# Industria Textilă

ISSN 1222–5347

5/2014

Revistă **cotată ISI** și inclusă în **Master Journal List** a Institutului pentru Știința Informării din Philadelphia – S.U.A., începând cu vol. 58, nr. 1/2007/
***ISI rated*** *magazine, included in the* ***ISI Master Journal List*** *of the Institute of Science Information, Philadelphia, USA, starting with vol. 58, no. 1/2007*

Editată în 6 nr./an, indexată și recenzată în:
*Edited in 6 issues per year, indexed and abstracted in:*
**Science Citation Index Expanded (SciSearch®), Materials Science Citation Index®, Journal Citation Reports/Science Edition, World Textile Abstracts, Chemical Abstracts, VINITI, Scopus, Toga FIZ technik ProQuest Central**







Recunoscută în România, în domeniul Științelor inginerești, de către **Consiliul Național al Cercetării Științifice din Învățământul Superior** (C.N.C.S.I.S.), în **grupa A** /
*Aknowledged in Romania, in the engineering sciences domain, by the* ***National Council of the Scientific Research from the Higher Education*** *(CNCSIS), in* ***group A***

# it Sumar

# Contents

# Comfort-related properties of woven fabrics produced from Dri-release® yarns

EMİNE UTKUN


## REZUMAT – ABSTRACT

**Proprietăţile de confort ale ţesăturilor produse din fire Dri-release®**

*Scopul acestui studiu a fost de a produce ţesături pentru îmbrăcăminte sport cu un grad ridicat de confort, deci cu o valoare adăugată mare. În prima etapă a studiului a fost proiectată o ţesătură nouă cu structură bistrat pentru a fi utilizată pentru producerea îmbrăcămintei sport. Au fost create patru ţesături diferite utilizând firele de bumbac, Tencel LF®, bambus şi Modal®, precum şi firele Dri-release®. Ulterior, au fost analizate, verificate statistic şi comparate proprietăţile de confort termic ale acestor ţesături. La finalului studiului, au fost indicate ţesăturile cu proprietăţi optime de utilizare.*

*Cuvinte-cheie: Dri-release®, confort termic, ţesătură*

**Comfort-related properties of woven fabrics produced from Dri-release® yarns**

*The aim of this study was to manufacture active-wear fabrics that have a high clothing comfort, hence, a high added value. In the first stage of the study, a new double-layer woven fabric was designed to be used for active-wear and four different fabrics were manufactured by utilizing cotton, Tencel LF®, bamboo and Modal® yarns in addition to Dri-release® yarn. Then, thermal comfort properties of these fabrics were analyzed, statistically reviewed and compared to each other. At the end of the study, fabrics with optimum usage properties were suggested.*

*Key-words: Dri-release®, thermal comfort, woven fabric*


Today, clothing comfort appears as a significant factor when people make their clothing selection. Researches conducted on this subject are important in terms of raising people's life standards. Clothing comfort is divided into sub-components as thermal comfort, sensory comfort, body movement comfort and psychological (aesthetical) comfort [1].

Thermal comfort is a property related to the ability of clothing to keep the body temperature within the required temperature limits and to transfer the produced sweat. Thermal comfort sense is the state where a person is satisfied with the temperature or moisture rate of the available environment and does not request any change in existing atmospheric conditions [2, 3, 4]. There is a common agreement in literature and the researchers of the subject consider that air permeability, water vapor permeability and liquid transfer properties as well as the thermal resistance and thermal conductivity properties are the most important properties of clothing in order to maintain thermal comfort [1, 3, 4, 5, 6, 7, 8, 9, 10].

Clothing with good thermal comfort has an efficient role in maintaining the heat and moisture balance of a person by transferring the heat and moisture of body that change under different atmospheric conditions and/or during different activities [11].

Within the scope of this study, the aim was to manufacture active-wear fabrics that have high clothing comfort, hence, a high added value, considering the fact that different fibers and fabric structures can be used for active-wear. Accordingly, in the first stage of the study, a new double-layer woven fabric was designed to be used for casual wear and four different fabrics were manufactured by utilizing cotton, Tencel LF®, bamboo and Modal® yarns in addition to Dri-release® yarn. Then, thermal comfort properties of these fabrics were analyzed, statistically reviewed and compared to each other. At the end of the study, fabrics with optimum usage properties were suggested.

While designing a fabric, functional properties and basic structural parameters of fabrics must be fully understood [12]. A fabric consists of fibers and air. The still-air amount in fabric is more important than the fiber amount when thermal resistance is considered; still-air provides more thermal resistance in comparison to a great number of textile fibers [2, 13, 14, 15]. Regarding this matter, Cubric et al. (2012) put forward that the amount of still-air within the structure of knitted fabrics played an important role in terms of the thermal properties of fabric [16].

In the light of this information, the main idea of designing fabrics within the scope of the study was to form a double-layer structure and in this way, to preserve an air stratum between the fabric layers. In addition to that, multiple yarn types were used together in fabric manufacturing. Therefore, the aim was to utilize the properties of different fibers simultaneously.

The general properties of the fibers used within the study are as follows.

### Dri-release®

Dri-release® is the trademark of Optimer. While 85–90% of this product consists of polyester fiber with hydrophobic properties, 10–15% of it consists of cotton, which is a hydrophilic fiber. In Dri-release® yarn, two different fibers are jointly used and they make a single yarn, thus, the properties of both fibers are separately utilized and the properties – mainly thermal comfort – of the manufactured goods are aimed to be improved. The natural fiber part absorbs the moisture on skin and transfers it inside the fabric. The synthetic fiber part wards off the moisture towards the upper part of clothing where it can easily vaporize by means of air current on the fabric. Dri-release® is a product which is used in active-wear, socks and underwear manufacturing [17, 18, 19, 20].

### Cotton

Cotton fiber, which is a vegetable raw material of textile, has an extensive area of use. Cotton fiber is used especially in underwear and active-wear manufacturing due to its softness, its high resistance to wetness, its durability against washing, its hygiene property and its high capacity to hold moisture [21].

### Tencel®

Tencel® fiber is the trademark of Lenzing. It is a tree-based fiber which is obtained via nano-fibril technology. Its most prominent feature is that it is soft due to its smooth fiber structure, that it is high-strength and that it provides quite high water absorption [22].

### Bamboo

This fiber, which is obtained from the cellulose of bamboo plant, has good properties of moisture absorption, moisture vaporization and ventilation thanks to the micro gaps and micro holes [22, 23].

### Modal®

Modal® is a fiber obtained from the cellulose of beech. It is the trademark of Lenzing. The most prominent feature of this fiber is that it is soft and radiant. Among the other properties, its low fiber hardness, smooth fiber surface, low yarn imperfection, high strength, natural softening material content and high chroma can be listed [22].

## EXPERIMENTAL PART

### Materials

Values related to the weft yarns of the fabrics within the scope of the study are shown in table 1, and values related to the warp yarns of the fabrics within the scope of the study are shown in table 2.

Table 1

CHARACTERISTICS OF THE WEFT YARNS OF THE FABRICS

| Yarn Code | Yarn Count (Nm) | Raw Material | Twist Coefficient (αe) | Direction of Twist |
|---|---|---|---|---|
| Y1 | 20/1, ring | % 100 Dri-release® (%85 Polyester, %15 Cotton) | 3,7 | Z |
| Y2 | 20/1, ring | % 100 Tencel LF® | 3,7 | Z |
| Y3 | 20/1, ring | % 100 Rayon made from Bamboo | 3,7 | Z |
| Y4 | 20/1, ring | % 100 Modal® | 3,7 | Z |

Table 2

CHARACTERISTICS OF THE WARP YARNS OF THE FABRICS

| Yarn Code | Yarn Count (Nm) | Raw Material | Twist Coefficient (αe) | |
|---|---|---|---|---|
| | | | First Layer (Z) | Second Layer (S) |
| Y5 | 80/2, ring | % 100 Cotton | 3,7 | 3,1 |

The fabrics were woven on a dobby weaving loom and kept in 50°C water for 90 minutes without adding any substance, and then, they were left to dry. The basis weight and thickness values, numbers of warp and weft yarns per unit area and the codes of warp and weft yarns are shown in table 3. In order that the fabric codes can be apprehended easily, the codes were prepared by using the numbers of yarn codes which are used in manufacturing the fabrics.

The fabrics were manufactured in original modified twill structure (figure 1). Modified twill structure was double-layered. While a double-layer structure was

Table 3

CHARACTERISTICS OF THE FABRICS

| Fabric No | Weight (g/m²) | Thickness (mm) | Warp Density (warp/cm) | Weft Density (weft/cm) | Code of Warp Yarn | Code of First-Layer Weft Yarn | Code of Second-Layer Weft Yarn |
|---|---|---|---|---|---|---|---|
| 1-1 | 121 | 0,55 | 22 | 28 | Y5 | Y1 | Y1 |
| 1-2 | 123 | 0,52 | 23 | 29 | Y5 | Y1 | Y2 |
| 1-3 | 140 | 0,56 | 23 | 29 | Y5 | Y1 | Y3 |
| 1-4 | 128 | 0,53 | 23 | 30 | Y5 | Y1 | Y4 |

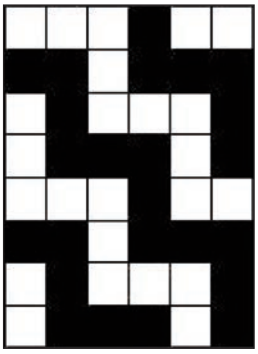

Fig. 1. Modified twill texture report

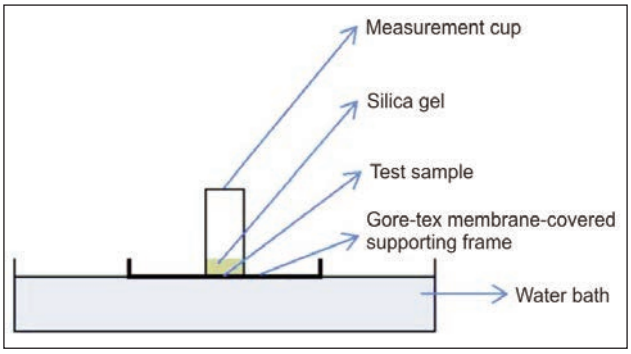


Fig. 2. Testing apparatus of Gore cup method

developed in the fabrics, among the self-tie methods, weft joining method was used. The texture reports of the fabrics are equal, however, their junction points were changed in order to use different yarns on front and reverse sides.

### Method

All of the experimental studies in this section except water permeability test were conducted in the Textile Laboratories in Tampere Technical University, Faculty of Automation, Mechanical and Material Engineering, Department of Fiber Materials Science. Water permeability test was conducted in the Textile Laboratories in Technical Administration of TSI Denizli Textile Laboratory. All of the fabric samples were conditioned by keeping under standard atmospheric conditions (20 ± 2°C temperature and 65% ± 5 relative humidity) for 24 hours before the experimental studies. The data obtained were analyzed by utilizing the SPSS 15.0 statistical package software. The measurements are described as follows. The weight values of the fabrics were identified according to SFS 3192:1974 standard, and the thickness values of the fabrics were identified according to SFS-EN ISO 5084:1997 standard.

### Thermal resistance – Thermal conductivity

Thermal resistance and conductivity of the fabrics were measured via thermal resistance measuring device according to ISO 5085-1:1989 standard and double plate method [24]. Test samples with diameter of 33 cm were prepared for each fabric sample.

### Water vapor permeability

Water vapor permeability of the fabrics was measured according to Gore cup method. Test samples with diameter of 9 cm were prepared for each fabric sample. The materials used during the test were measurement cup, rubber ring, silica gel, Gore-tex membrane-covered supporting frame and water bath. The testing apparatus is shown in figure 2.

The measurement cup is filled with silica gel and the brim of the cup is covered with samples via rubber rings. This apparatus is weighed on a precision scale and the $m_0$ value is obtained. On the other hand, water bath is prepared and the Gore-tex covered supporting frame, which is a highly permeable membrane in terms of water vapor, is placed on this water bath. Previously prepared sample is placed on this frame. This testing apparatus is kept for four hours and the $m_1$ value is obtained by measuring the cup weight again at the end of these four hours. The $m_1$ and $m_0$ values, which are obtained from the test results, are subtracted from each other and the water vapor permeability value is calculated.

### Air permeability

Air permeability of the fabrics was measured according to SFS-EN ISO 9237:1996 standard [25] The measurements were conducted via Karl Schröder D-6940 air permeability measuring device by applying 100 Pa pressure on a surface area of 20 $cm^2$.

### Water permeability

Water permeability of the fabrics was measured according to TS 257 EN 20811/T1 – Textile Fabrics-Determination of Resistance to Water Penetration-Hydrostatic Pressure Test standard [26]. The measurements were conducted via Textest FX 3000 Hydrostatic Head Tester measuring device by applying 60 mbar/minute water pressure rate of increase.

## RESULTS AND DISCUSSION

The mean values, standard deviations and measurement units of thermal comfort property, which were obtained from the standard measurements conducted on the fabrics, are shown in table 4.

The significance value within the study was acknowledged as ($p$) 0.05. If significance value ($p$) of a parameter was higher than 0.05 ($p > 0.05$), it was interpreted that the parameter did not make a statistically significant difference.

Fabric 1-1 was considered as the control group in interpretation of the analysis. One-way Analysis of Variance (ANOVA) was conducted on the independent samples in order to determine if different yarn types used in conjunction with Dri-release® yarn have a statistically significant difference on the thermal resistance, thermal conductivity, water vapor permeability, air permeability and water permeability values of the fabrics.

Table 4

RESULTS OF THE STANDARD MEASUREMENTS OF THE FABRICS

| Fabric code | Thermal resistance ($m^2$·K/W) | | | Thermal conductivity W/(m·K) | | | Water vapor permeability ($g/m^2$·24h) | | | Air permeability ($l/m^2$·s) | | | Water permeability (mbar) | | |
|---|---|---|---|---|---|---|---|---|---|---|---|---|---|---|---|
| | N | Mean | Standard deviation | N | Mean | Standard deviation | N | Mean | Standard deviation | N | Mean | Standard deviation | N | Mean | Standard deviation |
| 1-1 | 4 | 0,008 | 0,001 | 4 | 0,110 | 0,007 | 4 | 4868 | 112 | 5 | 1770 | 148 | 5 | 10,2 | 0,3 |
| 1-2 | 4 | 0,009 | 0,001 | 4 | 0,090 | 0,008 | 4 | 4812 | 96 | 5 | 1770 | 57 | 5 | 6,5 | 0,4 |
| 1-3 | 4 | 0,003 | 0,001 | 4 | 0,338 | 0,075 | 4 | 4817 | 104 | 5 | 1230 | 27 | 5 | 7,3 | 0,6 |
| 1-4 | 4 | 0,008 | 0,001 | 4 | 0,114 | 0,012 | 4 | 4899 | 89 | 5 | 1660 | 129 | 5 | 9,2 | 0,3 |

The hypotheses of ANOVA analysis, which were conducted for each property, are as follows.

"H0": There is no difference between the fabrics in terms of thermal comfort property.

"H1": There is a difference between the fabrics in terms of thermal comfort property.

Before the variance analysis, Levene Test was conducted and variance homogeneity was tested. It was interpreted that the variances were homogeneous if the result was $p > 0.05$, and that the variances were not homogeneous if the result was $p < 0.05$ in Levene Test. In order to define the relationship between the fabrics, Tukey HSD multiple comparison test was conducted in the cases that the variances were homogeneous, and Games-Howell multiple comparison test was conducted in the cases that the variances were not homogeneous. The results obtained are described in the provided tables.

## Thermal resistance

According to the results of Levene Test, $F = 0,105$ and significance level was $p = 0,955$; in this case, it was observed that distribution variances were homogeneous. According to the results of ANOVA, $F = 71,636$ and $p = 0,000$. Therefore, "H1" hypothesis was accepted; in other words, there was a statistically significant difference between the thermal resistance values of the fabrics. According to Tukey HSD multiple comparison test, which was conducted after ANOVA test, while the fabrics 1-1, 1-2 and 1-4 made a group, the fabric 1-3 made another group.

## Thermal conductivity

According to the results of Levene Test, $F = 6,725$ and significance level was $p = 0,007$; in this case, it was observed that distribution variances were not homogeneous. According to the results of ANOVA, $F = 37,321$ and $p = 0,000$. Therefore, "H1" hypothesis was accepted; in other words, there was a statistically significant difference between the thermal resistance values of the fabrics. According to Games-Howell multiple comparison test, which was conducted after ANOVA test, there was a significant difference between the thermal conductivity of the fabric 1-3 and the thermal conductivity of the fabrics 1-1, 1-2, 1-4. In addition to that, there was a significant difference between the thermal conductivity values of the fabrics 1-1 and 1-2.

## Water vapor permeability

According to the results of Levene Test, $F = 0,301$ and significance level was $p = 0,824$; in this case, it was observed that distribution variances were homogeneous. According to the results of ANOVA, $F = 0,698$ and $p = 0,571$. Therefore, "H0" hypothesis was accepted; in other words, there was no statistically significant difference between the water vapor permeability values of the fabrics.

In addition, according to the correlation analysis conducted between the thickness and water vapor permeability values of fabrics, Pearson correlation coefficient was measured as –0.953 at 0.05 significance level. In other words, while the thickness value of fabrics increases, the water vapor permeability value decreases.

## Air permeability

According to the results of Levene Test, $F = 1,877$ and significance level was $p = 0,174$; in this case, it was observed that distribution variances were homogeneous. According to the results of ANOVA, $F = 30,889$ and $p = 0,000$. Therefore, "H1" hypothesis was accepted; in other words, there was a statistically significant difference between the air permeability values of the fabrics. According to Tukey HSD multiple comparison test, which was conducted after ANOVA test, while the fabrics 1-1, 1-2 and 1-4 made a group, the fabric 1-3 made another group.

In addition, according to the correlation analysis conducted between the air permeability and thermal resistance values of fabrics, Pearson correlation coefficient was measured as 0.893 at 0.05 significance level. In other words, while the air permeability value of fabrics increases, the thermal resistance value increases as well.

### Water permeability

According to the results of Levene Test, $F = 1,431$ and significance level was $p = 0,271$; in this case, it was observed that distribution variances were homogeneous. According to the results of ANOVA, $F = 96,222$ and $p = 0,000$. According to these results, "H1" hypothesis was accepted; in other words, there was a statistically significant difference between the water permeability values of the fabrics. According to Tukey HSD multiple comparison test, which was conducted after ANOVA test, each of the fabrics 1-1, 1-2, 1-3 and 1-4 made a separate group.

Besides these analyses, according to the correlation analysis conducted between the water vapor permeability and water permeability values of fabrics, Pearson correlation coefficient was measured as 0.922 at 0.05 significance level. In other words, while the water vapor permeability value of fabrics increases, the water permeability value increases as well.

## CONCLUSIONS

Thermal and moisture transfer properties of active-wear fabrics must be very good in order that they can have optimum properties. Thermal conductivity, water vapor permeability, air permeability and water permeability values of the fabrics, which were developed within the scope of the study, were aimed to be high. At the end of the assessment of the measurements and analysis which were conducted on the fabrics, table 5 was generated.

It is observed that the thermal properties of the fabric 1-1, which is considered as the control group, are higher in comparison to the other fabrics. It follows the fabric 1-3 only in terms of thermal conductivity value. It is assumed that this is because of the micro holes which are available in the structure of bamboo fiber.

Considering the obtained results, if the fabrics should be sorted out according to their preferability as an active-wear fabric, the final listing is as follows.

Table 5

| EVALUATION OF THE MEASUREMENTS | | | | | |
|---|---|---|---|---|---|
| **Fabric code** | **Thermal resistance** | **Thermal conductivity** | **Water vapor permeability** | **Air permeability** | **Water permeability** |
| 1-1 | 1 | 2 | 1 | 1 | 1 |
| 1-2 | 1 | 3 | 1 | 1 | 4 |
| 1-3 | 2 | 1 | 1 | 2 | 3 |
| 1-4 | 1 | 2 | 1 | 1 | 2 |

Note: While the figure 1, which is used in the table, indicates that the fabric provides the highest value for the mentioned property, an increase on the figure indicates that the mentioned value lowers.

1) Fabric 1-1
2) Fabric 1-4
3) Fabric 1-3
4) Fabric 1-2

As it is obvious from the results, high-comfort fabrics can be manufactured by using cotton and Dri-release® yarns. This combination is followed by the fabric 1-4, which is a mix of cotton-Dri-release®-Modal® and by the fabric 1-3, which is a mix of cotton-Dri-release®- bamboo. It can be proposed that these fabrics can be used as active-wear fabrics. However, it was observed that the results were not as good as expected although the fabric 1-2, which is a mix of cotton-Dri-release®-Tencel LF®, was designed as an active-wear fabric, and it is not recommended to use for active-wear items.

### Acknowledgements

My profound thanks to M.Sc. Minna VARHEENMAA, to Teija JOKI from Tampere Technical University, and to the Technical Direction of Denizli Textile Laboratory of Turkish Standards Institution that helps to carry out the experimental studies, and to Kaçanoğlu Textile in the presence of Selahattin KAÇANOĞLU in the production of the fabric samples.

## BIBLIOGRAPHY

[1] Li Y. *The Science of Clothing Comfort.* The Textile Institute Publications, Textile Progress, Manchester, 2001, vol. 31 (½), p.138.

[2] Taylor HM. *Textiles for indoor thermal comfort, part 1 - clothing.* In: Textiles, 1982, vol. 11, issue 3, p. 66-71.

[3] Behera BK, Ishtiaque SM and Chand S. *Comfort properties of fabrics woven from ring-, rotor-, and friction- spun yarns.* In: Journal of the Textile Institute, 1997, vol. 88, issue 3, p. 255-264.

[4] Das A and Ishtiaque SM. *Comfort characteristics of fabrics containing twist-less and hollow fibrous assemblies in weft.* In: Journal of Textile and Apparel, Technology and Management, 2004, vol. 3, issue 4, p. 1-7.

[5] Barker RL. *From fabric hand to thermal comfort: the evolving role of objective measurements in explaining human comfort response to textiles.* In: International Journal of Clothing Science and Technology, 2002, vol. 14, issue ¾, p. 181-200.

[6] Hes L and Kus Z. *Improved thermal contact comfort of garments caused by functional underwear.* In: The Fiber Society Spring Symposium, Loughborough University, UK, 30 June – 2 July 2003.

[7] Celcar D, Meinander H and Geriaak J. *A study of the influence of different clothing materials on heat and moisture transmission through clothing materials, evaluated using a sweating cylinder.* In: International Journal of Clothing Science and Technology, 2008, vol. 20, issue 2, p. 119-130.

[8] Özdil N, Süpüren G, Özçelik G and Pruchova J. *A study on the moisture transport properties of the cotton knitted fabrics in single jersey structure.* In: Journal of Textile and Apparel, 2009, vol. 19, issue 3, p. 218-223.

[9] Majumdar A, Mukhopadhyay S and Yadav R. *Thermal properties of knitted fabrics made from cotton and regenerated bamboo cellulosic fibres.* In: International Journal of Thermal Sciences, 2010, vol. 49, p. 2042-2048.

[10] Onofrei E., *Identification of the most significant factors influencing thermal comfort using principal component analysis and selection of the fabric according to the apparel end-use*. In Industria Textila, 2012, vol. 63, issue 2, pp. 91-96.

[11] Marmaralı, A., Kretzschmar, S.D., Özdil, N. and Oğlakçıoğlu, N.G. *Parameters that affect thermal comfort of garment.* In: Journal of Textile and Apparel, 2006, vol.16, issue 4, p. 241-246.

[12] Behera BK and Karthikeyan B. *Artificial neural network-embedded expert system for the design of canopy fabrics.* In: Journal of Industrial Textiles, 2006, vol. 36, issue 2, p. 111-123.

[13] Fourt L. and Hollies NRS. *Clothing-Comfort and Function.* Marcel Dekker Publishers, New York, 1970, p. 254.

[14] Hollies NRS and Goldman RF. *Clothing Comfort-Interaction of Thermal, Ventilation, Construction and Assessment Factors,* Ann Arbor Science Publishers, Michigan, 1977, p.189.

[15] Bhattacharjee D. and Kothari VK. *Heat transfer through woven textiles.* In: International Journal of Heat and Mass Transfer, 2009, vol. 52, p. 2155-2160.

[16] Cubric IS, Skenderi Z, Mihelic-Bogdanic A and Andrassy M. *Experimental study of thermal resistance of knitted fabrics.* In: Experimental Thermal and Fluid Science 2012; 38:223-228.

[17] Chaudhari SS, Chitnis R S and Ramkrishnan R. *Waterproof breathable active sports wear fabrics*, http://www.sasmira.org/sportwear.pdf (Accessed 31 July 2013)

[18] Wardiningsih W. *Study of comfort properties of natural and synthetic knitted fabrics in different blend ratios for winter active sportswear.* Master of Science Thesis, RMIT University, Melbourne, 2001.

[19] Skomra E. *A comparative study of athletic apparel made from cotton.* Master of Science Thesis, Eastern Michigan University, 2006.

[20] Marmaralı A. and Blaga M. A *research about knitted fabric structures with optimum thermal properties which are produced by using new special fibers.* Report for the Ege University and Gheorghe Asachi Technical University within bilateral Project Romania-Turkey, International Round Table, 25-26 September 2009, Iaşi, Romania.

[21] Gürcüm, H.B. *Tekstil Malzeme Bilgisi.* Güncel Publishers, Turkey, 2010, p.520.

[22] Avcı, H. *Comfort properties of socks produced with new fibers.* Master of Science Thesis, İstanbul Technical University, Turkey, 2007.

[23] Karahan, H.A., Öktem, T. and Seventekin, N. *Natural bamboo fiber.* In: Journal of Textile and Apparel, 2006, vol. 4, p. 236-240.

[24] ISO 5085-1. Textiles. Determination of thermal resistance, part 1: low thermal resistance, 1989.

[25] SFS-EN ISO 9237. Textiles. Determination of permeability of fabrics to air, 1996.

[26] TS 257 EN 20811/T1. Textile fabrics – Determination of water tightness-hydrostatic pressure test, 1996.

**Author:**

*Asist. Prof. Dr.* EMİNE UTKUN
Buldan Vocational Training School
Program of Fashion Design
Pamukkale University
Denizli 20400
Turkey
e-mail: eutkun@pau.edu.tr

# Conferring antimicrobial properties to fabrics by sonochemical embedding of nanoparticles

HORTENSIA CLARA RADULESCU
MIRCEA VINATORU
JAMIE BEDDOW
VERONICA LAZAR
LAURENTIU DINCA
EADAOIN JOYCE
CARMEN GHITULEASA
TIMOTHY MASON

**REZUMAT – ABSTRACT**

**Conferirea de proprietăţi antimicrobiene materialelor textile prin impregnare ultrasonică cu nanoparticule**

*Obiectivul principal în domeniul cercetării textile din ultima decadă l-a constituit dezvoltarea de procese şi tehnologii prin care să se îmbunătăţească sau să se adauge funcţionalităţi suplimentare materialelor textile clasice. Această lucrare prezintă rezultatele privind evaluarea activităţii antimicrobiene faţă de un număr de specii bacteriene şi fungice a unei ţesături din amestec PES/Bbc impregnat cu nanoparticule de oxid de cupru cu ajutorul ultrasunetelor. Sunt prezentate rezultate adiţionale privind caracterizarea materialului textil şi a nanoparticulelor prin SEM cuplat cu EDS şi IRT (Termografie în Infraroşu).*

*Cuvinte-cheie: Activitate antimicrobiană, ultrasunete, MRSA, Acinetobacter baumannii, Candida albicans, oxid de cupru, durabilitate la spălare*

**Conferring antimicrobial properties to fabrics by sonochemical embedding of nanoparticles**

*The main focus of textile research in the last decade has been to develop processes and technologies which improve or add extra functionality to classical textiles. This paper presents the antimicrobial activity against a range of bacterial and fungal species of a PES/CO woven textile impregnated by means of ultrasound with nanoparticles of copper oxide. Supplementary data regarding textile and nanoparticle characterization, such as SEM coupled with EDS and IRT (Infrared Thermography) are also presented.*

*Key-words: Antimicrobial activity, ultrasounds, MRSA, Acinetobacter baumannii, Candida albicans, copper oxide, wash durability*

## INTRODUCTION

### *Antimicrobial textiles*

The use and applications of antimicrobial textiles have increased in recent years following a global trend in health care systems and a general societal concept, where personal and home hygiene have become an ever more important requirement for a healthier and better life [1].

The antimicrobial function is imparted to textiles by a range of chemical agents, including: silver ions, natural biopolymers like the chitosan or vegetal extracts, N-halamine molecules, alkyl ammonium ions, metals and metallic salts and quaternary ammonium salts [2–4].

Antimicrobial agents act in various ways: by disrupting the structure and integrity of the microbial cellular membrane; by interacting with the genetic material (RNA and DNA); and by altering the structure of essential proteins.

Maybe the most important application of antimicrobial textiles is the medical sector [5]. Such textiles can be included in preventive measures taken by the hospitals to avoid the transmission of diseases [6, 7]. Woven textiles may be used in hospitals as bed sheets and pillow covers as well as protective garments for patients and medical personnel. The durability of the antimicrobial property on the surface of textiles is a matter of concern and a serious challenge in developing such products [8, 9].

Depending on the type of textile fibre and the end use of the final product the antimicrobial functionality may be incorporated in three ways: (a) direct incorporation into the fibres during their formation, especially in the case of artificial fibres (i.e Rhovil'As from Rhovil, Amicor and Amicor Plus from Courtaulds); (b) as finishing on the fibres (i.e Eosy from Unitka); (c) and as finishing on the textile products (i.e Sanitized from Sanitized AG) [10–13].

### *Ultrasonic treatment*

Ultrasound induces voids, bubbles in liquid media when a power threshold is reached. These bubbles are not stable and after several acoustic cycles collapse releasing locally tremendous amounts of energy in terms of temperature (5,000ºK) and pressure (~2,000 atm). If there are some chemical compounds dissolved in the liquid, then they will suffer decomposition due to bubbles' collapse. If the compounds dissolved in the liquid generate metal oxides when the bubbles collapse, then they will end up as nanoparticles. Copper and zinc ammonia complexes in ethanol

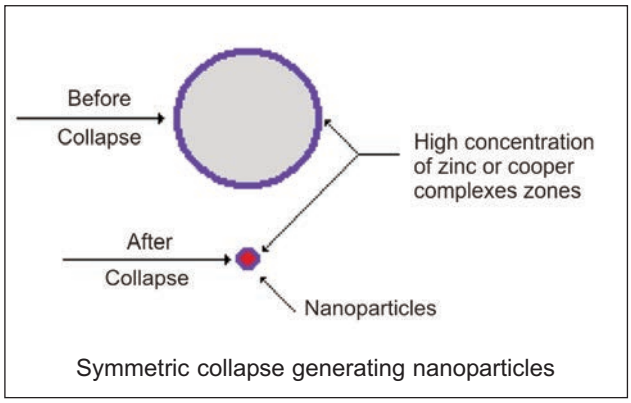


Fig. 1. Acoustic bubble collapse

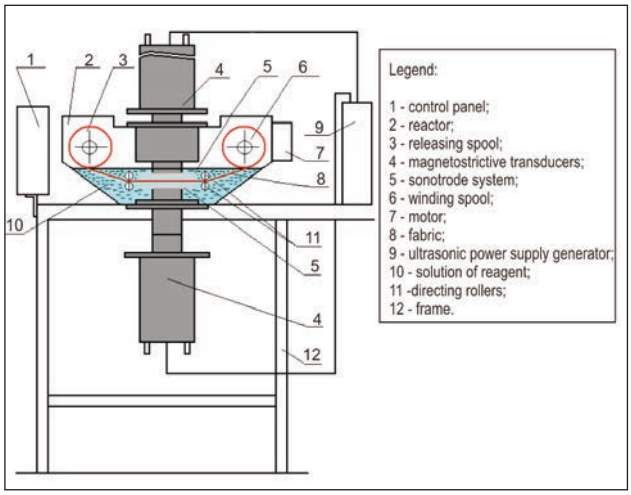


Fig. 2. Schematic of laboratory scale machine for ultrasonic impregnation of textiles with antimicrobial nanoparticles

solution were chosen for this process. The addition of a fabric material in this setting will change some of the bubble collapse from a symmetrical mode to an asymmetrical mode (figure 1).

In this project a single step process in which ultrasound causes both the formation of metal oxide nanoparticles (CuO) and simultaneously impregnates these nanoparticles into textile fibres was employed [14–16]. The pilot ultrasonic machines are based on the original laboratory scale unit, schematically presented in figure 2.

During this project two pilot ultrasonic machines designed to impregnate fabrics with nanoparticles were built. Each one was based on different ultrasonic transducers:

– The one existing in Romania was based on magnetostrictive flat ultrasonic transducers.
– The other one existing in Italy was based on piezoceramic tubular ultrasonic transducers.

Magnetostrictive transducers have the advantage of a high level of tolerance to process conditions, but they have a low level of efficiency in transformation of electricity into mechanical vibration, while the piezoceramic transducers are more sensitive to process condition, but have higher transformation efficiency.

Both prototypes were run in a continuous mode to produce 500 mm wide rolls of fabric impregnated with CuO NPs. Several samples are reported here for their antimicrobial properties.

### *New developments*

This paper presents the antimicrobial activity of a PES/CO woven fabric that was coated with copper oxide nanoparticles (CuO NPs) with the aid of ultrasound energy. The microorganisms tested were represented by bacteria species *Acinetobacter baumannii* and MRSA and as fungal species, *Candida albicans*. The antibacterial and antifungal activities were maintained after 30 and 60 washing cycles. The ultrasound methods proved to be efficient in imparting antimicrobial function to the textile materials. The ultrasound treatment process was developed and optimized during the FP7 project SONO, that proposed to develop a technology able to deposit metallic oxide nanoparticles on the surface of textile materials for biomedical applications and related economic domains.

## EXPERIMENTAL PART

### *Textile material*

67 % polyester: 33 % cotton plain weave fabric (469 yarns/10 cm, yarn count 22.2 tex, in warp; 225 yarn/10 cm, yarn count 36.1 tex in weft; fabrics weight 198 g/m$^2$), of 50 cm width was used. Two types of samples were obtained: one on the Davo pilot scale (based on magnetostrictive flat ultrasonic transducers) named sample D and the second on the Klopman pilot scale (based on piezoceramic tubular ultrasonic transducers) named sample K. Fabric pattern is diagonal 2/1.

### *CuO Nanoparticles deposition*

The sonochemical coating of fabrics was carried out according to a previously published procedure [14]. In the pilot scale machines 500 mm wide rolls of fabric were fed on a motorized roller system through the acoustic cavitation zone close to the ultrasonic transducers. Both the fabric and the sonotrodes were submerged in a solution containing the precursors for the sonochemical production of CuO NPs. This solution

contained between 0.01 and 0.05 M copper acetate dissolved in a 9:1 mixture of ethanol and water. For the coating procedure the solution was heated to approximately 50°C, the pH was adjusted to between 8 and 9. The fabric was then fed at a constant rate through machine. After this the fabrics were washed thoroughly with clean water and ethanol and then dried.

### *Washing of textiles*

Specimens of both samples coated with CuO NPs on the ultrasound equipment were washed at 75°C on a Rotawash (SDL Atlas) machine with a liquid detergent, pH neutral (4 ml/L). The washing was done for 30 and 60 washing cycles according to SR EN ISO 6330: 2001 standard (Textiles – Domestic washing and drying procedures for textiles testing).

### *Antimicrobial activity*

Antimicrobial activity was carried out according to ISO 20743 standard (Textiles. Determination of antibacterial activity of antibacterial finished products) absorption method [18]. The method gives a quantitative assessment of the antimicrobial activity at the surface of textile materials. The antimicrobial testing consists in establishing the cell reduction between a control sample and a treated sample after an incubation period of 24–72 hours. The value of reduction is expressed as logarithm function after the following formula:

$$A = F - G \quad (1)$$

where:

*A* – antimicrobial (antibacterial/antifungal) efficiency value;

*F* – growth value on the control fabric sample;

*G* – growth value on the treated fabric sample.

The antibacterial testing was carried out against methicillin-resistant *Staphylococcus aureus* (MRSA), strain NCTC 10442, and *Acinetobacter baumannii*, strain NCTC 10303. The antifungal testing was carried out against *Candida albicans* according to AATCC 10231.

The tested microbial strains are considered important in causing nosocomial infections and they are also resistant to usual antibiotic therapy.

### *Scanning Electron Microscopy (SEM)*

The surface morphology of coated samples was investigated by a FEI Quanta 200 Scanning Electron Microscope with a GSED detector, at a 8000X – 16 000X magnification and accelerating voltage of 12.5 kV – 20 kV. The samples were examined before washing and after 60 cycles of washing and the copper oxide nanoparticles diameters were measured with the SEM xTm software.

### *Energy Dispersive X-ray analysis (EDX)*

EDX was used to identify the elemental composition of the PES/CO coated fabrics. The analysis was done with a FEI Quanta 200 Scanning Electron Microscope coupled with EDX detector. The detector has the ability to convert the X-ray energy emitted by the samples into voltage signals that are specific to different chemical elements. The EDX analysis was applied before washing and after 60 cycles of washing.

### *Infrared Thermography (IRT)*

The uniformity of conductive thermal transfer was analysed with a FLIR P 620 thermocamera, for the evaluation of thermophysiological comfort. The samples were fixed on the top of heating plate heated to 37°C, the normal temperature of human body. The thermal infrared radiation emitted by the textile fabrics was detected with the thermocamera in the spectral band between 7.5 and 13 μm. Thermograms were generated from these results, which indicate the distribution of temperature on the surface of the analysed samples. The thermograms were analysed with the soft Flir Quick Report, adding the rectangle and isotherm function and samples' emissivity with the value 0.95.

## RESULTS AND DISCUSSIONS

### *SEM and EDX before and after washing*

Scanning electron microscopy was used to investigate the surface morphology of the uncoated and coated textile materials and to identify the presence of CuO nanoparticles. Investigations were carried out before and after 60 washing cycles (figures 3 and 4). The nanoparticles of CuO were identified on the surface of the samples before washing, and after

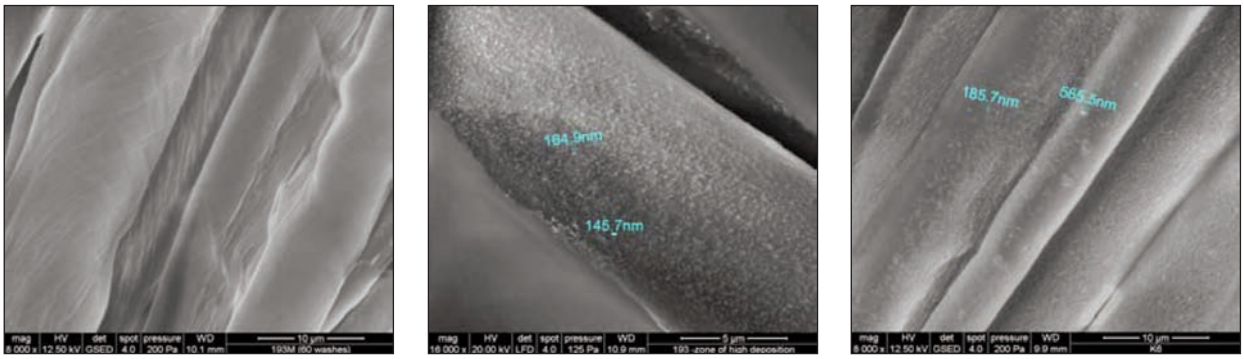


Fig. 3. SEM micrograph of the uncoated samples (left), coated sample D (middle) and coated sample K (right) before washing

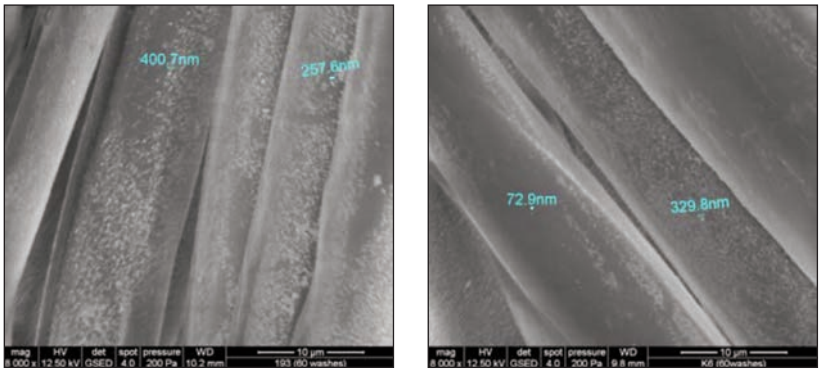


Fig. 4. SEM micrograph of the coated sample D (left) and coated sample K (right) after 60 washes

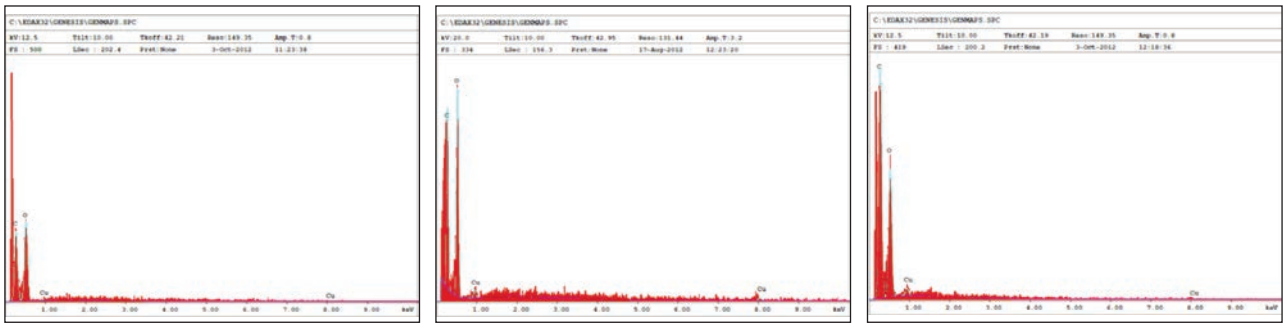

A B C

Fig. 5. EDX spectra of sample D before (B) and after 60 washing cycles (C) and of uncoated fabric (A)

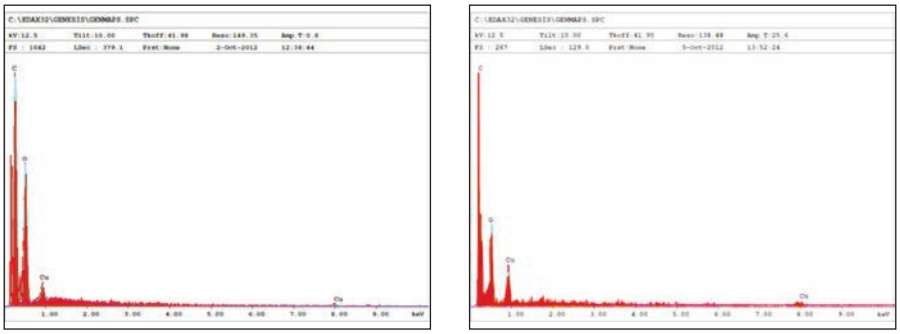

D E

Fig. 6. EDX spectra of sample K before (D) and after 60 washing cycles (E)

60 cyles. The washing did not affect the Nps coating for any of the samples. The range of Nps diameters observed was between 70–600 nm.

The presence of CuO nanoparticles on the surface of D and K samples was further confirmed by the EDX identification of Cu emission line. The Cu line was observed for the coated samples before and after 60 washing cycles. The coating was maintained after the laundering operation (figures 5 and 6).

### *Infrared thermography (IRT) before and after washing*

The pictures in figures 7 and 8 are the thermograms for the uncoated and coated samples. The isotherm of 37 ± 0.5 °C appears in the thermograms with grey colour and also the scale of temperatures which is represented by different colours. The thermograms of all samples (before and after washing) have a very large area of isotherm. This showed that they were thermally conductive, because a large area of the analysed surface had values of temperature near the temperature of the plate (37°C). For this reason, we can consider that the treatment and the washing do not modify the thermal conductivity of the textile material samples.

The non-uniformity of the thermal transfer through uncoated and coated samples is measured with the help of parameter Δt (0°C) which represents the difference between the maximal (tmax) and minimal (tmin) temperature inside the rectangles from thermograms. Figure 9 shows that, after washing, the uncoated and

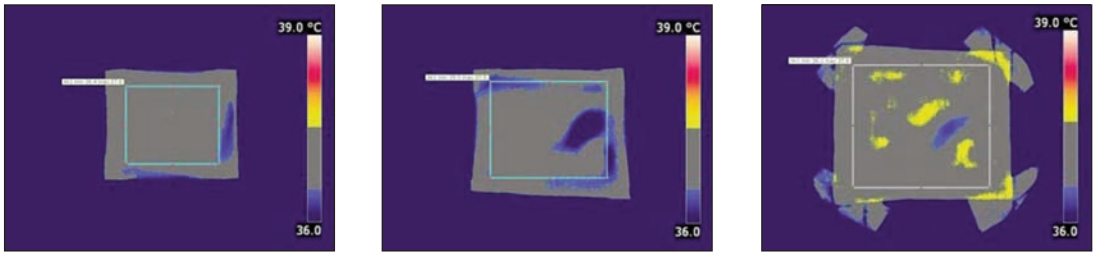


Fig. 7. IRT thermograms for the uncoated (left), sample D (middle) and sample K (right) before washing

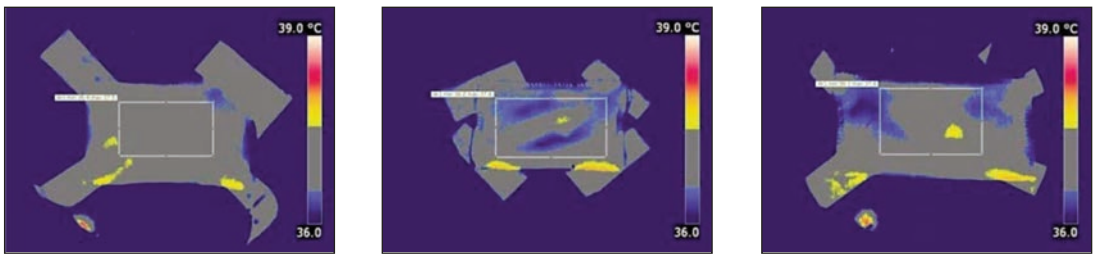


Fig. 8. IRT thermograms for the uncoated (left), sample D (middle) and sample K (right) after 60 washes

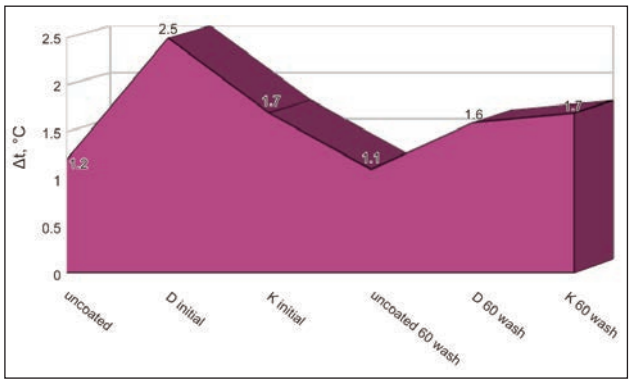


Fig. 9. Infrared thermography analysis for uncoated and CuO Nps coated samples before and after 60 washing cycles

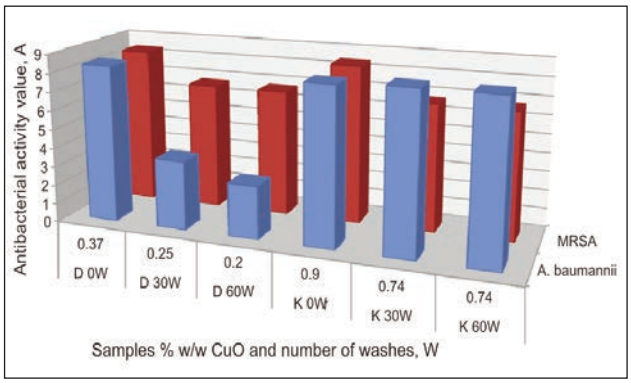


Fig. 10. Antibacterial activity towards MRSA and *Acinetobacter baumannii* for samples D and K after 0, 30 and 60 washing cycles

K samples maintain the non-uniformity values. For sample D the non-uniformity decreases.

### *Antimicrobial testing before and after washing*

### *Antibacterial assessment*

The antibacterial assessment was performed on initial CuO Nps coated D and K samples and after the laundering operation for 30 and 60 washing cycles. The antibacterial efficacy was compared with the uncoated fabric and the viable cell reduction was logarithmically expressed by parameter A. The results from antibacterial efficacy tests on the CuO NPs PES/Cotton fabrics are presented in figure 10. The antibacterial activity of both fabrics was very high, with A values > 5. Following overnight incubation of the fabric samples with the test bacteria no viable bacteria cells were recovered. The antibacterial activity levels after 60 washing cycles were still high (A>2) and in figure 4 CuO NPs can still be seen on the fibres after the washing treatment. There was some decrease in the antibacterial activity levels after

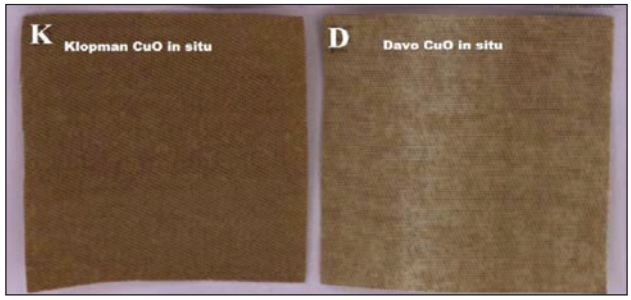


Fig. 11. White PEC sonochemically impregnated with CuO NPs. (left) sample from Klopman machine (right) sample from Davo machine

washing presumably due to the loss of some CuO from the fabrics. Both fabrics lost between 0.16 and 0.17 % w/w of the CuO. The slightly greater drop in activity observed with the Davo fabric may have been due to the lower amount of CuO deposited in the first place (0.37 % w/w CuO on D and 0.9% w/w CuO on K) (figure 11).

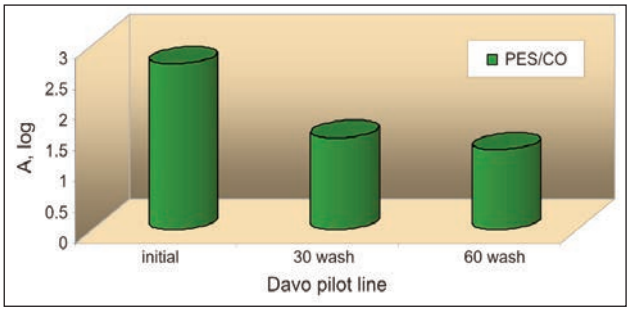


Fig. 12. Antifungal activity towards *Candida albicans* for sample D obtained on the Davo pilot line before and after 30 and 60 washing cycles

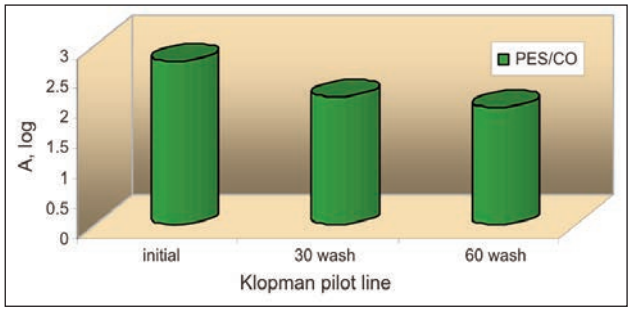


Fig. 13. Antifungal activity towards *Candida albicans* for sample K obtained on the Klopman pilot line before and after 30 and 60 washing cycles

### *Antifungal assessment*

The antifungal assessment was performed on initial CuO Nps coated D and K samples and after the laundering operation for 30 and 60 washing cycles. The antifungal activity efficiency was measured compared with the uncoated fabric and the cell reduction was logarithmically expressed by parameter A. The initial coated fabrics, both samples D and K expressed a high antifungal value, close to 3, representing a cell reduction > 99.9%. The fungal cell reduction remained at the same value after 30 washing cycles as well as after 60 washing cycles, for each samples, which means that the laundering cycles will no longer affect the antifungal efficiency and that the CuO Nps are stable/permanent embedded on the surface of the fabrics. The fungal cell reduction is showing higher value for the K sample after 30 and 60 washing cycles, similar to the antibacterial cell reduction results, sustaining the correlation hypothesis between the antimicrobial activity and the amount of CuO deposited on the textile materials. The antifungal results are presented in figures 12 and 13.

## CONCLUSIONS

Nanoparticles of copper oxide have been embedded onto a textile surface by means of ultrasounds. The CuO coating is analysed through Scanning Electron Microscopy (SEM), Energy dispersive x-ray analysis (EDX) and Infrared termography (IRT) and the antimicrobial efficiency of the CuO Nps is determined for the treated samples and for the treated samples after 30 and 60 washing cycles. The antibacterial efficiency as well as antifungal efficiency is very high for the initial coated samples. The sample obtained on the Klopman pilot line is showing excellent antimicrobial activity also after 30 and 60 washing cycles. The antimicrobial activity is lower for the D sample after the washing cycles, being correlated with a smaller amount of CuO Nps deposited on the fabrics surface (0.37 % w/w CuO on D and 0.9% w/w CuO on K). The sonochemical process can be used for a range of textiles and for various different nanoparticles. The technology has the potential to be both economically competitive and environmentally green. The formation of the nanoparticles and their impregnation are accomplished in a single step process, and no toxic chemicals are used.

## ACKNOWLEDGEMENTS

This research was funded by the EU Framework 7 grant (Project number: 228730). The authors would like to thank Professor A. Gedanken's group at Bar-Ilan University as well as all the other partners involved in the SONO project. Executive Agency for Higher Education, Research, Development and Innovation Funding (UEFISCDI), Romanian Ministry of Education Research for cofinancing the INCDTP participation in the SONO project.

## BIBLIOGRAPHY

[1] Rajendran, R., Balakumar, C., Ahammed, H.A.M., Jayakumar, S., Vaideki, K., Rajesh, E.M. *Use of zinc oxide nano particles for production of antimicrobial textiles*. In: International Journal of Engineering, Science and Technology, 2010, vol. 2, issue 1, p. 202

[2] Vigo, T.L. *Antimicrobial Polymers and Fibres: Retrospective and Prospective*. In Bioactive Fibres and Polymers, Eds J. V. Edwards and T.L. Vigo, American Chemical Society, Washington, DC, 2001

[3] Sivaramakrishnan, C.N. *Antimicrobial finishes*. In: Colourage, 2007, vol. LIV, issue 9, p. 50

[4] Gokarneshan, N., Gopalakrishnan, P.P., Jeyanthi, B. *Influences of Nanofinishes on the Antimicrobial Properties of Fabrics*. In: ISRN Nanomaterials, 2012, vol. 2012, p.1

[5] Takai, K., Ohtsuka, T., Senda, Y., Nakao, M., Yamamoto, K., Matsuoka, J., Hirai, Y., *Antibacterial Properties of Antimicrobial-Finished Textile Products*. In: Microbiol. Immunol., 2002, vol. 46, issue 2, p. 75

[6] Gao, Y., Cranston, R. *Recent Advances in Antimicrobial Treatments of Textiles*. In: Textile Research Journal, 2008, vol. 78, issue 1, p. 60

[7] Sun, G. *Durable and Regenerable Antimicrobial Textiles*, In Bioactive Fibres and Polymers, Eds J. V. Edwards and T.L. Vigo, American Chemical Society, Washington, DC, 2001

[8] Ureyen, M.E., Gurkan, P., Namligoz, E.S., Armakan, D.M., Dogan, A. *Antibacterial and Physical Properties of Knitted Cotton Fabrics Treated with Antibacterial Finishes*,. In: AATCC Review, 2010, vol. 10, issue 1, p. 48

[9] Lam, Y.L, Kan, C.W., Yuen, C.W.M. *A study of Metal Oxide on Antimicrobial Effect of Plasma Pre-treated Cotton Fabric*. In: Fibers and Polymers, 2013, vol. 14, issue 1, p. 52

[10] Sedelnik, Natalia. *Health-Promoting Properties of Blankets Made with the Bioactive Fibre 'Rhovyl AS' in the Pile*. In Fibres & textiles in Eastern Europe, October/December 2002

[11] Sedelnik, Natalia. *Health Properties of Polyacrylonitrile Blankets Made with the Anti-Microbial Fibre Amicor Plus.* In Fibres & textiles in Eastern Europe, 2006, vol. 14, issue 59, p. 120

[12] Papaspyrides, C.D., Pavlidou, S., Vouyiouka, S.N. *Development of advanced textile materials: Natural fibre composites, anti-microbial, and flame-retardant fabrics*. In: Proceedings of the Institution of Mechanical Engineers, Part L: Journal of Materials: Design and Applications. 2009, vol. 223, issue 2, p. 91

[13] Mohamed Abo El-Ola, S., Mohamady ElAdwi, M. *Concurrent antibacterial finishing and transfer printing of different types of fabrics.* Journal of Industrial Textiles, April 2012 vol. 41, issue 4, p. 309

[14] Abramov, O.V., Gedanken, A., Koltypin, Y., Perkas, N., Perelshtein, I., Joyce, E., Mason, T.J. *Pilot scale sono-chemical coating of nanoparticles onto textiles to produce biocidal fabrics*. In: Surface and Coatings Technology, 2009, vol. 204, p. 718

[15] Perelshtein, I., Applerot, G., Perkas, N., Wehrschuetz-Sigl, E., Hasmann, A., Guebitz, G., Gedanken, A. *CuO-Cotton Nanocomposite: Formation, Morphology, and Antibacterial Activity*. In: Surface and Coatings Technology, 2009, vol. 204, issue 1-2, p. 54

[16] Neral, B.; Sostar-Turk, S.; Fijan, S.. *The soil removal and disinfection efficiency of chemo-thermal and LCO2 treatment for hospital textiles*. In: Industria Textila, 2012, vol. 63, issue 5, pp. 246-251

[17] Haji, A; Barani, H; Qavamnia, S. S. *In situ synthesis and loading of silver nanoparticles on cotton fabric*. In: Industria Textila, 2013, vol. 64, issue 1, pp. 8-12

[18] BS EN ISO 20743:2007, *Textiles – Determination of Antibacterial Activity of Antibacterial Finished Products*, British Standards Institution, London, 2007

**Authors:**

*Scientific Res. PhD St.* CLARA RADULESCU,
National Research and Development Institute
for Textiles and Leather Bucharest (INCDTP)
Lucretiu Patrascanu, 16, 030508 Bucharest, Romania

University of Bucharest, Faculty of Biology,
Doctoral School in Biology
e-mail: clara.radulescu@certex.ro

LAURENTIU DINCA
*Dr. Ing.* CARMEN GHITULEASA
National Research and Development Institute
for Textiles and Leather Bucharest (INCDTP)
Lucretiu Patrascanu, 16, 030508 Bucharest, Romania
e-mail: certex@certex.ro

*Dr.* EADAOIN JOYCE,
*Dr.* MIRCEA VINATORU,
*Dr.* JAMIE BEDDOW,
*Prof. Dr.* TIMOTHY MASON
The Sonochemistry Centre, Coventry University,
Faculty of Health & Life Sciences,
Priory Street, Coventry, UK, CV1 5FB

*Prof. Dr.* VERONICA LAZAR
University of Bucharest, Faculty of Biology,
Department of Botany and Microbiology

# Effects of thermal aging on Kevlar and Nomex fabrics

BANU OZGEN GULSAH PAMUK


## REZUMAT – ABSTRACT

**Efectele îmbătrânirii termice a materialelor textile din fibre Kevlar și Nomex**

*În lucrare este studiată îmbătrânirea termică a fibrelor de înaltă performanță, Kevlar și Nomex. Au fost efectuate teste de îmbătrânire accelerată termic, pe eșantioane de țesături realizate din fibre 100% Kevlar, 100% Nomex și din amestecuri ale acestora. Materialele textile au fost supuse unor tratamente termice de îmbătrânire la temperaturi de 220°C și 300°C, pentru diferite perioade de timp. Efectele îmbătrânirii termice au fost evaluate prin teste de determinare a pierderilor de masă și a rezistenței la tracțiune. Studiul a arătat că structura și proprietățile probelor s-au schimbat după fiecare expunere termică, dar amploarea modificărilor a variat în funcție de tipul materialului, de temperatură și de durata cumulată a expunerii.*

*Cuvinte-cheie: Kevlar, Nomex, îmbătrânire termică, pierdere de masă, rezistență la tracțiune*

**Effects of thermal aging on Kevlar and Nomex fabrics**

*The focus of this work is the thermal aging of high-performance fibres, Kevlar and Nomex. Accelerated thermal aging tests were carried out on fabric samples made up of 100% Kevlar, 100% Nomex and their combinations. Fabrics were subjected to thermal aging treatments at 220°C and 300°C temperatures for various time periods. The effects of thermal aging were evaluated through mass loss and tensile strength tests. The study revealed that the structure and properties of specimens changed after each thermal exposure, but the magnitude of changes varied with material type, temperature and cumulative duration of exposure.*

*Key-words: Kevlar, Nomex, thermal aging, mass loss, tensile strength*


Kevlar® (Kevlar is the commercial name given by DuPont Inc., USA) is a para-aramid made up of poly (p-phenylene terephthalamide) or PPTA. Kevlar fibres are characterized by high tensile modulus, strength, good thermal stability and low density [1]. Nomex® is also a DuPont registered trademark for its family of aromatic polyamide (meta-aramid) fibres which is prepared from meta-phenylenediamine and isophthaloyl chloride in an amide solvent and is inherently flame resistant (FR) [2]. In military and fire fighters' clothing Kevlar and Nomex fabrics are widely used as protective clothing [3]. During their lifetime, materials used in protective clothing age under the action of various environmental and operation aggressors (temperature, light, moisture etc.). These factors constitute a severe limitation to the use of protective materials. The consequences of the degradation of these materials' functional properties are high, not only in terms of economic costs, but also in terms of safety.

The major destructive consequence of ageing in fire fighters' protective clothing is degradation. In terms of textiles, degradation is defined as weakening and loss of properties that are necessary for the satisfactory performance due to the changes occurring as a result of the ageing process [4].

Alexandrescu et al. [5] made investigations to obtain environmentally friendly materials for thermal protection and insulation in order to be used in the manufacture of air-tight packings, membranes, sleeves, protective cases and curtains, protective equipment for high temperature and fire hazard areas. Winterhalter et al. [3] developed low cost combat uniform fabrics that provide flame protection with combinations of Kevlar and Nomex yarns. Prior to material development, the flame threat and hazard was investigated and characterized. Jain et al. [6] stated that thermally aged Nomex fibres manifested several residual effects like reduction in X-ray crystallinity, mass loss and deterioration in tensile characteristics. They also observed surface damages in the form of longitudinal openings, holes, material deposits. Arrieta et.al. [7] studied the thermal aging of high-performance fibres used in the making of fire protective garments. They carried out accelerated thermal aging tests on fabric samples made up of a blend of Kevlar® (poly p-phenylene terephthalamide) and PBI (poly benzimidazole) staple fibres and they defined the overall aging process with a model. Parimala and Vijayan [8] and Jain and Kalyani [9] studied the loss of tensile strength after exposure to elevated temperatures of Kevlar fibers. They found experimental evidence suggesting that the decrease in tensile strength is caused by the diminished crystallinity brought about by elevated temperatures. In this study, tensile strength and mass loss degrees of fabrics made of Kevlar, Nomex and their combinations were evaluated under various aging temperatures and the results were statistically analysed.

Table 1

| PROPERTIES OF YARNS AND FABRICS USED FOR THE EXPERIMENTS | | | | | | |
|---|---|---|---|---|---|---|
| **Fabric no.** | **Weft yarn type** | **Warp yarn type** | **Weft yarn count**, *Nm* | **Warp yarn count**, *Nm* | **Weft density**, picks/cm | **Warp density**, ends/cm |
| *1* | 100% Kevlar | 100% Kevlar | 50 | 50 | 20 | 40 |
| *2* | 100% Nomex | 100 %Nomex | 50 | 50 | 20 | 40 |
| *3* | 50% Kevlar - 50% Nomex | 50% Kevlar - 50% Nomex | 50 | 50 | 20 | 40 |
| *4* | 100% Nomex | 50% Kevlar - 50% Nomex | 50 | 50 | 20 | 40 |
| *5* | 50% Kevlar - 50% Nomex | 100% Nomex | 50 | 50 | 20 | 40 |

## EXPERIMENTAL PART

### Materials used

*Nm* 50 Kevlar and Nomex yarns were used in various combinations for the woven fabric production. Plain woven fabric structure was chosen for the experiments since most Kevlar fabrics for ballistic and body protection purposes are plain woven [7]. The properties of yarns used in fabrics, weft and warp densities for each fabric type were given in table 1.

### Thermal aging treatments

Samples of all fabric types were prepared for both warp and weft direction in the size of 70 x 350 mm$^2$. Samples were kept for selected durations in the oven in a hanging position and with a distance from the oven walls.

The temperature domain for the accelerated aging tests should reflect the real temperatures encountered by fire fighters while in service. The exposure conditions faced by fire fighters have been classified in three categories depending on temperatures and heat flux: routine (up to 60°C and/or 2.1 kW/m$^2$), hazardous (up to 300°C and/or 10 kW/m$^2$), and emergency (above 300°C and/or 10 W/m$^2$) [10]. Thus, the aging temperatures of 220°C and 300°C were selected considering the tabulated continuous operating temperatures of respectively, 260°C and 200°C for Kevlar and Nomex® as well as the 100–300°C standard conditions reported for fire fights in operation.

The durations of cumulative exposures were 2, 10, 20, 30 days for 220°C and 1, 2, 5, 10 days for 300°C. The durations of exposure for 300°C were selected shorter than the periods for 220°C, since effects of aging on the mass loss and strength were observed faster at high temperatures.

### Mass loss

Fabric weights were measured before aging process and after each selected exposure period. Tests were performed on conditioned fabric samples under standard atmospheric conditions (20 ± 2ºC temperature and 65% ± 2 relative humidity). Percentage variation in weight (*%wl*) accompanying thermal ageing was estimated as:

$$\%wl = (\Delta w/w_0) \times 100 \quad (1)$$

where $\Delta w = w_0 - w_{heat\ treated}$, $w_0$ and $w_{heat\ treated}$ are the weights of samples prior to and after heat treatment, respectively.

### Mechanical testing

Breaking force was selected as the parameter to quantify the advance of the aging process. The samples, which were cut in the dimensions of 70 mm x 350 mm, were ravelled to give a test width of 50 mm and later the tensile properties were performed with Zwick/Roell Z010 universal testing machine equipped with 10 kN load cell and operated at a cross-head speed of 100 mm/minute, according to the ISO 13934-1 standard test method. For each fabric type, three replicates were measured.

### Experimental design

Statistical calculations were done using Minitab Release 14 program. The effect of two variables (fabric type and time) on thermal aging was investigated according to full factorial experimental design with three replicates. Five levels were selected for fabric type and four levels were selected for time. Thermal aging at 220°C and 300°C were assessed separately for each fabric direction (weft and warp). The levels are given in table 2 and table 3.

Table 2

| THE LEVELS OF FABRIC TYPE AND TIME FOR THERMAL AGING AT 220ºC | | | | | |
|---|---|---|---|---|---|
| **Factor** | Range and level of values | | | | |
| **Fabric type** | 1 | 2 | 3 | 4 | 5 |
| **Time** | 48 | 240 | 480 | 720 | |

Table 3

| THE LEVELS OF FABRIC TYPE AND TIME FOR THERMAL AGING AT 300ºC | | | | | |
|---|---|---|---|---|---|
| **Factor** | Range and level of values | | | | |
| **Fabric type** | 1 | 2 | 3 | 4 | 5 |
| **Time** | 24 | 48 | 120 | 240 | |

Table 4

| AVERAGE MASS LOSS PERCENTAGES (%) AFTER THERMAL AGING AT 220ºC | | | | | | | | |
|---|---|---|---|---|---|---|---|---|
| Fabric type | 48 hours | | 240 hours | | 480 hours | | 720 hours | |
| | Weft direction | Warp direction | Weft direction | Warp direction | Weft direction | Warp direction | Weft direction | Warp direction |
| 1 | 4.29 | 4.07 | 4.51 | 4.26 | 4.95 | 5.06 | 5.12 | 5.40 |
| 2 | 3.51 | 3.43 | 3.72 | 3.67 | 3.75 | 3.91 | 4.38 | 4.32 |
| 3 | 3.92 | 3.47 | 4.15 | 4.25 | 4.29 | 4.22 | 4.44 | 4.48 |
| 4 | 3.03 | 3.76 | 3.89 | 3.88 | 3.92 | 3.90 | 3.99 | 3.95 |
| 5 | 3.45 | 3.8 | 3.67 | 3.87 | 4.05 | 4.31 | 4.47 | 4.53 |

Table 5

| AVERAGE MASS LOSS PERCENTAGES (%) AFTER THERMAL AGING AT 300ºC | | | | | | | | |
|---|---|---|---|---|---|---|---|---|
| Fabric type | 24 hours | | 48 hours | | 120 hours | | 240 hours | |
| | Weft direction | Warp direction | Weft direction | Warp direction | Weft direction | Warp direction | Weft direction | Warp direction |
| 1 | 4.01 | 3.98 | 4.20 | 4.02 | 7.21 | 6.81 | 9.33 | 8.99 |
| 2 | 3.12 | 3.12 | 3.19 | 3.15 | 4.63 | 4.50 | 5.04 | 4.92 |
| 3 | 3.98 | 4.03 | 4.86 | 4.79 | 5.22 | 5.08 | 6.46 | 6.72 |
| 4 | 4.56 | 4.86 | 4.68 | 5.04 | 5.10 | 5.43 | 6.76 | 6.41 |
| 5 | 4.14 | 3.98 | 4.25 | 4.72 | 5.15 | 5.07 | 6.13 | 5.64 |

## RESULTS AND DISCUSSIONS

### Mass loss after thermal aging

Prior to tensile testing, mass loss percentages were measured at standard atmosphere conditions from samples being exposed to heat for several hours. The results were showed in table 4 and table 5 for 220°C and 300°C respectively. Average mass loss percentages varied in the range of 3.03 and 8.99%.

In order to test the significance of factors, Analysis of Variance (ANOVA) is used. The *p* value is the indicator of the significance of the test. If the *p* value is below 0.05, it indicates that the test parameter is significant at 5% level of significance. This analysis showed that fabric type and time are both statistically significant since *p* value is less than 0.05. However the statistical analysis showed that the interaction among two factors was insignificant in every case except in weft direction at 300°C.

$R^2$ is the determination coefficient (square of the correlation coefficient) between the dependent variable mass loss and independent variables fabric type and time. With respect to table 6 and table 8, it is seen that $R^2$ increased when the temperature increases from 220°C to 300°C. Similar relation is seen between table 7 and table 9. On the other side, $R^2$ values are not high enough in warp directions. This means that the relationship between mass loss and the factors (fabric type and time) is stronger in the weft direction.

Factors that influence the mass loss after thermal aging were evaluated by using factorial plots; main effects and interactions. Main effects of each parameter (fabric type and time) on mass loss after thermal aging are displayed in figures 1–4.

As can be seen from these figures, mass loss reached to the maximum value for both directions

Table 6

| ANOVA FOR MASS LOSS IN WEFT DIRECTION AT 220ºC | | | | | | |
|---|---|---|---|---|---|---|
| Source | DF | Seq SS | Adj SS | Adj MS | F | P |
| Fabric type | 4 | 7.74656 | 7.74656 | 1.93664 | 28.18 | 0.000 |
| Time | 3 | 5.63223 | 5.63223 | 1.87741 | 27.32 | 0.000 |
| Interaction | 12 | 1.08279 | 1.08279 | 0.09023 | 1.31 | 0.250 |
| Error | 40 | 2.74927 | 2.74927 | 0.06873 | - | - |
| Total | 59 | 17.21084 | - | - | - | - |

$R^2$ = 84.03%

Table 7

| ANOVA FOR MASS LOSS IN WARP DIRECTION AT 220ºC | | | | | | |
|---|---|---|---|---|---|---|
| **Source** | *DF* | *Seq SS* | *Adj SS* | *Adj MS* | *F* | *P* |
| **Fabric type** | 4 | 5.7176 | 5.7176 | 1.4294 | 6.47 | 0.000 |
| **Time** | 3 | 5.7777 | 5.7777 | 1.9259 | 8.72 | 0.000 |
| **Interaction** | 12 | 2.0044 | 2.0044 | 0.1670 | 0.76 | 0.689 |
| **Error** | 40 | 8.8341 | 8.8341 | 0.2209 | - | - |
| **Total** | 59 | 22.3338 | - | - | - | - |

$R^2$ = 60.45%

Table 8

| ANOVA FOR MASS LOSS IN WEFT DIRECTION AT 300ºC | | | | | | |
|---|---|---|---|---|---|---|
| **Source** | *DF* | *Seq SS* | *Adj SS* | *Adj MS* | *F* | *P* |
| **Fabric type** | 4 | 29.7721 | 29.7721 | 7.4430 | 32.17 | 0.000 |
| **Time** | 3 | 72.9929 | 72.9929 | 24.3310 | 105.17 | 0.000 |
| **Interaction** | 12 | 20.9810 | 20.9810 | 1.7484 | 7.56 | 0.000 |
| **Error** | 40 | 9.2540 | 9.2540 | 0.2313 | - | - |
| **Total** | 59 | 133.0000 | - | - | - | - |

$R^2$ = 93.04%

Table 9

| ANOVA FOR MASS LOSS IN WARP DIRECTION AT 300ºC | | | | | | |
|---|---|---|---|---|---|---|
| **Source** | *DF* | *Seq SS* | *Adj SS* | *Adj MS* | *F* | *P* |
| **Fabric type** | 4 | 27.3208 | 27.3208 | 6.8302 | 6.86 | 0.000 |
| **Time** | 3 | 58.9785 | 58.9785 | 19.6595 | 19.75 | 0.000 |
| **Interaction** | 12 | 21.7607 | 21.7607 | 1.8134 | 1.82 | 0.077 |
| **Error** | 40 | 39.8161 | 39.8161 | 0.9954 | - | - |
| **Total** | 59 | 147.8761 | - | - | - | - |

$R^2$ = 73.07%

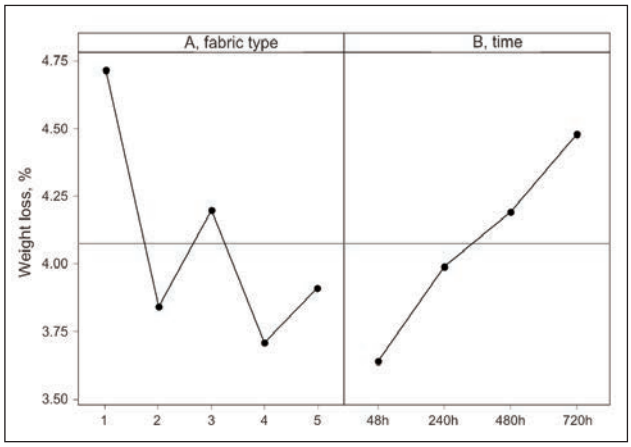


Fig. 1. Main effects diagram for weight loss in weft direction at 220ºC

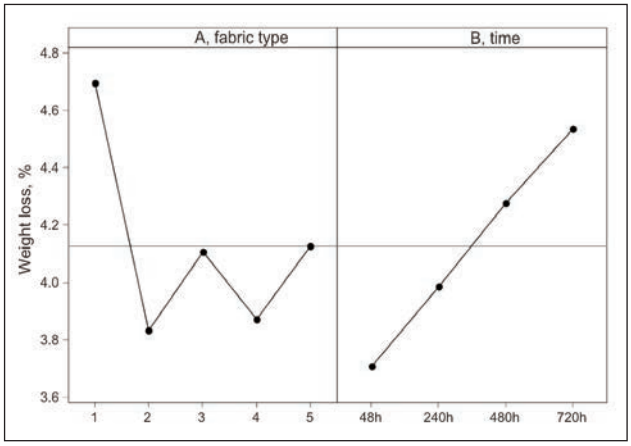


Fig. 2. Main effects diagram for weight loss in warp direction at 220ºC

(weft and warp) in fabric type *1*. The effect of thermal aging was minimum in fabric type *4* in weft direction at 220°C. On the other hand, minimum loss was observed in fabric type *2* in warp direction at 220°C and in both directions at 300°C. As the time that samples exposed to heat increased, the amount of mass loss increased.

An interactions plot is a plot of means for each level of a factor with the level of a second factor held constant. Interactions plots are useful for judging the

presence of interactions, which means that the difference in the response at two levels of one factor depends upon the level of another factor. Parallel lines in an interactions plot indicate no interaction. The greater the departure of the lines from being parallel, the higher the interaction degree. To use an interaction plot, data must be available from all combinations of levels.

Figures 5–8 show the plots of interaction. At 220°C in weft and warp direction fabric types *2, 4* and *5* intersected each other (fig. 5 and fig. 6). However, at 300°C fabric type *2* run parallel to others in both

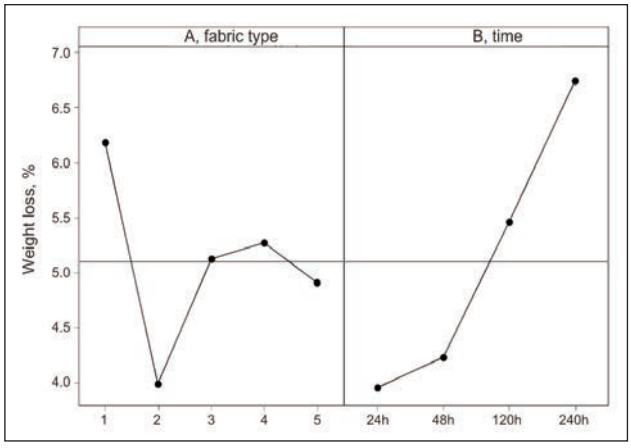


Fig. 3. Main effects diagram for weight loss in weft direction at 300ºC

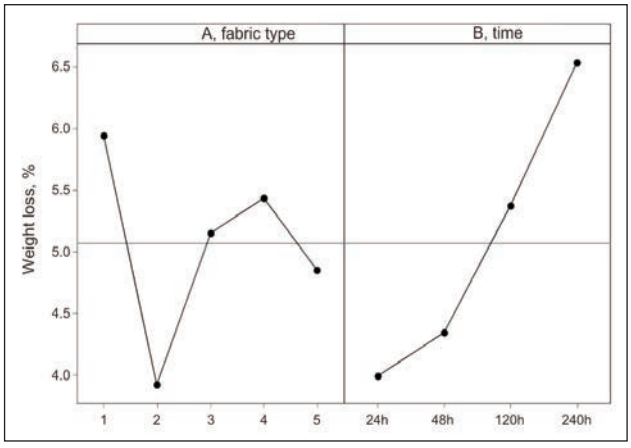


Fig. 4. Main effects diagram for weight loss in warp direction at 300ºC

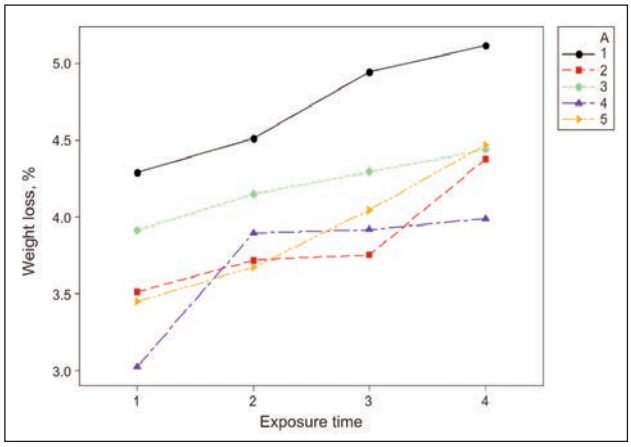


Fig. 5. Interaction diagram for weight loss in weft direction at 220ºC

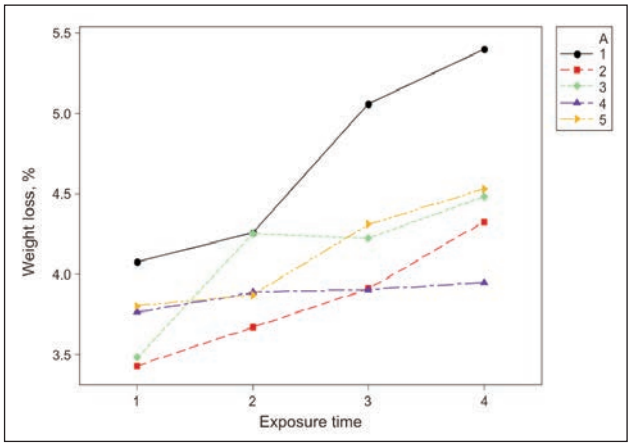


Fig. 6. Interaction diagram for weight loss in warp direction at 220ºC

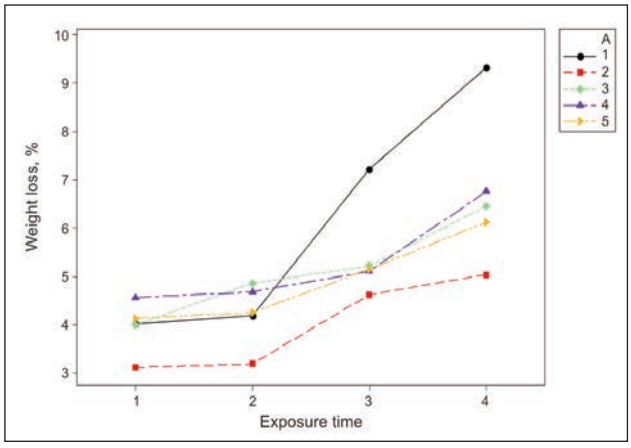


Fig. 7. Interaction diagram for weight loss in weft direction at 300ºC

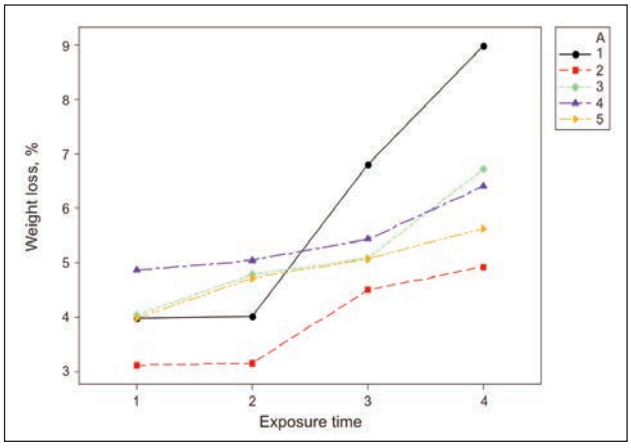


Fig. 8. Interaction diagram for weight loss in warp direction at 300ºC

Table 10

| AVERAGE TENSILE STRENGTH LOSS PERCENTAGES (%) AFTER THERMAL AGING AT 220ºC | | | | | | | | |
|---|---|---|---|---|---|---|---|---|
| Fabric type | 48 hours | | 240 hours | | 480 hours | | 720 hours | |
| | Weft direction | Warp direction | Weft direction | Warp direction | Weft direction | Warp direction | Weft direction | Warp direction |
| 1 | 68.52 | 55.54 | 86.69 | 78.68 | 88.78 | 85.34 | 94.41 | 89.37 |
| 2 | 0.43 | 2.61 | 1.34 | 3.11 | 2.64 | 3.28 | 2.73 | 4.21 |
| 3 | 14.06 | 42.88 | 17.52 | 55.26 | 17.60 | 55.96 | 18.25 | 56.56 |
| 4 | 23.90 | 1.92 | 25.09 | 3.90 | 25.13 | 4.92 | 25.71 | 6.40 |
| 5 | 1.89 | 44.09 | 3.99 | 51.12 | 5.43 | 52.28 | 5.76 | 54.19 |

Table 11

| AVERAGE TENSILE STRENGTH LOSS PERCENTAGES (%) AFTER THERMAL AGING AT 300ºC | | | | | | | | |
|---|---|---|---|---|---|---|---|---|
| Fabric type | 24 hours | | 48 hours | | 120 hours | | 240 hours | |
| | Weft direction | Warp direction | Weft direction | Warp direction | Weft direction | Warp direction | Weft direction | Warp direction |
| 1 | 55.79 | 51.46 | 68.66 | 59.97 | 93.42 | 88.70 | 95.16 | 94.82 |
| 2 | 0.16 | 0.58 | 0.55 | 2.73 | 0.57 | 3.00 | 2.25 | 5.94 |
| 3 | 15.92 | 52.11 | 16.19 | 55.19 | 16.30 | 56.85 | 19.36 | 58.93 |
| 4 | 23.07 | 0.91 | 23.53 | 2.27 | 24.02 | 3.73 | 25.94 | 10.47 |
| 5 | 2.65 | 50.81 | 3.10 | 51.27 | 3.85 | 54.47 | 5.69 | 54.78 |

directions, in other words fabric type *2* disrupted the interaction (fig. 7 and fig. 8). When all four graphs were examined, it was obviously seen that the increase in mass loss was greater when fabric type *1* was used.

## Strength loss after thermal aging

After mass loss measurements, the samples being exposed to thermal aging were tested to evaluate their strengths. Reductions in tensile strength were represented as percentage in table 10 and table 11. Average tensile loss percentages varied in a wide range. Minimum decrease was observed in fabric type *2* as 0.16% while maximum decrease was observed in fabric type *1* as 94.82%.

Since the p values in the ANOVA table are less than 0.05, there is a statistically significant relationship between the variables at the 95% confidence level (tables 12–15). The $R^2$ value indicates how much variability in the observed response values can be explained by the factors and their interactions. $R^2$ values stated in tables 12–15 are all over 0.98. This implies that 98% of the variations for tensile strength loss after thermal aging are explained by the independent variables.

Main effects and interactions plots were used to evaluate the factors that influence tensile loss after thermal aging. Main effects of each parameter (fabric type and time) on tensile strength loss after thermal aging were showed in figures 9–12. Generally, minimum tensile strength loss was observed in fabric type *2*, whereas maximum reduction was observed in fabric type *1*. Only at 300ºC maximum strength loss values were very close for fabric types *3, 4* and *1* in

Table 12

| ANOVA FOR TENSILE STRENGTH LOSS IN WEFT DIRECTION AT 220ºC | | | | | | |
|---|---|---|---|---|---|---|
| **Source** | *DF* | *Seq SS* | *Adj SS* | *Adj MS* | *F* | *P* |
| **Fabric type** | 4 | 55 495.5 | 55 495.5 | 1 3873.9 | 804.83 | 0.000 |
| **Time** | 3 | 1 717.8 | 1 717.8 | 572.6 | 33.22 | 0.000 |
| **Interaction** | 12 | 476.7 | 476.7 | 39.7 | 2.30 | 0.024 |
| **Error** | 40 | 689.5 | 689.5 | 17.2 | - | - |
| **Total** | 59 | 58 379.6 | - | - | - | - |

$R^2$ = 98.82%

Table 13

| ANOVA FOR TENSILE STRENGTH LOSS IN WARP DIRECTION AT 220ºC | | | | | | |
|---|---|---|---|---|---|---|
| **Source** | *DF* | *Seq SS* | *Adj SS* | *Adj MS* | *F* | *P* |
| **Fabric type** | 4 | 58 602.8 | 58 602.8 | 14 650.7 | 979.88 | 0.000 |
| **Time** | 3 | 2 382.4 | 2 382.4 | 794.1 | 53.11 | 0.000 |
| **Interaction** | 12 | 1 002.7 | 1 002.7 | 83.6 | 5.59 | 0.000 |
| **Error** | 40 | 598.1 | 598.1 | 15.0 | - | - |
| **Total** | 59 | 62 585.9 | - | - | - | - |

$R^2$ = 99.04%

Table 14

| ANOVA FOR TENSILE STRENGTH LOSS IN WEFT DIRECTION AT 300ºC | | | | | | |
|---|---|---|---|---|---|---|
| **Source** | *DF* | *Seq SS* | *Adj SS* | *Adj MS* | *F* | *P* |
| **Fabric type** | 4 | 54 421.9 | 54 421.9 | 13 605.5 | 1 5149.17 | 0.000 |
| **Time** | 3 | 2 255.0 | 2 255.0 | 751.7 | 63.49 | 0.000 |
| **Interaction** | 12 | 1 899.3 | 1 899.3 | 158.3 | 13.37 | 0.000 |
| **Error** | 40 | 473.6 | 473.6 | 11.8 | - | - |
| **Total** | 59 | 59 049.8 | - | - | - | - |

$R^2$ = 99.20%

Table 15

| ANOVA FOR TENSILE STRENGTH LOSS IN WARP DIRECTION AT 300ºC | | | | | | |
|---|---|---|---|---|---|---|
| **Source** | *DF* | *Seq SS* | *Adj SS* | *Adj MS* | *F* | *P* |
| **Fabric type** | 4 | 61 368.5 | 61 368.5 | 15 342.1 | 2 863.57 | 0.000 |
| **Time** | 3 | 3 338.5 | 3 338.5 | 1 112.8 | 207.71 | 0.000 |
| **Interaction** | 12 | 2 353.6 | 2 353.6 | 196.1 | 36.61 | 0.000 |
| **Error** | 40 | 214.3 | 214.3 | 5.4 | - | - |
| **Total** | 59 | 67 274.9 | - | - | - | - |

$R^2$ = 99.68%

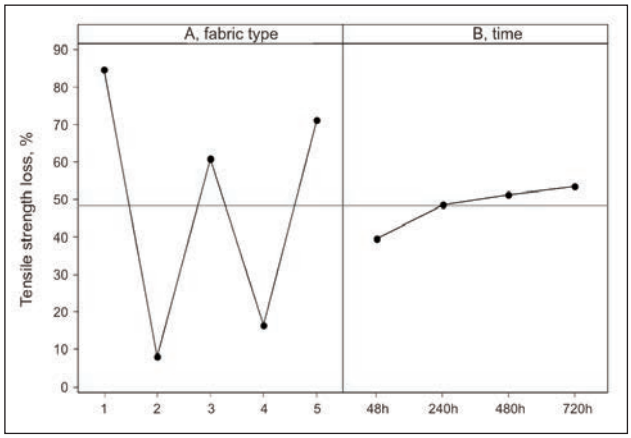


Fig. 9. Main effects diagram for tensile strength loss in weft direction at 220ºC

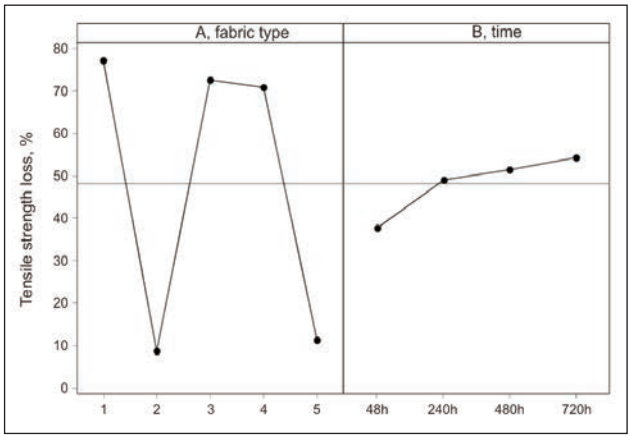


Fig. 10. Main effects diagram for tensile strength loss in warp direction at 220ºC

warp direction. Also the main effects diagrams indicated that tensile strength loss increased with the increase of heat exposure time.

Interaction diagrams were given in figures 13–16. These plots showed apparent interaction because the lines do not have the same tendency, implying that the effect of time upon tensile strength loss output depended upon the fabric type. These results were also compatible with the values given in tables 12–15.

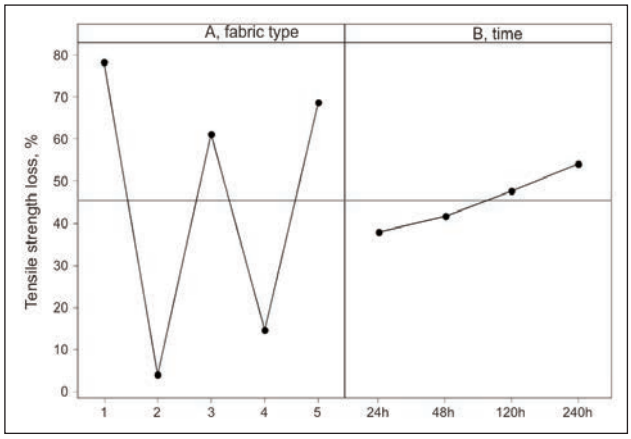


Fig. 11. Main effects diagram for tensile strength loss in weft direction at 300ºC

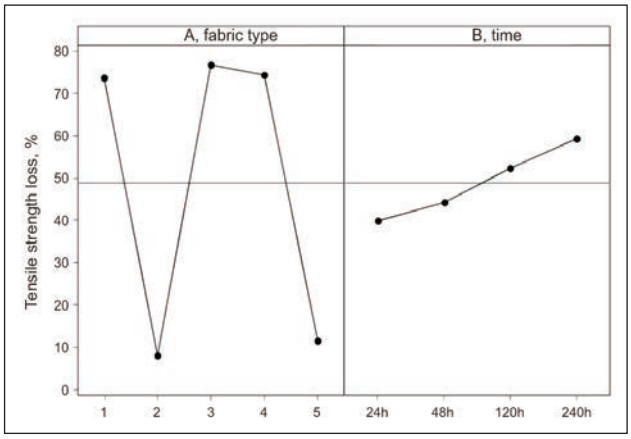


Fig. 12. Main effects diagram for tensile strength loss in warp direction at 300ºC

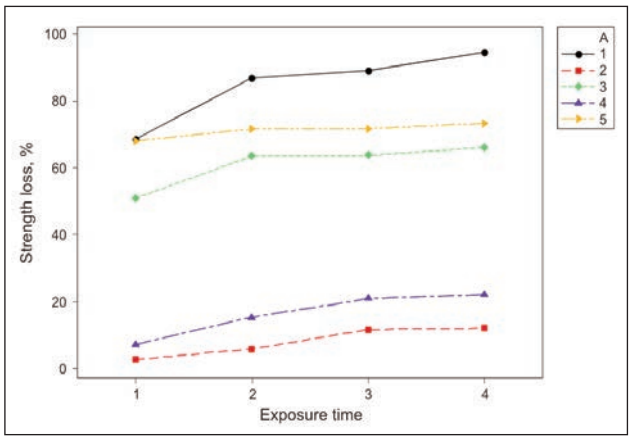


Fig. 13. Interaction diagram for tensile strength loss in weft direction at 220ºC

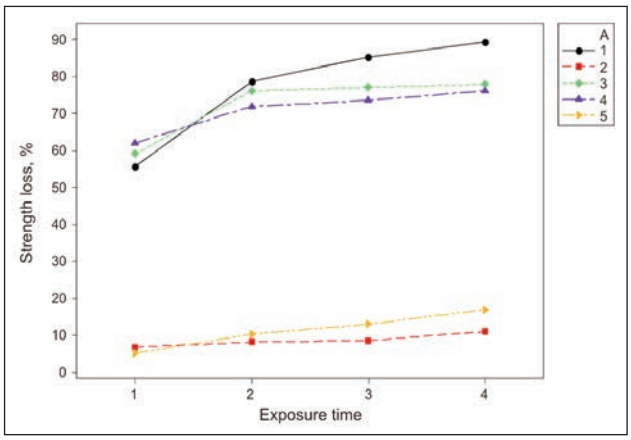


Fig. 14. Interaction diagram for tensile strength loss in warp direction at 220ºC

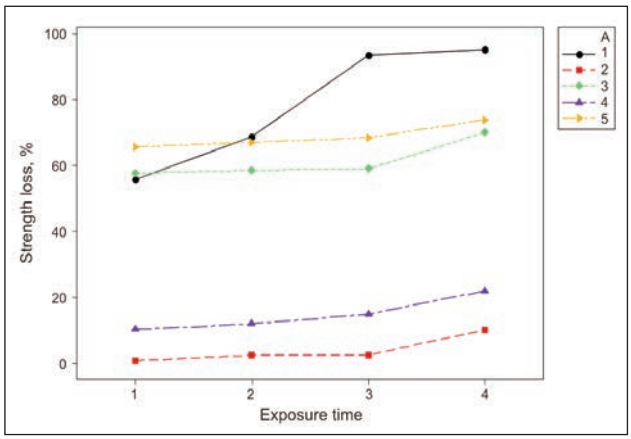


Fig. 15. Interaction diagram for tensile strength loss in weft direction at 300ºC

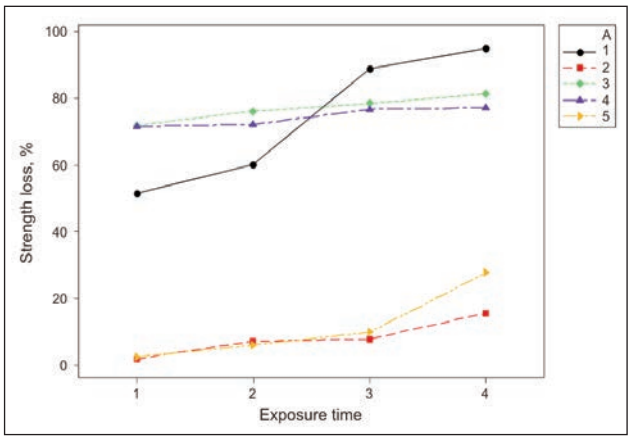


Fig. 16. Interaction diagram for tensile strength loss in warp direction at 300ºC

## CONCLUSIONS

Protective clothings are exposed to environmental conditions such as flame and elevated temperature. The performance of protective clothing has a significant influence on the level of protection provided. In this study, woven fabrics produced from various combinations of Kevlar and Nomex yarns were exposed to 220°C and 300°C for duration ranging from 24 hours to 30 days to investigate the effects of thermal aging. Mass loss and tensile strength values of fabrics were measured before and after exposure and results were statistically analysed.

The study revealed that the structure and properties of specimens changed in a similar manner after each

thermal exposure, but the magnitude of changes varied with both temperature and cumulative duration of exposure. The changes in the specimens observed at higher temperatures and shorter durations were similar to the changes observed at lower temperatures and longer duration. As temperature increased, the percentage of mass loss was also increased. It was also concluded that material type had an effect on mass loss results. According to the test results, highest mass loss values were achieved for 100% Kevlar fabrics for both temperatures. Percentage of mass loss was decreased when amount of Nomex yarns used in fabric production was increased.

The effect of thermal exposure on tensile strength was dependent on the fabric type, temperature and exposure duration. Highest strength loss was also measured for 100% Kevlar fabrics for both temperatures. The percentage of strength loss for 100% Kevlar was about 95%, while this value was calculated as 4% for 100% Nomex fabrics.

## BIBLIOGRAPHY


[1] *Technical Guide – Kevlar aramid fiber*. Dupont Advanced Fibers Systems, USA

[2] *Technical Guide for NOMEX brand fibers*. Dupont Advanced Fibers Systems, USA

[3] Winterhalter, C. A., Lomba, R. A., Tucker, D. W., Martin, O. D. *Novel approach to soldier flame protection*. In: Journal of ASTM International, 2005, vol. 2, issue 2, pp. 1-8

[3] Rezazadeh, M., Torvi, D. A. *Assessment of factors affecting the continuing performance of firefighters' protective clothing: a literature review*. In: Fire Technology, 2011, vol. 47, pp. 565–599

[4] Alexandrescu, L., Popa, M., Georgescu, M., Leca, M. *Development of new processes intended to obtain fireproof non-asbestos textiles covered with nanodispersions based on modified polychloroprene elastomers*. In: Industria Textilă, 2013, vol. 64, issue 5, pp. 277-284

[5] Jain, A., Vijayan, K. *Thermally induced structural changes in Nomex fibres*. In: Bulletin of Material Science, 2002, vol. 25, issue 4, pp. 341-346

[6] Arrieta, C., David, E., Dolez, P., Khanh, T. *Thermal aging of a blend of high-performance fibers*. In: Journal of Applied Polymer Science, 2010, vol. 115, pp. 3 031–3 039

[7] Parimala, H. V., Vijayan, K. *Effect of thermal exposure on the tensile properties of Kevlar fibres*. In: Journal of Material Science Letters, 1993, issue 12, pp. 99-101

[8] Jain, A., Kalyani, V. *Thermal aging of Twaron fibers*. In: High Performance Polymers, 2003, issue 15, pp. 105-129

[9] Rossi, R. *Fire fighting and its influence on the body*. In: Ergonomics, 2003, vol. 46, pp. 1 017-1 033



**Authors:**

BANU OZGEN
GULSAH PAMUK
Ege University Emel Akın Vocation School
Izmir, Turkey
e-mail: banu.ozgen@ege.edu.tr

**Corresponding author:**
GULSAH PAMUK
e-mail: gulsah.pamuk@ege.edu.tr


# The frictional and lint shedding characteristics of regenerated cellulosic yarns

GONCA ÖZÇELİK KAYSERİ


## REZUMAT – ABSTRACT

**Proprietăţile de frecare şi formare a scamelor de pe firele din celuloză regenerată**

*Pe lângă parametrii tradiţionali ai firelor precum uniformitatea, neregularitatea, rezistenţa şi alungirea, frecarea joacă un rol important în ceea ce priveşte calitatea şi eficienţa prelucrării firelor deoarece acestea sunt supuse frecării de tip fir-fir şi fir-metal de mai multe ori în timpul producţiei. Ca efect perturbator al frecării, procesul de formare a scamelor apare în timpul producţiei şi trebuie ţinut sub control pentru a reduce defectele de prelucrare şi pentru a creşte eficienţa producţiei. Această lucrare prezintă un studiu al celor mai importante caracteristici care afectează condiţiile de producţie prin utilizarea a trei generaţii de fire din celuloză regenerată (100% viscoză, 100% fibră modală, 100% Lyocell) în trei categorii diferite de fineţe a firului (60 tex, 30 tex, 20 tex) şi trei coeficienţi diferiţi de torsiune a firului ($\alpha_e$=3, $\alpha_e$=3.5, $\alpha_e$=4). Proprietăţile de frecare de tip fir-fir ($\mu_{YY}$), fir-metal ($\mu$YM) şi de formare a scamelor (LF) în cazul acestor fire au fost determinate cu ajutorul instrumentului Constant Tension Transport. Au fost evaluate din punct de vedere statistic rezultatele coeficientului de frecare şi valorile factorului de determinare a scămoşării. Rezultatele au arătat că natura firului şi densitatea liniară a firului au un efect deosebit de important asupra proprietăţilor de frecare şi de formare a scamelor de pe fire, în timp ce coeficientul de torsiune a firului influenţează numai valorile coeficientului de frecare fir-fir.*

*Cuvinte-cheie: formarea scamelor, frecare de tip fir-fir, frecare de tip fir-metal, lyocell, fibră modală, viscoză*

**The frictional and lint shedding characteristics of regenerated cellulosic yarns**

*Besides the traditional yarn parameters such as evenness, imperfection, strength and elongation, the friction plays an important role in yarn quality and processing efficiency since the yarns are subjected to friction between the yarns or against metal surfaces several times during production. As a disturbing effect of friction, lint shedding occurs during production and it should be also kept under control in order to reduce the processing faults and to increase the production efficiency.*

*The present paper reports a study on these important features affecting the production conditions by using three generations of regenerated cellulosic yarns (100% viscose, 100% modal, 100% lyocell) in three different yarn counts (60 tex, 30 tex, 20 tex) and three different yarn twist coefficients ($\alpha_e$=3, $\alpha_e$=3.5, $\alpha_e$=4). Yarn-to-yarn friction ($\mu_{YY}$), yarn-to-metal friction ($\mu_{YM}$) and lint shedding (LF) characteristics of these yarns were determined by Constant Tension Transport instrument. The friction coefficient results and lint factor values were evaluated statistically. The results have revealed that yarn material and yarn linear density have significant effect on the frictional and lint shedding features of the yarns whereas yarn twist coefficient has influence only on the yarn-to-yarn friction coefficient values.*

*Key words: lint shedding, yarn-to-yarn friction, yarn-to-metal friction, lyocell, modal, viscose*


The demand for higher manufacturing speeds and the constantly growing quality requirements in production call for the exact knowledge of fiber characteristics. The friction behaviours of fibers and yarns are considered as key parameters in many processes and arise from interaction between two surfaces. During the knitting and weaving process, the moving yarn is flexed, turned and pressed to machinery parts having various curved surfaces. As reaction, yarn tension and therefore yarn-to-yarn and yarn-to-metal friction increase [1, 2, 3].

Lint shedding is also one of the parameters that should be under control to reduce processing faults and to increase production efficiency. As the production speeds in textile industry increase, fluff, an accumulation of loose fibers detached from the yarn body becomes a major cause leading to serious process troubles [4].

Measurement of yarn friction can help to improve the several properties in subsequent processes such as in spinning process (influencing the strength of yarns, increasing the wear of guides, determining the tensions developed in fiber and yarn handling equipment, determining optimum wax type, minimization of friction variations between cones), in knitting process (ensuring constant quality, reducing breaks and down time, reducing fly, increasing needle lifetime), in weaving process (affecting the shear, formability and handle of woven fabrics), in finishing process (selection of the right finishing agents) [5–8].

There have been several studies on the effects of the fiber and yarn properties and also the production conditions on the frictional characteristics of yarns. Čiukas and Svetnickienė performed an experiment on the friction properties of flax, bamboo, bamboo-flax, soy, cotton-sea cell yarns. The highest friction ratio belonged to the flax yarns whereas the lowest values were obtained from soy yarns [2].

Chattopadhyay et al. found that the increase in twist of yarn led to a reduction in the frictional force of both

ring and rotor spun yarns. The ring spun yarn and finer yarns were found to have a higher frictional force [8, 9]. Kilic and Sülar obtained the lowest yarn to yarn friction coefficient values from vortex yarns and the highest values were found with ring yarns. The highest yarn to metal and yarn to ceramic friction coefficients were observed from vortex yarns and the lowest values were generally obtained from compact yarns. Yarn-to-yarn friction coefficient decreased while yarn-to-metal and yarn-to-ceramic friction coefficients increased for all of the input tensions with the increasing ratio of tencel LF [10]. According to the study conducted by Ghosh et.al, OE friction yarns showed maximum friction followed by rotor, air-jet, and ring spun yarns; however, a reverse order was noticed for yarn to metal friction [7]. Ramkumar et al. mentioned the influence of the fiber type and tension applied on the friction values [11]. Altas et al. investigated the relation between friction and physical properties of carded and combed ring spun yarns. It was found that with the higher yarn diameter and yarn hairiness, yarn-to-metal friction coefficient values decreased but didn`t have any effect on the yarn-to-yarn friction coefficient values. The effect of yarn twist was not obvious according to the results [12].

The study of fly generation during manufacturing has also attracted the attention of many researchers for decades and especially due to the legal regulations requiring a clean working environment for employees, its importance has been gradually increasing. Excessive lint indicates fiber loss, which reduces the strength of the yarn. It also creates problems for fabric production machines, working environment and appears as defects on the fabric. Most of the researches have revealed that lint generation is caused by the fiber properties and is also related to the processing parameters during the production of the fabric. However the main reason for fluff formation is the friction between yarn and knitting elements that occurs where the moving yarn passes over machine parts. Among all fiber properties, the fiber length has the greatest effect on the amount of fly generated. The spun yarns produced by various spinning technologies differ significantly from each other in their surface characteristics and therefore in frictional features. In production of yarns, blending with a synthetic fiber also reduces the fly generation due to an increase in the fiber mean length. Additionally, yarn moisture content, production speed, input tension and the number of rollers on the machine are crucially important in terms of fly generation. Trials to reduce the fluff trouble by using chemicals or installing suction units to the different parts of the machines are also suggested [4, 7,13–18].

With the growing demand for more comfortable, healthier and environmentally friendly products, efforts in research and development activities in the textile industry have focused on the utilization of renewable and biodegradable resources as well as environmentally friendly manufacturing processes in textiles. In this aspect, new kinds of regenerated fibers, which are alternative to conventional ones have gained importance in apparel and home textile manufacturing [19]. Although all regenerated cellulosic fibers have the same chemical composition, they differ in density, molecular mass, degree of polymerization, super molecular arrangement, degree of crystallinity, orientation and also in physical characteristics [20]. Viscose was the first generation of these cellulosic fibers. The distinguishing property of viscose is its low wet strength. As a result, it becomes unstable and may stretch or shrink in wet conditions. Modal is the second generation, high wet modulus (HWM) rayon which has virtually the same properties as regular viscose plus high wet strength and softness. Lyocell is the third generation fiber and its advantages include environmental friendliness of the chemical processing combined with its softness, drape, and resistance to growth of bacteria which create odors. In recent years, regenerated cellulosic fibers bear valuable properties and the usage of these fibers in different products is constantly increasing.

There are many studies dealing with the frictional and lint shedding features of various kinds of yarns. However, there is not a detail and comparative study on the frictional and lint shedding characteristics of these three generations of regenerated cellulosic yarns. Therefore in this study, the frictional and lint generation characteristics of most commonly used regenerated cellulosic yarns made from viscose, modal and lyocell fibers are investigated.

## EXPERIMENTAL PART

### Material

In order to investigate the effect of the parameters such as yarn material type (100% viscose, 100% modal and 100% lyocell), yarn linear density (60 tex, 30 tex, 20 tex) and yarn twist coefficient ($\alpha_e$=3, $\alpha_e$=3.5, $\alpha_e$=4) on the yarn-to-yarn, yarn-to-metal friction coefficient values and lint shedding characteristics, 27 yarns were produced. Fiber linear density used in the production of all yarns was 1.7 dtex and fiber staple length was 38 mm. Yarn production was carried out in Pinter Merlin Spa ring spinning machine with the spindle speed of 8000 rev/min and at the same production conditions for all yarn types.

The basic physical properties of the yarns such as mass coefficient of variation (CVm), diameter (D), diameter variation (CV (D)), hairiness (H) and hairiness coefficient of variation (CV (H)) values were measured by USTER TESTER 5 S800 evenness tester, as given in table 1.

### Testing method and equipment

The measurements of yarn-to-yarn friction coefficient and yarn-to-metal friction coefficient tests were carried out by using CTT Dynamic Friction Tester and the lint amount of the yarns were determined by CTT Lint Generation Tester by changing the test module of Lawson Hemphill Constant Tension Transport instrument as given in figure 1. Since fiber testing instruments are mainly developed in United States, ISO standards do not exist and ASTM standards are

Table 1

| BASIC PHYSICAL PROPERTIES OF THE PRODUCED YARNS | | | | | | | |
|---|---|---|---|---|---|---|---|
| **Yarn material** | **Yarn twist coefficient** | **Yarn linear density** | **$CV_m$** | **D** | **CV (D)** | **H** | **CV (H)** |
| **Viscose** | $\alpha_e$=3 | 60 tex | 9.6 | 0.379 | 1.15 | 10.10 | 2.30 |
| | | 30 tex | 10.3 | 0.263 | 1.33 | 6.97 | 2.73 |
| | | 20 tex | 12.9 | 0.211 | 1.71 | 6.27 | 4.39 |
| | $\alpha_e$=3.5 | 60 tex | 8.5 | 0.352 | 2.25 | 8.90 | 7.95 |
| | | 30 tex | 10.6 | 0.243 | 1.85 | 5.75 | 7.60 |
| | | 20 tex | 12.3 | 0.197 | 0.78 | 4.73 | 2.43 |
| | $\alpha_e$=4 | 60 tex | 8.6 | 0.330 | 0.76 | 7.11 | 2.33 |
| | | 30 tex | 10.2 | 0.232 | 0.00 | 4.64 | 2.99 |
| | | 20 tex | 11.9 | 0.186 | 0.31 | 4.21 | 5.97 |
| **Modal** | $\alpha_e$=3 | 60 tex | 8.8 | 0.358 | 0.58 | 10.25 | 2.26 |
| | | 30 tex | 10.6 | 0.246 | 1.31 | 7.10 | 8.97 |
| | | 20 tex | 13.3 | 0.196 | 0.68 | 6.35 | 3.27 |
| | $\alpha_e$=3.5 | 60 tex | 8.8 | 0.337 | 1.29 | 9.56 | 7.49 |
| | | 30 tex | 10.4 | 0.235 | 0.88 | 6.52 | 10.6 |
| | | 20 tex | 12.5 | 0.187 | 0.00 | 5.16 | 6.60 |
| | $\alpha_e$=4 | 60 tex | 8.8 | 0.320 | 0.90 | 8.21 | 5.90 |
| | | 30 tex | 10.7 | 0.224 | 1.36 | 5.39 | 2.07 |
| | | 20 tex | 12.3 | 0.182 | 2.01 | 4.72 | 6.42 |
| **Lyocell** | $\alpha_e$=3 | 60 tex | 9.9 | 0.366 | 1.77 | 13.8 | 12.3 |
| | | 30 tex | 11.7 | 0.246 | 0.19 | 8.56 | 7.92 |
| | | 20 tex | 15.6 | 0.198 | 1.07 | 7.74 | 4.85 |
| | $\alpha_e$=3.5 | 60 tex | 9.3 | 0.331 | 1.85 | 10.4 | 4.74 |
| | | 30 tex | 11.8 | 0.236 | 0.67 | 8.19 | 2.28 |
| | | 20 tex | 13.3 | 0.180 | 0.82 | 6.12 | 5.49 |
| | $\alpha_e$=4 | 60 tex | 9.2 | 0.317 | 0.55 | 9.06 | 1.87 |
| | | 30 tex | 11.3 | 0.223 | 1.04 | 6.93 | 6.48 |
| | | 20 tex | 13.3 | 0.185 | 0.73 | 6.36 | 8.05 |

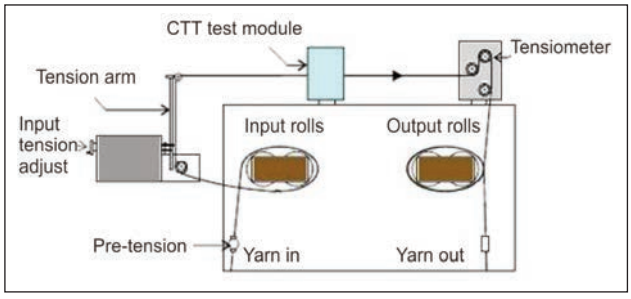


Fig. 1. Schematic view of CTT instrument [23]

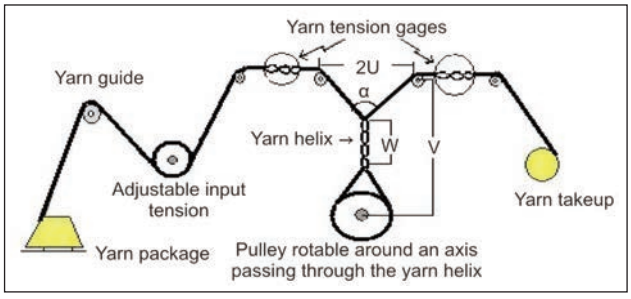


Fig. 2. Schematic diagram of the elements required for twisted strand [21]

applied in most cases. Therefore in this study, friction tests were carried out according to ASTM standards as well.

## Yarn to yarn friction coefficient ($\mu_{YY}$) measurements

The yarn-to-yarn friction test was carried out by CTT Friction Tester which measures the frictional properties of the moving yarn as it is wrapped around itself as given in figure 2. This test complies with the ASTM D 3412-13 twisted strand method [21]. A length of yarn is moved at 100 m/min speed in contact with itself (3 turns) at a specified wrap angle (35°apex angle). As a result of this contact, the output tension on the yarn changes. The software calculates the coefficient of yarn friction using the input and output tension values as well as the number of wraps and apex angle according to the formula given below (1).

$$\mu = \frac{\ln \dfrac{T_2 - \Delta T/2}{T_1 + \Delta T/2}}{2 \cdot \pi \cdot n_\alpha} \qquad (1)$$

Table 2

| PEARSON CORRELATION COEFFICIENT (r) AND p VALUES OF CORRELATION ANALYSIS | | | | |
|---|---|---|---|---|
| | | **Hairiness (H)** | **Diameter (D)** | **Unevenness ($CV_m$)** |
| **Yarn to yarn friction ($\mu_{YY}$)** | r<br>p | –0.560<br>*0.002** | –0.216<br>0.279 | –0.168<br>0.403 |
| **Yarn to metal friction ($\mu_{YM}$)** | r<br>p | 0.579<br>*0.002** | 0.897<br>*0.000** | –0.824<br>*0.000** |
| **Lint factor (LF)** | r<br>p | 0.620<br>*0.001** | 0.635<br>*0.000** | –0.535<br>*0.004** |
| *statistically significant according to α=0.05 confidence level | | | | |

where $\alpha = 2 \cdot \arctan\left(\frac{U}{V - W}\right)$

Where: μ is the coefficient of friction, $T_1$ is mean input tension, $T_2$ is mean output tension, $\Delta T$ = zero twist tension (the difference value between input and output tensions with no yarn friction), $n$ = number of wraps (3 turns), and α = apex angle (35°) ($W$: inter twisted portion of yarn, $U$: the distance between the upper pulley axes, $V$: the distance between the lower pulley axis and a line connecting the upper pulley axes).

### Yarn to metal friction coefficient ($\mu_{YM}$) measurements

The measurements of yarn-to-metal friction coefficients of yarns were carried out according to ASTM D 3108-13 standard by using CTT Friction Tester. A length of yarn is run at a constant speed of 100 m/min and in contact with metal surface using a specified wrap angle (180º) (figure 3). The yarn input and output tensions are measured, and the coefficient of friction is calculated by means of Amontons' law given in equation 2 [22].

$$e^{\mu\theta} = \frac{T_2}{T_1} \qquad \mu = \frac{\ln (T_2/T_1)}{\theta} \qquad (2)$$

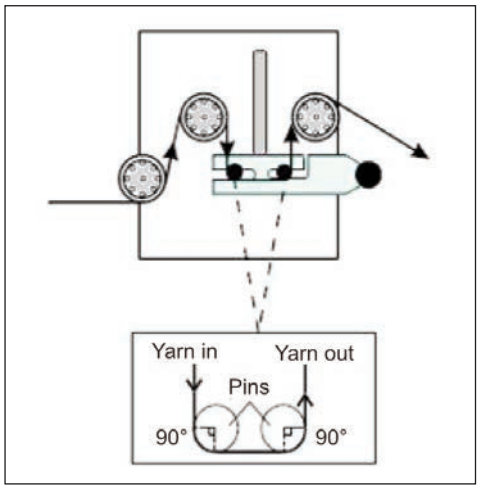


Fig. 3. The position of the yarn in yarn-to-metal friction test [22]

### Lint factor measurements

Lint shedding characteristics of the investigated yarns were measured by the CTT Lint Generation Tester. The CTT lint tester measures the amount of the lint generated during 1 km test long while the yarn is running under constant tension at test speed of 100 m/min and determines how much lint a yarn will generate under the condition of yarn to yarn friction. In this way, the yarn is tested dynamically to simulate the actual production conditions more closely and provides timely accurate data. As the yarn is moving, the generated lint is collected on a piece of paper under the vacuum sealed enclosure. The amount of collected lint is expressed as mg/km and stated as lint factor (LF) [23].

## RESULTS AND DISCUSSION

In order to investigate the relationship between the frictional and lint generation properties of the regenerated cellulosic yarns (viscose 100%, modal 100% and lyocell 100%) with the basic physical properties of the yarns (hairiness, diameter and mass coefficient of variation), the Pearson correlation coefficient values were calculated. The correlation coefficients ($r$) and $p$ values are given in table 2.

As it can be seen from the correlation analysis, yarn hairiness has a negative significant effect on the yarn-to-yarn friction coefficients of the yarns whereas positive correlation is determined with $\mu_{YM}$ values. As the yarn hairiness increases, lint shedding also increases and this correlation is found to be statistically significant as well. In yarn-to-yarn friction test, as the yarn is rubbed itself, a more hairy surface may led to a sliding effect and could cause a decrease in yarn-to-yarn friction values whereas on contrary, this surface structure results in higher friction when rubbing the yarn with metal pin since one of the rubbing surface is constant and solid. Therefore, it can be stated that the rougher surface causes higher friction and this result is compatible with the study carried out by Kilic and Sülar [10].

Yarn diameter has positive and statistically significant correlation with both $\mu_{YM}$ and $LF$ values. Coarser yarn has a bigger friction surface with the metal pin

Table 3

| PEARSON CORRELATION COEFFICIENT (r) AND p VALUES OF CORRELATION ANALYSIS | | | |
|---|---|---|---|
| | **Yarn-to-yarn friction ($\mu_{YY}$) Yarn-to-metal friction ($\mu_{YM}$)** | **Yarn-to-yarn friction ($\mu_{YY}$) Lint factor (LF)** | **Yarn-to-metal friction ($\mu_{YM}$) Lint factor (LF)** |
| r | –0.111 | –0.268 | 0.453 |
| p | *0.325* | *0.015** | *0.000** |
| * statistically significant according to α=0.05 confidence level | | | |

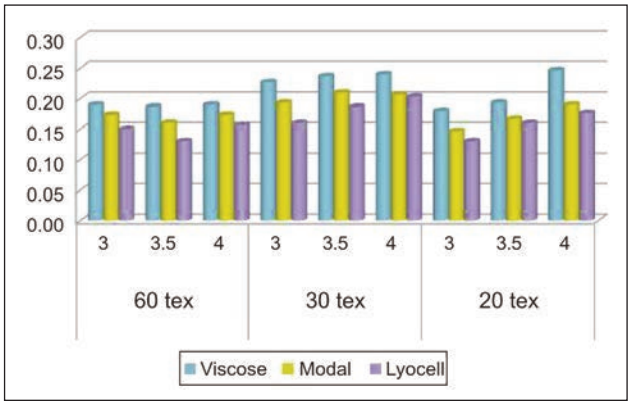


Fig. 4. The graphic of the yarn-to-yarn friction values of the produced yarns

and this gives rise to higher friction values as found parallel with the study of Kalyanaraman [24].

The correlation coefficient is found statistically significant between $CV_m$, $\mu_{YM}$ and *LF* values of the yarns. As the yarn gets thinner the mass variation of the yarn becomes worse but the $\mu_{YM}$ and *LF* values decrease, so the correlation has been found in a negative tendency.

Table 3 indicates the Pearson correlation coefficients (*r*) and p values of $\mu_{YM}$, $\mu_{YY}$ and *LF* values. Although the correlation coefficients are statistically significant for $\mu_{YM}$ – *LF*, and $\mu_{YY}$ – *LF* values, the power of the relation between these data is not so high. However, the correlation between the yarn to metal friction and lint shedding is relatively high (*r* = 0.453).

## The results of yarn to yarn friction coefficient ($\mu_{YY}$) values

The mean values of the yarn-to-yarn friction coefficients ($\mu_{YY}$) are given in figure 4. The results indicate that the highest yarn-to-yarn coefficient values belong to the viscose yarns in all produced yarn linear densities and twist coefficients whereas the lowest values are obtained from lyocell yarns. The hairiness of the lyocell yarn is higher compared to the viscose and modal yarns as can be seen from the results in table 1. The fibers protruding from the yarn structure may cause compensating effect when the yarns are rubbed each other and could cause lower friction forces. With the increasing of yarn twist coefficient, $\mu_{YY}$ values increase. This may be the fact that with the higher twist levels, the structure of the yarn gets compact and the diameter of the yarns decreases leading to higher friction forces.

In order to determine the effects of yarn type, yarn linear density and twist coefficient on the yarn-to-yarn friction values of the viscose, modal and lyocell yarns statistically, variance analysis (ANOVA) was carried out. According to α = 0.05 confidence level, all of the investigated parameters have been found statistically importance effects on $\mu_{YY}$ values (*p* = 0.000). In order to compare the levels of the factors with each other, multiple comparison statistical test (Student Newman Keuls-SNK) was carried out and the means for groups in homogenous subsets are displayed in table 4. According to the results, three subsets are formed based on the mean values of yarn material, yarn linear density and twist coefficient values. Therefore, it can be stated that 95% confidence limits of each group do not overlap and the differences between the mean values are statistically significant.

## The results of yarn-to-metal friction coefficient ($\mu_{YM}$) values

Figure 5 indicates the results of the yarn-to-metal friction coefficient values ($\mu_{YM}$) of the produced yarns. Similar to yarn-to-yarn friction results, the lowest $\mu_{YM}$ values were obtained with lyocell yarns and the highest friction coefficient values belonged to the viscose yarns. As the yarn gets coarser since the friction area between the yarn and metal pin increases, the friction

Table 4

| MULTIVARIATE COMPARISON RESULTS FOR YARN-TO-YARN FRICTION VALUES | | | | | | | | | | | |
|---|---|---|---|---|---|---|---|---|---|---|---|
| **Yarn material** | **Subset** | | | **Yarn linear density** | **Subset** | | | **Yarn twist coefficient** | **Subset** | | |
| | **1** | **2** | **3** | | **1** | **2** | **3** | | **1** | **2** | **3** |
| **Lyocell** | 0.162 | | | **60 tex** | 0.168 | | | **$\alpha_e$=3** | 0.172 | | |
| **Modal** | | 0.180 | | **30 tex** | | 0.177 | | **$\alpha_e$=3.5** | | 0.181 | |
| **Viscose** | | | 0.210 | **20 tex** | | | 0.207 | **$\alpha_e$=4** | | | 0.198 |
| *Significant value (p)* | *1.000* | *1.000* | *1.000* | *Significant value (p)* | *1.000* | *1.000* | *1.000* | *Significant value (p)* | *1.000* | *1.000* | *1.000* |

Table 5

| MULTIVARIATE COMPARISON RESULTS FOR YARN-TO-METAL FRICTION VALUES | | | | | | | | | |
|---|---|---|---|---|---|---|---|---|---|
| **Yarn material** | **Subset** | | | **Yarn linear density** | **Subset** | | | **Yarn twist coefficient** | **Subset** |
| | **1** | **2** | **3** | | **1** | **2** | **3** | | **1** |
| **Lyocell** | 0.329 | | | **60 tex** | 0.314 | | | **$\alpha_e$=3.5** | 0.3400 |
| **Modal** | | 0.346 | | **30 tex** | | 0.324 | | **$\alpha_e$=3** | 0.3437 |
| **Viscose** | | | 0.355 | **20 tex** | | | 0.392 | **$\alpha_e$=4** | 0.3463 |
| *Significant value (p)* | *1.000* | *1.000* | *1.000* | *Significant value (p)* | *1.000* | *1.000* | *1.000* | *Significant value (p)* | *0.107* |

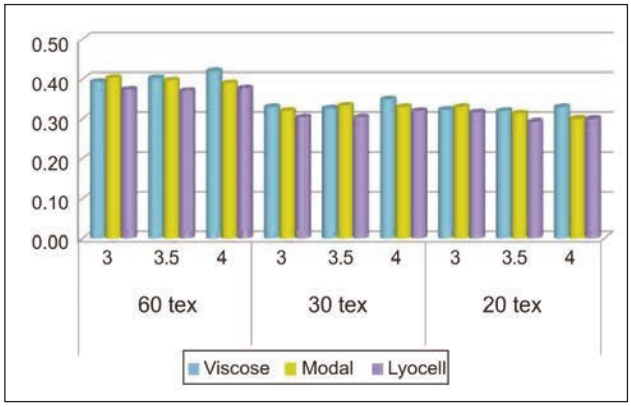


Fig. 5. Yarn-to-metal friction values of the produced yarns

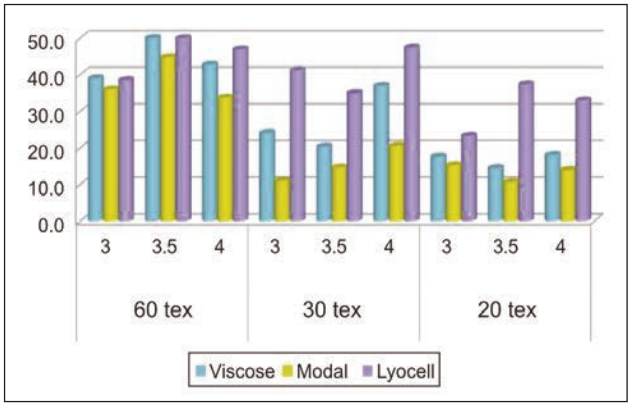


Fig. 6. Lint factor values (mg/km) of the produced yarns

values increase as well. The results reveal that the friction values of the yarns in different twist coefficients are generally similar to each other so the effect of twist factor is not obvious and this finding is compatible with the previous studies [10, 12].

The analysis of variance test has been carried out in order to determine whether the yarn type, yarn linear density and yarn twist coefficient have statistically significant effects on yarn-to-metal friction values. According to the analysis, the influence of the yarn material and yarn linear density have been found statistically important ($p$ = 0.000) but yarn twist coefficient has no significant influence on $\mu_{YM}$ values ($p$ = 0.127). According to the results of the multiple comparison test as given in table 5, since there is no statistically crucial effect of yarn twist coefficient, all the investigated yarns in terms of yarn twist coefficients take place in the same subset. However, for yarn material and yarn linear density, 3 subsets are formed, which means that the 95% confidence ranges of all the levels of each factor do not overlap and the differences between the mean values are important.

## The results of lint factor (LF) values

The lint factor values (mg/km) of the produced yarns are given in figure 6. The results have indicated that the highest lint shedding occurred by the lyocell yarns due to the higher hairiness characteristic of these yarns. However, modal yarns produced less fluff during yarn-to-yarn friction and therefore lowest lint factor values (*LF*) were obtained with these yarns. As the yarn diameter increases and the yarn gets coarser, due to the higher friction area and higher hairy structure of the yarns, lint generation increases. Yüksekkaya stated that according to many researchers, coarser yarns had higher hairiness, and since fly formation was related to the yarn hairiness, coarser yarn generated high lint levels [13].

Based on the variance analysis carried out for the determination of the influences of the investigated parameters on lint shedding characteristics of the yarns, yarn material and yarn linear density have been found significant ($p$ = 0.000) whereas there isn`t any important difference between the lint factor values of the yarns in terms of yarn twist coefficient ($p$ = 0.124). The results of the multiple comparison test given in table 6 indicates that the average of the lint factor values for modal yarns is quite low compared to that of viscose and lyocell yarns. In terms of yarn linear density, 3 subsets are formed since the differences between the lint factors of the yarns in different yarn counts are statistically important. All the yarns produced in three twist coefficients are in the same subset since the effect of twist coefficient on lint shedding is not statistically significant.

## CONCLUSIONS

The final quality of textile materials depends mostly on the surface mechanical properties of fibers, yarns,

Table 6

| MULTIVARIATE COMPARISON RESULTS FOR LINT FACTOR VALUES | | | | | | | | | |
|---|---|---|---|---|---|---|---|---|---|
| **Yarn material** | **Subset** | | | **Yarn linear density** | **Subset** | | | **Yarn twist coefficient** | **Subset** |
| | **1** | **2** | **3** | | **1** | **2** | **3** | | **1** |
| **Modal** | 22.242 | | | **60 tex** | 20.425 | | | **$\alpha_e$=3** | 27.318 |
| **Viscose** | | 30.307 | | **30 tex** | | 27.902 | | **$\alpha_e$=4** | 32.593 |
| **Lyocell** | | | 40.52 | **20 tex** | | | 44.742 | **$\alpha_e$=3.5** | 33.159 |
| *Significant value (p)* | *1.000* | *1.000* | *1.000* | *Significant value (p)* | *1.000* | *1.000* | *1.000* | *Significant value (p)* | *0.152* |

and fabrics. With the advent of modern spinning systems, frictional properties of fiber assemblies have gained much more importance. In recent years, three generations of regenerated cellulosic yarns such as viscose, modal and lyocell yarns have found a wide usage area in textile sector and the knowledge of the physical characteristics of these yarns has gained increasing importance especially for the determination of production parameters and conditions. Therefore, within the scope of this study, it was aimed to investigate the frictional (yarn-to-yarn and yarn-to-metal) and one of the disturbing effects of the friction that is lint shedding properties of viscose, modal and lyocell yarns produced in three different yarn linear densities and in three different yarn twist coefficients. According to the results in terms of yarn material, yarn-to-yarn friction ($\mu_{YY}$) and yarn-to-metal friction ($\mu_{YM}$) values of the viscose yarns are found to be the highest whereas the lowest values belonged to the lyocell yarns. Since the hairiness of the lyocell yarns is higher compared to other regenerated cellulosic yarns, the hairy surface may lead to a sliding effect and therefore could cause a decrease in the friction forces. The rigidity of the yarns may also affect the friction since the rigidity of the lyocell yarns are lower and this relation can be also searched in further studies in detail. In terms of lint factor, a higher hairiness level of the yarns causes more lint shedding during friction and therefore the highest *LF* values were obtained from lyocell yarns.

The effect of twist coefficient on yarn-to-metal and lint factor values is not apparent and the mean values are close to each other, therefore there is not a statistical important relation. However, in terms of yarn-to-yarn friction measurements, twist coefficient has a statistical significant effect due to the more compact yarn structure and higher frictional forces.

As for the effect of yarn linear density, the results of yarn-to-metal and lint factor values are in the same tendency whereas yarn-to-yarn friction values indicate a contrary effect. As the yarn gets thinner, due to the lower diameter and surface area the contact points between yarns cause higher friction values because of the shearing effect but in yarn-to-metal friction test, as the yarn rubs to the solid metal surface, due to the higher linear density of yarn and smaller surface area, the contact points decrease and therefore the friction values decrease. The higher lint factor values of the yarns in higher diameter arise from the hairy and coarser yarn structure.

Since the frictional behaviour of yarns greatly affects their processing, physical properties, and the performance of the final products, the results of this study can be used for the optimization of process conditions of regenerated cellulosic yarns of which their usages are increasingly preferred in various fields of textile sector.


## FUNDING

The materials of this study have been supplied from a scientific project granted by Ege University with the project number of 10-MUH-032.


## BIBLIOGRAPHY


[1] Jawel, S.N., Patil, U.J. *Yarn friction & its importance, theory, factors, measurement*. In: The Indian Textile Journal, 2011, vol.35, issue 4, pp.14-28

[2] Svetnickienė,V., Čiukas, R. *Investigation of friction properties of yarns from natural fibres*. In: MECHANIKA, 2009, Vol. 75, issue 1, pp.73-77

[3] Gupta, S.B. *Surface Characteristics of Fibers and Textiles (Frictional Properties of Textile Materials)*. In: Surfactant Science Series, 2001, Vol.94, ISBN: 0-8247-0002-3, pp.60-74

[4] Koo, Y.S. *Yarn hairiness affecting fluff generation*. In: Fibers and Polymers, 2003, Vol. 4, issue 3, pp.119-123

[5] Kretzshmar, D.S., Further R. *USTER Zweigle Friction Tester Application Report,* 2010, pp. 5-6

[6] Liu, L., Chen, J., Zhu, B., Yu, T.X., Tao, X.M., Cao, J. *The yarn-to-yarn friction of woven fabrics*. In: Proceeding of the 9th international ESAFORM conference on material forming, Glasgow, UK, April 26–28 2006,

[7] Ghosh, A., Patanaik, A., Nandjiwala, R. D., Rengasamy, R. S. *A Study on Dynamic Friction of Different Spun Yarns*. In: Journal of Applied Polymer Science, 2008, Vol.108, issue 5, pp.3233-3238

[8] Jones, J.*Abrasion Characteristics of Ring-Spun and Open-End Yarns*, Master of Science Thesis, December 2001, Graduate Faculty of North Carolina State University

[9] Chattopadhyay, R., Banerjee, S.*The frictional behaviour of ring, rotor and friction spun yarn*. In: Journal of Textile Institute, 1996, Vol.87, issue 1, pp.59–67

[10] Kilic, B.G., Sülar, V. *Frictional properties of cotton-tencel yarns spun in different spinning systems*. In: Textile Research Journal, 2012, Vol. 82, issue 8, pp. 755–765

[11] Ramkumar, S. S., Shastri, L., Tock, R.W., Shelly, D. C., Smith, M. L., Padmanabhan, S. *Experimental Study of the Frictional Properties of Friction*. In: Spun Yarns Journal of Applied Polymer Science, 2003, Vol. 88, issue 10, pp. 2450-2454

[12] Altaş, S., Kadoğlu, H. *Comparison of the evenness, faults and hairiness of compact and conventional spun ring yarns*. In: Industria Textila, 2013, Vol.64, issue 2, pp.65-69

[13] Yuksekkaya, M.E.A *study of fly generation during raising*. In: The Journal of the Textile Institute, 2008, Vol. 99, issue 4, pp.169-176

[14] Koo, Y.S, Kim, H.D. *Friction of Cotton Yarn in Relation to Fluff Formation on Circular Knitting Machines*. In: Textile Research Journal, 2002, Vol.72, issue 17, pp.17-20

[15] Yuksekkaya, M.E. *Fiber Fly Generation of Soybean Yarns during Weaving.* In: Journal of Textile Science and Engineering, 2012, Vol.2, issue 7, pp.1-5

[16] Basu, A., Gotipamul, L.R. *Lint Shedding Propensity of Cotton and Blended Yarns*. In: Indian Journal of Fibre and Textile Research, 2003, Vol.28, issue 3, pp.288-294

[17] Bhomıck, N., Ghosh, S. *Fibre Shedding from Cotton Spun Yarn-A Serious Indoor Air Pollution in Knitting Industry.* In: 5th WSEAS Int. Conf. on Environment, Ecosystems and Development, 2007, Tenerife, Spain, December 14-16

[18] Koo, Y.S. *Waxing Effect on Lint Contamination in the Knitting Process*, In: Textile Research Journal, 2008, Vol. 78, issue 2, pp. 168-173

[19] Erdumlu N., Ozipek B. *Investigation of Regenerated Bamboo Fibre and Yarn Characteristics*. In: Fibres and Textiles in Eastern Europe, 2008, Vol. 16, issue 4, pp. 43-47.

[20] Kreze T., Malej S. *Structural Characteristics of New and Conventional Regenerated Cellulosic Fibers.* In: Textile Research Journal, 2003, Vol.73, issue 8, pp. 675-684.

[21] ASTM D 3412-13, Standard Test Method for Coefficient of Friction, Yarn to Yarn, 2013

[22] ASTM D 3108–13, Standard Test Method for Coefficient of Friction, Yarn to Solid, 2013

[23] Lawson-Hempfill, CTT User Manuel & Technical Documents

[24] Kalyanaraman A. R., *Yarn-friction Studies with the SITRA Friction-measuring Device*, In: The Journal of The Textile Institute, 1988, Vol. 79, issue 1, pp. 147-151

**Author:**

*Ass. Prof. Dr.* Gonca ÖZÇELİK KAYSERİ
Emel Akın Vocational Training School,
Ege University Campus, Bornova, İzmir, TURKEY
e-mail: gonca.ozcelik@ege.edu.tr

# Numerical study of flow around parachute based on macro-scale fabric permeability as momentum source term

HAN CHENG
XIAO CHEN
XIAO-XUE YAN
LI YU
YA-NAN ZHAN

**REZUMAT – ABSTRACT**

**Studiu numeric al fluxului de aer în jurul unei paraşute pe baza permeabilităţii ţesăturii la scară macro ca sursă de impuls**

*Pentru o acurateţe cât mai bună a simulării câmpului de curgere în jurul unei paraşute la coborârea finală, este descrisă în primul rând performanța permeabilităţii ţesăturii microporoase obținute cu ajutorul experimentelor și este utilizată interacțiunea fluid – structură pentru a obține forma aerodinamică a voalurii flexibile în stare de echilibru. Domeniul computaţional este format din domeniul de permeabilitate al ţesăturilor microporoase și domeniul câmpului de curgere în funcție de forma aerodinamică. Ecuația care stabileşte impulsul cu sursa de corecție care este afectată de permeabilitatea țesăturii este determinată în domeniul de permeabilitate, iar modelul clasic de turbulenţă k-ε este utilizat pentru a simula fluxul de aer în jurul paraşutei în domeniul câmpului de curgere. Caracteristicile de rezistenţă la rulare obținute prin această nouă metodă au o compatibilitate mai bună cu rezultatele testelor de largare faţă de simularea anterioară care verifică fezabilitatea și acurateţea noii metode. În plus, distribuția presiunii în voalură de-a lungul meridianului se obține pe baza permeabilităţii ţesăturii. Structura câmpului de curgere arată că în spatele voalurii există curent invers, curent turbionar, ventilaţie şi alte stări ale fluxului de aer. Metoda poate furniza nu numai baza pentru proiectarea paraşutei și selecția materialelor, dar poate furniza, de asemenea, un model de referinţă pentru analiza caracteristicilor ţesăturilor permeabile.*

*Cuvinte-cheie: paraşută, simulare numerică, ţesătură permeabilă, structura câmpului de curgere, vârtej de siaj, stare de curgere*

**Numerical study of flow around parachute based on macro-scale fabric permeability as momentum source term**

*For a more accurate simulation of the flow field around parachute in terminal descent, firstly the microporous fabric permeability performance obtained through experiments is described in modeling description, and the fluid-structure interaction is utilized to obtain the aerodynamic shape of flexible canopy in stable stage. Then the computation domain is divided into microporous fabric permeability domain and flow field domain according to the aerodynamic shape. The momentum governing equation with correction source term which is affected by the fabric permeability is established in permeability domain and the standard k-ε turbulence model is utilized to simulate the flow around the parachute in the flow field domain. The drag characteristics obtained by this new method is more consistent with airdrop test results than the past simulation which verifies the feasibility and accuracy of the new method. In addition, the canopy pressure distribution along the meridian is obtained considering fabric permeability. The flow field structure shows that behind the canopy there exist backflow, swirl flow, ventilation flow and other flow states. The method can not only provide the basis for parachute design and material selection, but also provide a reference for other permeable fabric operating characteristic analysis.*

*Key-words: parachute, numerical simulation, permeable fabric, flow field structure, wake vortex, flow state*

Parachute is a kind of high effective aerodynamic deceleration device, and the aerodynamic performance of parachute decides the deceleration and stability of the parachute-payloads system [1]. Except the aerodynamic shape, the aerodynamic performance is also affected by fabric permeability. The past research of the parachute aerodynamic performance mainly depends on the wind tunnel test [2–3]. However, due to the large area of parachute, it is difficult to carry out full-size test. It is also hard to achieve the same permeability similarity as other rigidity similarities for proper similarity model, so model test error is large. With the advances in numerical algorithms and computer hardware, numerical simulations become an important method of parachute theoretical studies.

Currently the numerical studies of fabric permeability mainly focus on micro-scale view [4], [5], small-scale grid is utilized to discretize spatial domain among the fabric fibers and the flow simulation is calculated among the fiber gaps. But the parachute aerodynamic performance analysis is macro issue, and the flow around parachute contains flow separation, vortex formation and shedding. If the fabric and flow field is discretized by small-scale grid, the grid number will reach hundreds of millions which is difficult to achieve

in current computing capacity. Therefore, in the conventional parachute aerodynamic performance analysis, the aerodynamic shape is often directly obtained through CAD software and processed as solid wall [6], [7]. With ignorance of fabric permeability in calculation, the flow field structure and aerodynamic performance don't agree with experiment results well.

In order to achieve the combination of macro-scale aerodynamic performance analysis and micro-scale fabric permeability, the large-scale body grid is utilized to discretize the permeability domain as description of complex aerodynamic shape. And the fabric permeability obtained through experiment is converted into momentum loss term for permeability domain solver, while the flow field domain surrounding the permeability domain is calculated utilizingturbulence model. The complicated aerodynamic shape in terminal stage is obtained through FSI which ensure its accurate description. Then this method is utilized for the calculation of a ringsail parachute, and the calculation results are consistent with airdrop test results well. In addition, the topology of canopy flow field is obtained, and the wake and aerodynamic characteristics around permeable canopy are analyzed.

## THE BASIC PARAMETERS OF RINGSAIL PARACHUTE

The ringsail parachute in this work consists of 24 canopy gores as shown in figure 1. The specific structural dimensions are shown in table 1. The materials used in the calculation are listed in table 2 (where all of the width of reinforcement band is 15 mm). The permeability of canopy fabric has important influence on the aerodynamic performance, and the fabric permeability can be described as Ergun equation as below [8]:

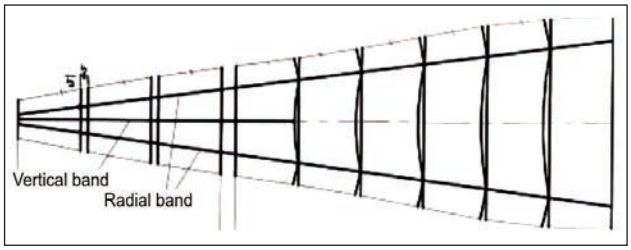


Fig. 1. Ringsail parachute canopy gore

$$\Delta P = (av_p + bv_p^2)\, e \quad (1)$$

where:

$a$, $b$ are viscosity coefficient and, respectively, inertia coefficient that describe the fabric permeability;

$e$ – the canopy thickness;

$v_p$ – the flow velocity through the canopy fabric;

$\Delta P$ – differential pressure from the canopy fabric test.

Air permeability under different differential pressures is measured through YG461D fabric permeability instrument and the experimental data are fitted. The viscosity coefficient $a$ and inertia coefficient $b$ of two fabric materials are obtained:

– ring:

$$a = 1.3 \times 10^6 \text{ kg/m}^3 \cdot \text{s}, \quad b = 6.47 \times 10^5 \text{ kg/m}^4 \quad (2)$$

– sail:

$$a = 1.89 \times 10^6 \text{ kg/m}^3 \cdot \text{s}, \quad b = 1.17 \times 10^6 \text{ kg/m}^4 \quad (3)$$

## GOVERNING EQUATIONS

### Flow governing equations

The opening speed of this ringsail parachute is only 30 m/s, so the flow field around the parachute is a typical incompressible flow problem. The standard $k$-epsilon model is utilized as the flow field governing equations, the general expression as below:

Table 1

| RINGSAIL PARACHUTE STRUCTURAL DIMENSIONS | | | | | | |
|---|---|---|---|---|---|---|
| **Nominal diameter**, $D_0$/m | **Canopy gore**, height/m | **Ring**, height/m | **Ring gap**, width/m | **Sail**, height/m | **Line**, length/m | **Number of lines** |
| 7.35 | 3.69 | 0.39 | 0.045 | 0.39 | 9.1 | 24 |

Table 2

| RINGSAIL PARACHUTE MATERIALS PARAMETERS | | | | |
|---|---|---|---|---|
| **Type** | **Density** | **Thickness** | **Tensile strength** | **Tensile elongation**, % |
| Ring | 80 g/m$^2$ | 0.15 mm | 1 000 N/5 cm | 30 |
| Sail | 35 g/m$^2$ | 0.1 mm | 450 N/5 cm | 28 |
| Vent reinforcement band | 9 g/m | 1 mm | 3 128 N | 34 |
| Reinforcement band | 3.7 g/m | 0.42 mm | 1 780 N | 30 |
| Line | 1.9 g/m | 2 mm (diameter) | 31 280 N | 8.5 |

$$\frac{\partial(\rho\phi)}{\partial t} + \mathrm{div}(\rho \boldsymbol{v}\phi) = \mathrm{div}(\Gamma \mathrm{grad}\,\phi) + S \qquad (4)$$

where:

$\phi$, $\Gamma$ are common variable and, respectively, diffusion coefficient;

$S$ – the source term.

For the continuity equation, momentum equation and $k$-epsilon turbulence model, the three terms are respectively:

$$\phi = 1, v_i, k, \varepsilon \qquad (5)$$

$$\Gamma = 0, \mu_{\mathrm{eff}}, \mu + \frac{\mu_t}{\sigma_k}, \mu + \frac{\mu_t}{\sigma_\varepsilon} \qquad (6)$$

where:

$$\mu_{\mathrm{eff}} = \mu + \mu_t,$$

$$S = 0, -\frac{\partial p}{\partial x_i} + \frac{\partial}{\partial x_j}(\mu_{\mathrm{eff}} \frac{\partial v_j}{\partial x_i}), \mu_t \frac{\partial v_i}{\partial x_j}(\frac{\partial v_i}{\partial x_j} + \frac{\partial v_j}{\partial x_i}) - \rho\varepsilon,$$

$$\frac{C_{1\varepsilon}\varepsilon}{k} \mu_t \frac{\partial v_i}{\partial x_j}(\frac{\partial v_i}{\partial x_j} + \frac{\partial v_j}{\partial x_i}) - C_{2\varepsilon}\rho\frac{\varepsilon^2}{k} \qquad (7)$$

where:

$\mu$, $\mu_t$, are the fluid dynamic viscosity and, respectively, turbulence viscosity coefficient;

$$\mu_t = \rho C_\mu \frac{k^2}{\varepsilon}$$

In this example, the corresponding coefficient values are, respectively, $C_{1\varepsilon}$ = 1.44, $C_{2\varepsilon}$ = 1.92, $C_\mu$ = 0.09. The turbulent Prandtl number of turbulent kinetic energy $k$ and dissipation rate $\varepsilon$ are 1.0 and 1.3.

## Fabric permeability model

The parachute canopy is a flexible stretchable permeable fabric structure and the flow field around a permeable canopy has always been a difficult problem. The source term correction method is utilized to include the influence of fabric permeability. The whole flow field computation domain is divided into two parts as canopy permeability domain and flow field domain around canopy. In the canopy permeability domain, the fabric permeability model is introduced into the source term in momentum equation, so the flow field momentum equation in the permeable fabric domain is:

$$\frac{\partial}{\partial t}(\rho v_i) + \frac{\partial}{\partial x_j}(\rho v_i v_j) = -\frac{\partial p}{\partial x_i} + \frac{\partial}{\partial x_j}(\mu \frac{\partial v_i}{\partial x_j}) + S_i \qquad (8)$$

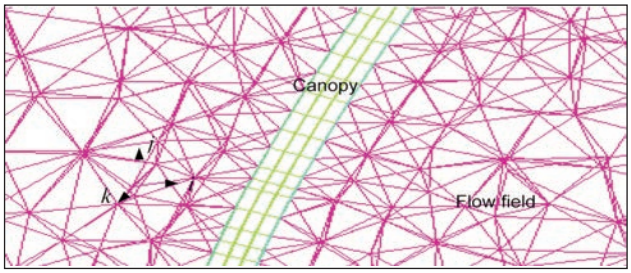


Fig. 2. The permeable canopy mesh and flow field mesh

where:

$S_i$ is the additional source term caused by the fabric permeability, the expression as below:

$$S_i = -\frac{\mu}{\alpha} v_i - C_2 \frac{1}{2} \rho |\boldsymbol{v}| v_i \qquad (9)$$

where:

$\alpha$ is permeability coefficient;

$C_2$ – the internal resistance factor.

The terms on the right side of this equation are viscosity loss terms and inertia loss terms. According to the one-dimensional Ergun description of fabric permeability (fig. 2) is presented in equation (10):

$$\Delta P = (a v_p + b v_p^2) e \qquad (10)$$

and

$$S_i = \frac{\Delta P}{e} e_n \qquad (11)$$

Then, the three-dimensional source term of fabric permeability is expressed as:

$$S_i = (-a v_i - b |\boldsymbol{v}| v_i) e_n \qquad (12)$$

where:

$e$ is the fabric thickness;

$e_n$ – the thickness of permeability domain.

## NUMERICAL SIMULATION METHOD

### Steady shape

This canopy shape is calculated through the fluid-structure coupling method [9]. Since the three-dimensional space-time discrete FSI method requires huge computation resources, in order to quickly obtain steady canopy shape, the simplified laminar flow model is utilized and the initial shape is simplified as conical shape. The coupling method is Arbitrary Lagrangian Eulerian method (specific methods in references [9], [10]). The final steady shape is obtained through calculation. The changing shapes through

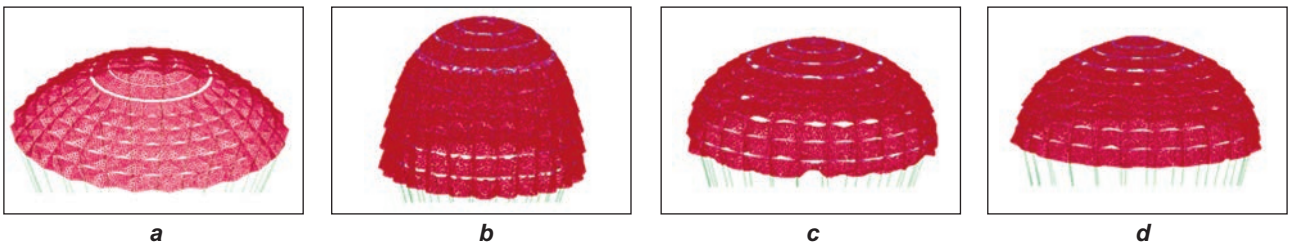

*a* *b* *c* *d*

Fig. 3. The changing shapes through coupling calculation ($t$ = 0, 0.15, 0.3, 0.45 s)

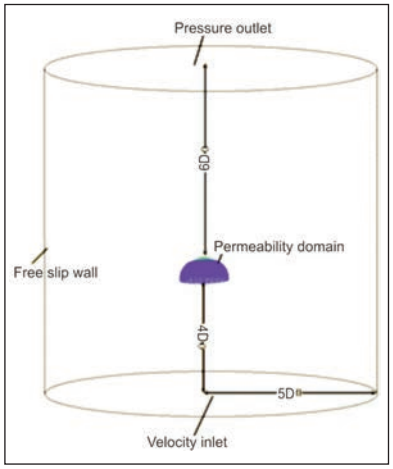


Fig. 4. The flow field computation domain

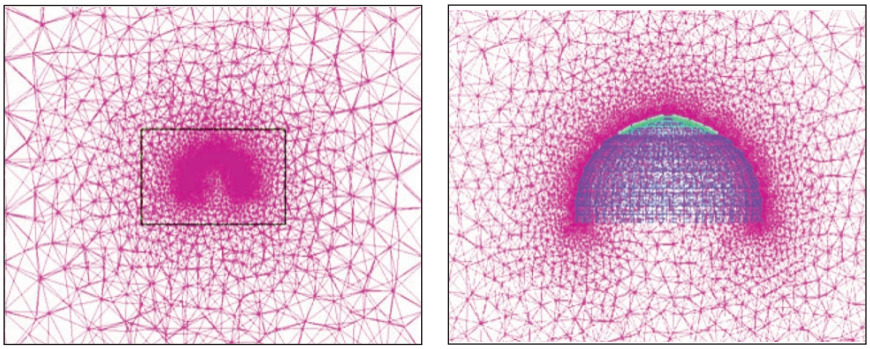

*a* *b*

Fig. 5. The flow field mesh of the symmetry plane with: *a* – partial domain; *b* – canopy central domain

FSI calculation are shown in figure 3, where figure 3 *d* is the steady shape.

## Mesh generation

The flow field calculation of the ringsail parachute is based on the steady shape (fig. 3 *d*).The flow field computational domain is shown in figure 4, where the boundary conditions are velocity inlet, pressure outlet, and the wall is free slip wall. The whole flow field computational domain is divided into two domains as canopy permeability domain and flow field domain around canopy, and the momentum equations are respectively equation (1) and equation (2). The canopy consists of 405,756 prismatic grids. The flow field mesh consists of 1,641,935 tetrahedron grids (fig. 5).

## Numerical results and analysis

Firstly, the steady calculation of ringsail parachute is conducted and the convergence residuals are less than 3 × 10E–4. The drag coefficient is 0.776 and the drag area is 32.8 $m^2$ in steady state through integration. This type of parachute has been tested in three airdrop tests (fig. 6) and the average drag area of test results is 30.9 $m^2$. The numerical results are consistent with test results, and these results show that the mesh is good enough to ensure fast and stable computation and the computational model is in high precision.

## The numerical results

Figure 7 is the pressure distribution and differential pressure coefficient in the canopy surface along meridian (dimensionless quantity). The results show that: except the vicinity of ventilation structure, the canopy internal pressures are almost the same but

Fig. 6. Ringsail parachute airdrop test

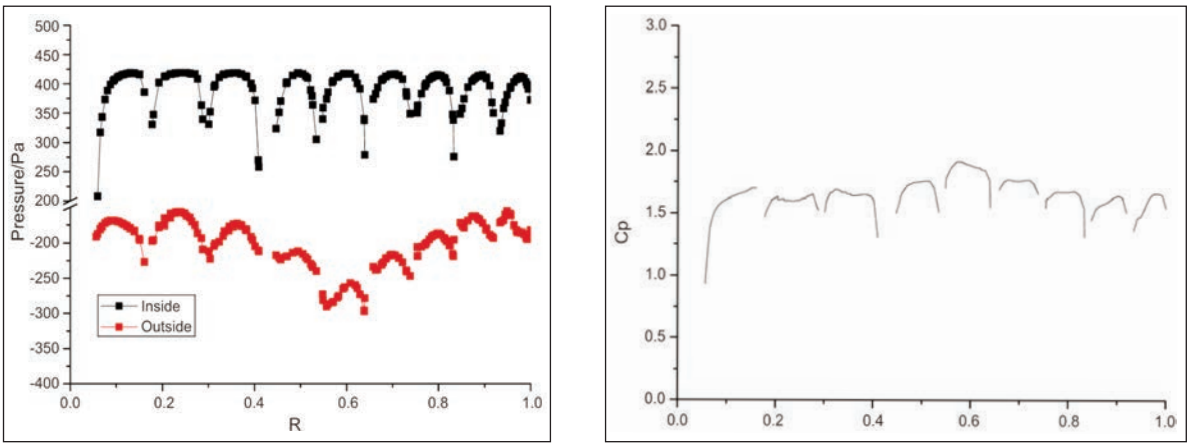


*a* *b*

Fig. 7. The pressure distribution results along canopy meridian with: *a* – the internal and external pressure distribution; *b* – differential pressure coefficient

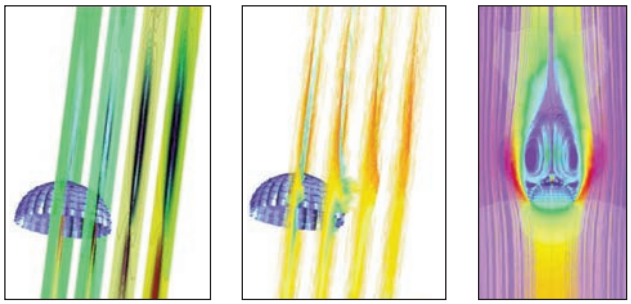

*a* *b* *c*

Fig. 8. The flow field along the flow direction (section location $r$ = 0, 0.5 $D_0$, 1 $D_0$, 1.5 $D_0$): *a* – pressure at different sections; *b* – pressure at different sections; *c* – the streamlines of center symmetry plane

the external static pressures along the meridian are not the same; the external static pressures of ring are close; the external static pressure of the second sail is the minimum but the differential pressure coefficient is the maximum, so the canopy stress here is the maximum; after this location the static pressure gradually increase along the meridian.

## Flow structure

Figure 8 is a flow field along the flow direction. According to figure 8, at the section with a distance of 1.5 x nominal diameter to the center, the pressure gradient is small and the normal velocity is almost 0. According to figure 8 *c* (the streamline distribution of central symmetry plane), the inlet streamlines and outlet streamlines are parallel to themselves, so the computation domain (fig. 4) fully meet the computation requirement.

Figure 9 is the flow field of canopy center plane. The results show that: the fluid clearly flow through the canopy fabric while the velocity is lower than the vent flow velocity and the free stream velocity. The results indicate that the momentum equation model with Ergun correction source term adopted in this work can effectively simulate the fabric permeability. Inside the canopy there is a positive pressure zone and behind the canopy there is a negative pressure zone. The differential pressure sustains the stable shape and produces the drag force that decelerates the payloads. The pressure gradient near canopy skirt edge is large. The further away from the canopy center, the smaller pressure gradient is.

Figure 10 shows the canopy surface streamline distribution. The results show that the flow field in the symmetry plane of wake vortex zone is very complex and there are spiral point, node and saddle point. The flow along the canopy edge forms the outer boundary. Behind the canopy center there are backflow. The backflow merges with the flow from vent and the saddle point emerges. After that the fluid spreads out and forms the inner boundary of wake. The front part of the inner boundary of wake is the first wake vortex

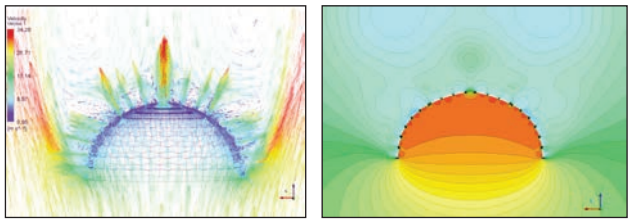

Fig. 9. The flow field of canopy center plane

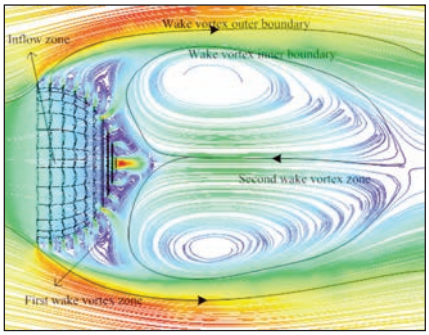


Fig. 10. Surface streamline in canopy center symmetry plane

zone. Because of the fabric permeability and structure ventilation, there are two main flow states as ventilation flow and small swirl flow. The number of small swirls is influenced by the number of ventilation gaps and the size of small swirls is influenced by the flow velocity through ventilation gaps. The wider the gap, the greater the velocity is, and then the first wake vortex zone is larger. There is a pair of central point in the second wake vortex zone. The greater the energy of backflow, the drag force is larger. The two wake vortex zone will influence each other. The energy increase in the first wake vortex zone will decrease the backflow energy in the second wake vortex zone, thus increase in structure ventilation will significantly reduce the drag of the parachute.

## CONCLUSIONS

The macro-scale fabric permeability is converted into the momentum source term and the flow field calculation of ringsail parachute with permeable canopy is conducted in this paper. The calculation results are compared with airdrop test results, and the drag is well consistent with the airdrop test results. The following conclusions are obtained through numerical results:

- The fluid penetration velocity through permeable fabric surface could be obtained and the flow field calculation of microporous fabric could be effectively completed with the method of adding additional source term in momentum equation.
- Except the gaps, the canopy internal static pressures are almost the same; the canopy external static pressure distribution in each ring is similar and the static pressure gradually increase along the meridian from the second sail of bottom canopy;

the differential pressure of the second sail is the maximum and the canopy at this location could be severely deformed in steady drop stage.

- The flow structure of wake is very complex and there will be backflow, swirl flow, ventilation flow and other flow state; the first wake vortex zone is right behind the canopy and mainly consists of ventilation flow and small swirls; the second wake vortex zone consists of backflow and big swirls which are in the opposite direction with swirls from the tail.
- The first wake vortex zone is affected by the influence of canopy structure vents, and the second zone is affected by the flow velocity and canopy area. The two wake vortex zone will influence each other. The enlargement of first wake vortex zone will cut down the backflow energy in the second wake vortex zone and reduce the drag. Thus increase in structure ventilation will significantly reduce the drag of the parachute.

## ACKNOWLEDGMENTS

This paper is supported by the National Natural Science Foundation of China (no. 11172137) and the Aeronautical Science Foundation of China (no. 20122910001).

## BIBLIOGRAPHY

[1] Niculescu, C., Butoescu, V., Sălișteanu, A., Olaru, S. *Equipment for paraglider- the emergency parachute*. In: Industria Textilă, 2010, vol. 61, issue 1, p. 11

[2] Barber, J., Johari, H. *Experimental investigation of personnel parachute designs using scale model wind tunnel testing.* In: AIAA, 2001-2074

[3] Yu, L., Ming, X., Cheng, L., J. *Experimental investigation on the flow-field of different vent canopy.* In: Acta Aerodynamica Sinica, 2008, vol. 26, issue 1, pp.19-24

[4] Yazdchi, K., Srivastava, S., Luding, S. *Microstructural effects on the permeability of periodic fibrous porous media.* In: International Journal of Multiphase Flow, 2011, vol. 36, pp. 956-966

[5] Melro, A. R., Camanho, P. P., Pinho, S. T. *Generation of random distribution of fibres in long-fibre reinforced composites.* In: Composites Science and Technology, 2008, vol. 68, pp. 2 092-2 102

[6] McQuilling, M., Lobosky, L., Sander, S. *Computational Investigation of flow around a parachute model*. In: Journal of Aircraft, 2011, vol. 48, issue 1, pp. 34–41

[7] Noetscher, G., Charles, R. D. *Benchmarking bluff body aerodynamics*. In: Report AIAA 2011-2607

[8] Aquelet, N., Wang, J., Tutt, B. A. et al. *Euler-Lagrange coupling with deformable porous shells*. In: ASME Pressure Vessels and Piping Division Conference. Vancouver, BC, Canada, 2006, pp. 23–27

[9] Cheng, H., Yu, L., Li, S. Q. *Numerical simulation of parachute inflation process based on ALE*. In: Journal of Nanjing University of Aeronautics & Astronautics, 2012, vol. 44, issue 3, pp. 290-293

[10] Souli, M., Ouahsine, A., Lewin, L. *ALE formulation for fluid-structure interaction problems*. In: Computer methods in applied mechanics and engineering, 2000, vol. 190, pp. 659-675

**Authors:**

HAN CHENG
Aviation Engineering Institute
Civil Aviation Flight University of China
46 Nanchang Road
Sichuan Guanghan 618307
P.R. China
e-mail: chenghanstorm@sina.com

LI YU
XIAO CHEN
YA-NAN ZHAN
XIAO-XUE YAN
College of Aerospace Engineering
Nanjing University of Aeronautics and Astronautics
29 Yudao Stress, Nanjing 210016, P. R. China

# Modeling of heat transfer through multilayer firefighter protective clothing

ELENA ONOFREI
STOJANKA PETRUSIC
GAUTHIER BEDEK
DANIEL DUPONT
DAMIEN SOULAT
TEODOR-CEZAR CODAU

**REZUMAT – ABSTRACT**

**Modelarea transferului de căldură prin îmbrăcămintea de protecție pentru pompieri**

*Acest articol este primul dintr-o serie de studii privind optimizarea performanțelor îmbrăcămintei de protecţie pentru pompieri, în ceea ce privește confortul termic și protecția contra radiațiilor termice de mică intensitate. Lucrarea se axează pe dezvoltarea unui model numeric de transfer termic adecvat estimării temperaturii și fluxului termic în echipamentele de protecție destinate pompierilor. Utilizând aplicațiile pachetului Comsol Multiphysics®, pentru determinarea transferului de căldură s-a folosit metoda elementului finit. Rezultatele aplicării acestui model au fost comparate cu cele experimentale, pentru un caz tipic de folosire a unui ansamblu de protecție format din trei straturi, în condiții obișnuite. S-a observat o bună corelaţie între rezultatele experimentale şi cele obţinute cu ajutorul modelului numeric. Acest model de transfer termic poate fi folosit în proiectarea îmbrăcămintei de protecție pentru pompieri şi pentru evaluarea performanțelor echipamentelor de protecție expuse diferitelor medii termice.*

*Cuvinte-cheie: transfer de căldură, îmbrăcăminte de protecție, model numeric*

**Modeling of heat transfer through multilayer firefighter protective clothing**

*This paper is the first in a series of studies on optimizing the performance of firefighter clothing, in respect of thermal comfort and skin protection from thermal injury that results from exposure to low-intensity thermal radiation. This paper focuses on the development of a heat transfer model suitable for predicting the temperature and heat flux in firefighter protective clothing exposed to low-intensity thermal radiation. The finite element method was used to evaluate the heat transfer by means of the Comsol Multiphysics® package. The model results were compared to experimental results for the case typical of routine conditions with a commonly used three-layer protective clothing assembly. Model predictions of the temperature agreed well with experimental temperature. This model could be used as an aid in the design of candidate protective clothing systems, by evaluating the performance of protective clothing systems in various thermal environments.*

*Key-words: heat transfer, firefighter protective clothing, numerical model*

Thermal comfort of the protective clothing is a topic of active research. According to generally accepted definition given by American Society of Heating, Refrigerating and Air Conditioning Engineers (ASHRAE), thermal comfort is “the condition of mind that expresses satisfaction with the thermal environment” [1]. Nonetheless, the concept of thermal comfort is not solely in a subjective domain since it depends to a certain extent on physiological processes in the body. It is in direct relation with a heat balance of the human body, i.e. the processes that lead to heat production and heat loss. The heat balance depends on a number of factors that could be classified into environmental, physiological and clothing factors. Therefore, the role of protective clothing in high-risk profession as fire fighting is of crucial significance for the thermal comfort of a wearer and its performance.

When firefighters are exposed to a heat stress, their body reacts by activating sweat glands, i.e. through evaporative cooling mechanism. The protective clothing protects the firefighters from environmental heat and moisture but simultaneously prevents their flow in the opposite direction, away from the body to the environment. Consequently, risks of heat stress and steam burn injuries strongly increase. In such hot environments, heat and moisture transfer properties of the protective clothing have prevailing impact on firefighters’ performances and their safety. Optimization of these coupled transfer phenomena from the skin through the garment could improve comfort of the wearers and hence their performance. Effective protective clothing should minimize heat stress while providing protection [2]. For this purpose, the firefighter protective clothing has to fulfill a variety of different demands according to the European standard EN 469: protection against heat from flames and thermal radiation, protection against hot liquids and other chemicals, resistance against abrasion and other mechanical stress, breathability, being not flammable, unshrinkable, easy to wash, light and comfortable [3].

Usually a protective clothing system for a firefighter consists of 3 or 4 layers:

- outer layer – that protects against all kind of thermal hazards and mechanical impact;
- thermal barrier – that is an insulating layer which protects against heat;
- moisture barrier – which protects against water and other fluids;

- inner layer – for increased thermal protection and to protect the last layer against abrasion.

Underwear is used between the jacket and skin and additionally a station uniform is worn between the underwear and firefighter jacket.

Investigations of comfort characteristics of firefighter protective clothing are complex because of the non-homogeneous internal structure, coupled heat and moisture transfer and other physical processes that occur in different space and time scales. During the last decade numerous studies have been carried out regarding the design and the mathematical modeling of different aspects of the physical behaviour of the protective clothing [4] – [7]. Two types of mathematical models have been developed: those that only consider heat transfer [7] – [9] and those that consider heat and moisture transfer [5], [10], [11].

According to Mäkinen [12], thermal environments are divided in three categories:

- Routine corresponds to a common intervention for firefighters characterized by low radiant heat flux from 0.42 to 1.26 kW/m$^2$ and air temperatures in the range of 10 to 60°C;
- Hazardous represents an intervention in the presence of high radiant heat flux from 1.26 to 8.37 kW/m$^2$ and air temperatures in the range of 60 to 300°C, and firefighters generally have less time to intervene;
- Emergency means extreme conditions from 8.37 to 125.6 kW/m$^2$ and air temperatures in the range of 300 to 1 000°C, and firefighters have only several seconds to escape.

Emergency conditions are quite rare and several studies were conducted on these conditions under the flash fire exposure [13] – [17]. Firefighters are most frequently exposed to low-level radiative heat flux [2]. Data obtained over the years show that most burn injuries sustained by firefighters occurred in thermal environments with low radiation level (classified as routine or hazardous conditions), as a result of prolonged exposure. Only a few studies have been conducted on thermal protective performance with prolonged exposure to low-level radiative heat flux. Moreover, firefighters working in these conditions often sweat, and that leads to significant changes in garments protective performance [5], [10], [11].

This paper presents initial results of research on heat transfer through multilayer protective textile structure for firefighters in conditions of low-level radiation.

## APPROACH AND METHODOLOGY

The physical model of a firefighter in a firefighting environment consists of three parts that are linked by heat and mass transfer: the human body that produces heat (metabolic heat) and water (sweat), the heat source from the environment and the protection system. In the initial phase of the study, only heat transfer is taken into account whereas the influence of moisture is not considered.

### Materials used

The fabrics selected for experiments are commonly used as high performance fabrics in the thermal protective clothing field. The studied multilayer system consists of three fabric layers: outer shell, thermal liner and moisture barrier.

Thickness of the monolayers was measured under the pressure of 1 ± 0.01 kPa, according to the standard ISO 5084:1996. Density was calculated from the values of fabric monolayer thickness and surface weight (determined using an analytical balance). The average of ten measurements was calculated.

The thermal properties of the fabric samples were measured with the Hot Disk TPS 2500 S instrument (Hot Disk AB, Gothenburg, SWEDEN), in agreement with the standard ISO 22007-2:2008. By applying the hot disk method, thermal conductivity, thermal diffusivity and specific heat capacity are simultaneously determined from a single measurement [18]. For each monolayer three measurements were performed and then the average of the measured parameters was calculated. General physical and thermal properties of monolayers are displayed in the table 1.

Table 1

PHYSICAL AND THERMAL PROPERTIES OF EACH MONOLAYER

| Property | Outer shell | Thermal liner | Moisture barrier |
|---|---|---|---|
| Fabric type | Woven | Nonwoven | Knitted (coated) |
| Composition | 100% Aramid | 100% Aramid | Polyurethane coated 100% Aramid |
| Thickness, mm | 0.5 ± 0.01 | 1.46 ± 0.03 | 0.47 ± 0.00 |
| Surface weight, g/m$^2$ | 242 ± 2 | 98 ± 2 | 195 ± 2 |
| Density, kg/m$^3$ | 489 ± 5 | 67 ± 2 | 418 ± 6 |
| Thermal conductivity, W/m · K | 0.1154 ± 0.0018 | 0.0633 ± 0.0015 | 0.0900 ± 0.0001 |
| Thermal diffusivity, mm$^2$/s | 0.248 ± 0.013 | 0.449 ± 0.001 | 0.213 ± 0.000 |
| Specific heat capacity, J/kg · K | 951 ± 44 | 2113 ± 89 | 1011 ± 3 |

## Experimental simulation of heat transfer through multilayer protective system

To perform the laboratory simulation of low-level radiant thermal hazards, six silicon carbide heating rods were employed as the radiant heat source as specified in ISO 6942:2002, for measuring radiant heat resistance. According to this standard, the levels of incident heat flux should be chosen from the following levels: low level 5 and 10 kW/m$^2$, medium level 20 and 40 kW/m$^2$ and high level 80 kW/m$^2$. However, other levels of incident heat flux may be chosen [19]. A copper plate calorimeter is used to record the temperature.

Thus, the radiation source was positioned to deliver 1 kW/m$^2$ inward heat flux. The calibration followed the standard, but the specimens were exposed to radiant heat flux for 40 minutes.

A protective shutter positioned between the radiant energy source and the specimen was used to block the radiant energy prior to the exposure of the specimen and to control the exposure time. At the end of exposure period the specimen was isolated from the heat source by closing the protective shutter and a cooling-down time followed.

The standard ISO 6942:2002 is used to determine the behavior of material for protective clothing, when exposed to a source of radiant heat, in steady-state conditions, but we extended the analysis also to transient conditions.

A Data Acquisition System connected to a computer equipped with TESTPOINT software was used for registering the results. Three specimens have been tested and the average values were determined.

## Numerical model

Due to the length scales of clothing thickness compared to their surface, a one-dimensional model is adopted as a valid assumption (fig. 1).

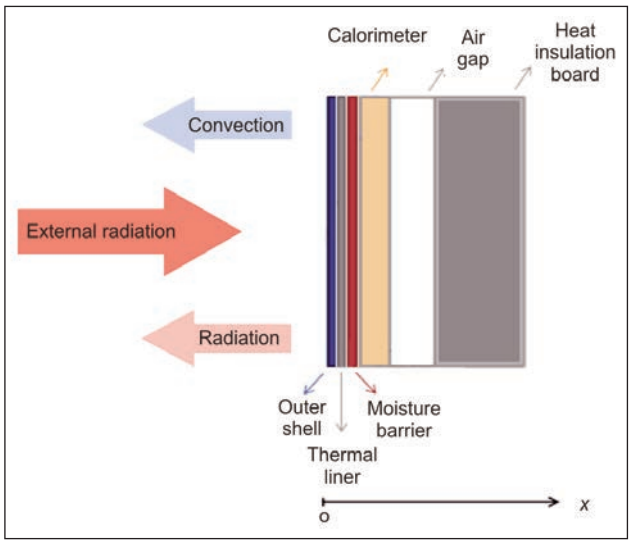


Fig. 1. Scheme of the experimental setup used for evaluation of the material assemblies when exposed to a source of low-radiant heat flux

For the development of the numerical model it was supposed that the temperature depends only on time and position, $T$ ($t$, $x$). Heat conduction and penetrating radiation through solid phase are considered for heat transfer within the fabric. Radiative heat transfer in the fabric is accounted for by introducing in the energy equation a source term similar to that in Torvi's model [8]. It is assumed that radiation penetrates through the outer layer of the fabric only. The conductive and radiative heat transfer mechanisms are considered through the air gap.

The energy balance in the infinitesimal element of the fabric, for one dimensional heat transfer, can be described in the form of differential equation (1):

$$\rho c_p \frac{\partial T}{\partial t} = -\frac{\partial}{\partial x} \cdot \left(-k \frac{\partial T}{\partial x}\right) + \gamma q_{rad} e^{-\gamma x} \quad \text{for } 0 < t \leq t_{exp}$$

$$\rho c_p \frac{\partial T}{\partial t} = -\frac{\partial}{\partial x} \cdot \left(-k \frac{\partial T}{\partial x}\right) \quad \text{for } t > t_{exp} \tag{1}$$

where:

$\rho$ is density, kg/m$^3$;

$c_p$ – heat capacity at constant pressure, J/kg · K;

$k$ – thermal conductivity, W/m · K;

$\gamma$ – extinction coefficient of the fabric, 1/m;

$q_{rad}$ – incident radiation heat flux, W/m$^2$;

$t_{exp}$ – time of exposure;

$x$ – linear horizontal coordinate.

The extinction coefficient that characterizes the decrease of thermal radiation as it penetrates into the fabric is given as:

$$\gamma = \frac{-\ln(\tau)}{l_{fab}} \tag{2}$$

where:

$\gamma$ is the transmissivity of the fabric;

$l_{fab}$ – the fabric thickness.

A constant inward heat flux, convective and radiative heat transfers are assumed on the left external boundary and a constant temperature (ambient temperature) is considered on the right side.

The general inward heat flux $Q$ (W/m$^2$) represents a heat flux that enters into domain. The emitted radiative heat flux is defined as:

$$Q_{rad-out} = \varepsilon \sigma (T_{amb}^4 - T_{surf}^4) \quad [\text{W/m}^2] \tag{3}$$

where:

$\varepsilon$ is emissivity of the fabric;

$\sigma$ – Stefan-Boltzmann constant, W/m$^2$K$^4$;

$T_{surf}$ – surface temperature, K;

$T_{amb}$ – ambient temperature, K.

Natural convection heat transfer due to the temperature gradient between the surface and the environment is described by the following equation:

$$Q_{conv} = h_c (T_{amb} - T_{surf}) \quad [\text{W/m}^2] \tag{4}$$

where:

$h_c$ is natural convection heat transfer coefficient ($W/m^2K$) that is calculated using the definition of the Nusselt number:

$$h_c = Nu \frac{k_{air}}{L} \quad (W/m^2K) \tag{5}$$

where:

$Nu$ is the Nusselt number;

$k_{air}$ – the thermal conductivity of the air, W/m·K;

$L$ – the characteristic length, m.

The Nusselt number was estimated using the empirical correlation of free convection on a vertical plate [20]. The heat flux by radiation across the air gap is the radiation heat exchange between two gray parallel surfaces [21]:

$$Q_{rad-air} = \frac{\sigma\left(T_{surf1}^4 - T_{surf2}^4\right)}{\left(\frac{1}{\varepsilon_1} + \frac{1}{\varepsilon_2} - 1\right)} \tag{6}$$

where:

$\varepsilon_1$ is emissivity of the inner surface of the calorimeter;

$\varepsilon_1$ – emissivity of the insulation board;

$\sigma$ – Stefan-Boltzmann constant, $W/m^2K^4$;

$T_{surf1}$ – temperature of the inside surface of the calorimeter, K;

$T_{surf2}$ – temperature of the insulation board surface, K.

The fabric initial temperature is considered equal to the ambient temperature.

$$T_{fab}(x, t=0) = T_{amb} \tag{7}$$

Based on data in the literature, an emissivity of 0.9 and a transmissivity of 0.01 were assumed for the fabric [7]. Emissivity of the inner surface of the calorimeter was considered 0.78 and the emissivity of the insulation board 0.96 [22]. The Finite Element Method (FEM) was used to evaluate the heat transfer by means of the Comsol Multiphysics® package.

## RESULTS AND DISCUSSIONS

Figure 2 shows the evolution of temperature over time according to measurements and numerical simulation, respectively. The temperature of the calorimeter starts rising sharply as the fabric system is exposed to the radiant flux at $t = 0$ and then gradually rises until the stabilization. The steady state condition is reached after approximately 1 600 seconds, and the temperature stabilized at approximately 75°C. After stopping the radiant flux ($t \geq 2\,400$), the temperature decreases until it reaches again the initial value of the environment.

The numerically predicted profiles follow the experimental data. During the heating period, the difference between the experimental and the numerical values can be explained by the fact that heat accumulates in front of the shutter and when the shutter opens this extra heat is added to the radiative flux. As result, there is a steeper temperature gradient compared with the predicted values. The differences between experimental and predicted values during cooling-down period are due to the cooling system of the shutter that speeds up the cooling effect, and was not considered in the numerical model.

Figure 3 displays the distribution of temperature in the complete system tested, including the multilayer textile structure along with cooper plate and insulation board. The most pronounced increase in temperature within the protective clothing is observed in the initial 10 minutes of exposure to low-level radiant flux. The difference between the outer surface of the outer shell temperature and the moisture barrier backside temperature is between 40% and 15% (between 22°C and 11.6°C difference) in this interval. At equilibrium, the difference becomes smaller (9.5% corresponding to a temperature difference of around 8°C). Thus, the thermal protective efficiency of the protective system is higher during the first 10 minutes of exposure.

The temperature profile through the textile structure (2.43 mm) is not linear due to different thermal properties of each monolayer. The sharpest temperature

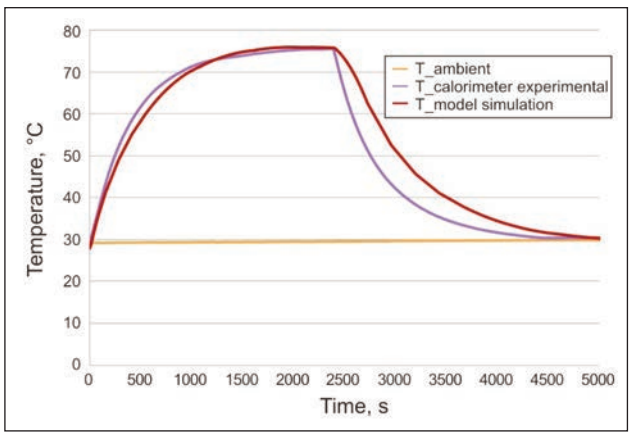


Fig. 2. Comparison of computational and experimental results

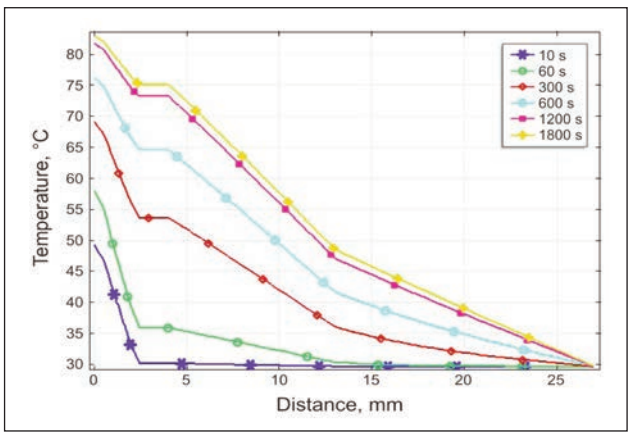


Fig. 3. Temperature distribution in the fabric at different time points, predicted by the numerical model

distribution profile (i.e. the best isolation capacity) was obtained across the thermal liner since this monolayer has the lowest thermal conductivity.
It is worth noting: since the tests are carried out at room temperature, the results do not necessarily correspond to the behavior of the materials at higher ambient temperature, and therefore are only to a limited extent suitable for predicting the performance of the protective clothing made from the materials under test.
Moreover, in real situation, air gaps exist between the fabric layers and between the last layer and the skin. The thickness of the air gap between the garment and the body depends on the particular location on the human body.
According to Song [7] the maximum air gaps occur for the leg (15–22 mm) and the minimum air gap occurs for the shoulders (0–1.6 mm). As air is a good insulator, the air gap will increase the degree of insulation and slow down heat transfer to the skin.

## CONCLUSIONS

A numerical model of heat transfer in protective clothing during exposure to low level of radiative heat flux was developed using the software Comsol Multiphysics® and the computational results were compared with the experimental ones. The predicted temperature values are in good agreement with the corresponding experimental measurements. At this stage, the model is restricted to dry fabrics, but further developments should include moisture effects.
This model could be used as an aid in the design of candidate protective clothing systems, by evaluating the performance of protective clothing systems in various thermal environments. Thus, the model can be used to determine the effect of various parameters such as fabric thickness and density, thermal properties such as thermal conductivity and specific heat capacity, optical properties etc., or of environmental conditions such as radiant heat flux and ambient temperature, on the protective performance of clothing. These properties and parameters can be varied dynamically during the simulation.

## FUTURE RESEARCH AND PERSPECTIVES

The transfer of moisture through a multilayer clothing system should be investigated. The heat and moisture transfers should be coupled in a model to perform a detailed thermal analysis of the clothing system. A skin model should be coupled with the heat and mass transfer model to predict burn injury, by estimating the time for occurrence of the 1st and 2nd degree burns from thermal radiation.


## ACKNOWLEDGEMENTS

The authors gratefully acknowledge the region Nord-Pas-de-Calais and the European Regional Development Fund for their financial support.


## BIBLIOGRAPHY


[1] ASHRAE Standard 55:2010. *Thermal Environmental Conditions for Human Occupancy*

[2] Song, G., Paskaluk, S., Sati, R. et al. *Thermal protective performance of protective clothing used for low radiant heat protection*. In: Textile Research Journal, 2011, issue 81, pp. 311-323

[3] European Standard EN 469:2006. *Protective clothing for firefighters. Performance requirements for protective clothing for firefighting*

[4] Onofrei E., *Identification of the most significant factors influencing thermal comfort using principal component analysis and selection of the fabric according to the apparel end-use*, In: Industria Textila, 2012, vol. 63, Issue: 2, pp. 91-96

[5] Korycki, R. *Method of thickness optimization of textile structures during coupled heat and mass transport*. In: Fibres & Textile in Eastern Europe, 2009, issue 17, pp. 33-38

[6] Loghin, C. *Îmbracăminte funcțională – Modelarea și simularea funcțiilor de protecție*. Iasi, PIM, 2008

[7] Song, G. *Modeling thermal protection outfits for fire exposures.* PhD Thesis, North Carolina State University, USA, 2002

[8] Torvi, D. *Heat transfer in thin fibrous materials under high heat flux conditions.* PhD Thesis, University of Alberta, USA, 1997

[9] Das, A., Alagirusamy, R., Kumar, P. *Study of heat transfer through multilayer clothing assemblies: A theoretical prediction*. In: AUTEX Research Journal, 2011, issue 11, pp. 54-60

[10] Sybilska, W., Korycki, R. *Analysis of coupled heat and water vapour transfer in textile laminates with a membrane*. In: Fibres & Textile in Eastern Europe, 2010, issue 18, pp. 65-69

[11] Li, Y., Zhu, Q. *Simultaneous heat and moisture transfer with moisture sorption, condensation, and capillary liquid diffusion in porous textiles*. In: Textile Research Journal, 2003, issue 73, pp. 515-524

[12] Mäkinen, H. *Firefighter's protective clothing.* In: Scott RA (ed.) Textiles for Protection. Cambridge, Woodhead, UK, 2005, pp. 622-647

[13] Song, G., Chitrphiromsri, P., Ding, D. *Numerical simulations of heat and moisture transport in thermal protective clothing under flash fire conditions*. In: The International Journal of Occupational Safety and Ergonomics, 2008, issue 14, pp. 89-106

[14] Chitrphiromsri, P. *Modeling of thermal performance of firefighter protective clothing during the intense heat exposure*. PhD Thesis, North Carolina State University, USA, 2004

[15] Chitrphiromsri, P., Kuznetsov, A. V. *Modeling heat and moisture transport in firefighter protective clothing during flash fire exposure*. In: Heat Mass Transfer, 2004, issue 41, pp. 206-215

[16] Ghazy, A., Bergstrom, D. J. *Influence of the air gap between protective clothing and skin on clothing performance during flash fire exposure.* In: Heat Mass Transfer, 2011, issue 47, pp. 1 275-1 288

[17] Mercer, G. N., Sidhu, S. H. *Mathematical modeling of the effect of fire exposure on a new type of protective clothing.* In: ANZIAM, 2008, issue 49, pp. C289–C305

[18] ISO 22007-2:2008. *Plastics – Determination of thermal conductivity and thermal diffusivity.* Part 2: *Transient plane heat source (hot disc) method*

[19] ISO 6942:2002. *Protective clothing – Protection against heat and fire – Evaluation of materials and material assemblies when exposed to a source of radiant heat*

[20] Comsol Multiphysics® package.

[21] Kothandaraman, C. P. *Fundamental of heat and mass transfer*. New Age International (P) Limited Publishers, Revised third edition, 2006, ISBN (13):978-81-224-2642-7, p. 608

[22] Tools and Basic information for design, engineering and construction of technical applications, http://www.engineeringtoolbox.com/emissivity-coefficients-d_447.html (accessed 21 October 2013)

**Authors:**

ELENA ONOFREI
Université Catholique de Lille
HEI, GEMTEX, Lille, F-59046 France
Technical University "Gheorghe Asachi"
Iasi, 700050, Romania

GAUTHIER BEDEK
DANIEL DUPONT
Université Catholique de Lille
HEI, GEMTEX, Lille, F-59046 France

STOJANKA PETRUSIC
DAMIEN SOULAT
TEODOR-CEZAR CODAU
Université Lille Nord de France
Lille, F-5900 France

ENSAIT, GEMTEX
Roubaix, F-59056 France

e-mail: eonofrei@yahoo.com; elena.onofrei@hei.fr

# Analysis of lubricants used for spinning of polyester filament yarns

IULIAN MANCAȘI
DANIELA FARÎMĂ
ALEXANDRA ENE

**REZUMAT – ABSTRACT**

**Analiza lubrifianților utilizați la filarea firelor filamentare de poliester**

*Prelucrarea firelor filamentare de poliester pe mașini specifice industriei textile este posibilă datorită tratării preliminare a filamentelor cu un amestec de substanțe, numit generic ulei de filare. Tratamentul se efectuează cu scopul de a reduce coeficientul de frecare statică și dinamică a firului din poliester filamentar. Dacă uleiul de filare este într-un procent de maximum 2%, prelucrarea mecano - textilă se desfășoară în condiții normale. Dacă uleiul de filare este prezent pe fir într-un procent mai mare, există dezavantajul ca, la contactul cu organele de lucru ale masinii de țesut, acesta să se acumuleze și să se depună pe țesătură. Cunoașterea compoziției uleiului de filare este absolut necesară în stabilirea unor rețete eficiente pentru eliminarea petelor de pe țesătură, acestea având un impact negativ asupra calității. În acest context, în lucrare este studiată compoziția uleiului de filare, folosind analizele spectrale RMN și FT-IR.*

*Cuvinte-cheie: fire, filamente, poliester, spectru RMN, spectru IR*

**Analysis of lubricants used for spinning of polyester filament yarns**

*The processing of the polyester filament yarns in the specific textile machinery industry requires a previous treatment of the filaments with mixtures of substances generically called spinning oils. The treatment is necessary in order to reduce the static and dynamic friction between the filament threads and different weaving machine surfaces. A satisfactory process takes place when the loading of filament threads with spinning oil is about 2%. When the loading is larger the spinning oil accumulates on the contact surfaces of the processing machine what creates unwanted oil spots on the textile. The knowledge of the spinning oil composition is absolutely necessary in order to develop cleaning materials for effective removing of the spots, ensuring by this way fabrics of good quality. In this order, this paper presents the identification of spinning oil compositions by using NMR and IR spectroscopy methods.*

*Key-words: filaments, yarns, polyester, NMR analysis, IR analysis*

It is known that the processing of polyester filament yarns requires the use of a lubricant usually called spinning oil to reduce the friction in the contact areas between the fibres and machine surfaces. There are important unwanted effects of this friction, from surface cracks to breakage of the filaments. The use of spinning oil is considered a necessary evil, the effects of which are both beneficial for protection of the filaments and generating unwanted oil spots on fabrics if the oil accumulates in too large quantities on the components of, for example, a weaving machine (yarn conductors and holders). Efficient washing recipes to eliminate stains on fabrics can be performed if the lubricant chemical composition is known. In this context, we used accurate methods like the Nuclear Magnetic Resonance (NMR) and infrared (IR) spectroscopy to identify chemical compositions and to measure concentrations [1] – [5].

## EXPERIMENTAL PART

The following polyester thread samples were analyzed:

- $M_1$ with $T_t$ = 75 den/f 36 · 1;
- $M_2$ with $T_t$ = 150 den/f 36 · 1;
- $M_3$ with $T_t$ = 150 den/f 36 · 2.

## Separation and identification of lubrication products

### *Extraction with chloroform*

Amounts of about 10 g of each thread sample were plunged in 50 ml of chloroform for 24 hours at room temperature. To avoid solvent evaporation the operation was performed in tightly closed desiccators. Finally the chloroform solutions were separated from fibres by filtering.

### *Solvent removal and extraction products*

Chloroform (b. p. 61°C) was first removed by free evaporation and then by forced evaporation at 60–65°C for 4 days. The solvent removal from the extraction products was initially proved organoleptic and subsequently by absence of any characteristic spectral signals. The extraction process led to two kinds of products for each sample of yarns: an oily liquid further on noted *LM* and a fine white powder, noted *SM*. The separation of the two kinds of extraction products was performed by washing with toluene of PA quality. This solvent dissolved only oil products *LM* leaving the white powder deposited on the glass bottom. Finally the *LM* products resulted after complete toluene evaporation.

## NMR and IR spectra

The proton NMR spectra were recorded from deuterated chloroform solutions at 400 MHz and 300 K by using a DRX 400 Bruker NMR spectrometer, while the Fourier Transform Infrared (FT-IR) spectra were obtained with a Vertex 80 Bruker FTIR spectrometer using liquid films coated on *KBr* tablets for oil products *LM* and *KBr* – solid sample mixture tablets in the case of solid products, *SM*.

## RESULTS AND DISCUSSIONS

### Spectral analyses of extraction products

One observes that the three spectra are identical between them what means that the same type of lubricant has been used in the manufacturing process of the three polyester yarns samples. The NMR spectra for the raw products, resulted by chloroform extraction, from the three polyester yarns samples are shown in figure 1, figure 2 and figure 3.

The following main signals are distinguished:

- 0.5–1.5 ppm – two intense signals, which according to the attribution rules would arrive from the alkyl type structures;
- 3.65 ppm – a singlet signal, which could be attributed to methylene and or methine groups in ether and/or alcoholic structures, $CH_2O$ or CHO or $CH_2OH$ or CHOH;
- 4.7 and 8.15 ppm – two singlet signals of equal intensities, which according to the position, shape and relative intensity can be attributed to short chains of polyethylene terephthalate (polyester).

A dilemma was if the ether or alcoholic groups are chemically bonded to sequences of polyethylene terephthalate. Therefore, a further analytical investigation of the extraction products was necessary.

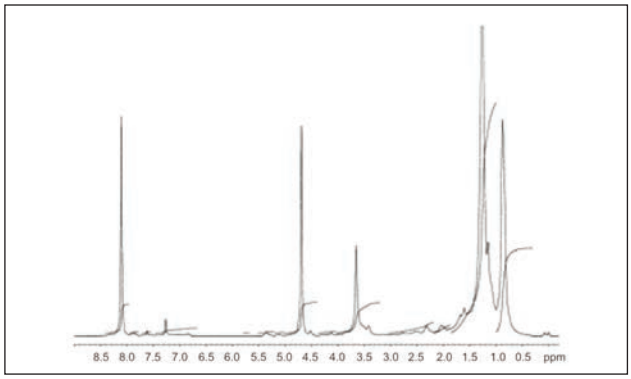


Fig. 1. Proton NMR spectrum for $M_1$ extract

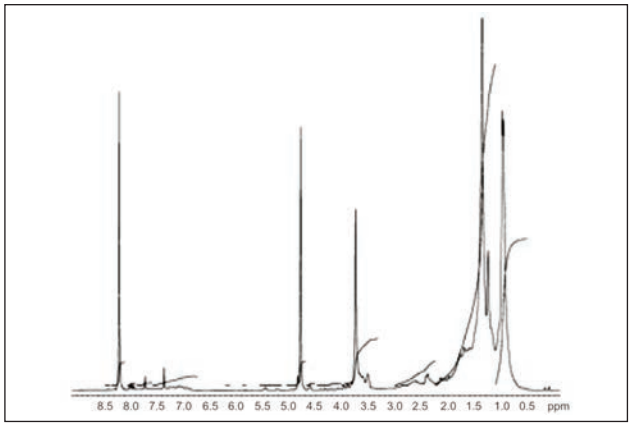


Fig. 2. Proton NMR spectrum for $M_2$ extract

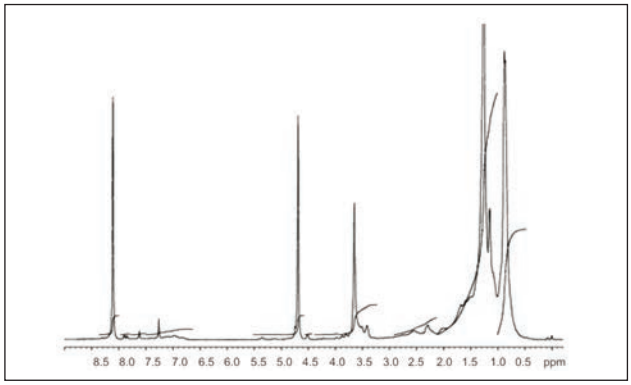


Fig. 3. Proton NMR spectrum for $M_3$ extract

### Analysis of the global extracts to identify the components

NMR spectra obtained for the viscous liquid *LM* and powder *SM* components separated from global extraction products by toluene washing are presented in figure 4 and figure 5.

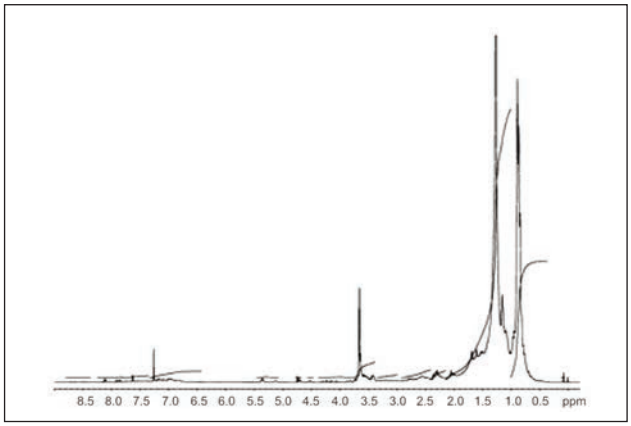


Fig. 4. Proton NMR spectrum of the liquid component, *LM*

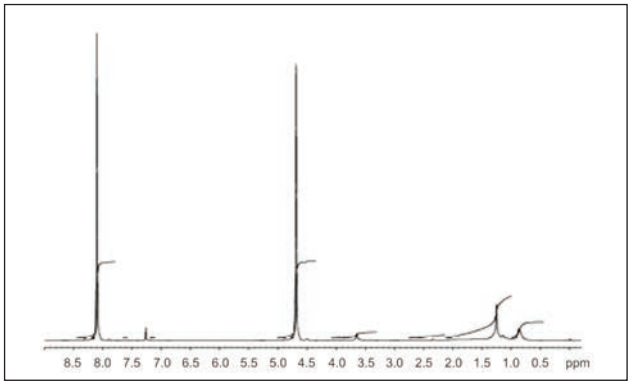


Fig. 5. Proton NMR spectrum of the powder component, *SM*

## Identification of oil (liquid) component

By comparing the spectrum in figure 4 with those in figures 1–3, one observes that the group of signals in the region 0.5–4 ppm appears in all cases, while the signals at 4.7 and 8.15 ppm are practically absent in figure 4. It results that the oily liquid components *LM* are not chemically linked to the sequences attributed to polyethylene terephthalate, therefore the alkyl and ether structures do not belong to of this polymer. Moreover, taking into account the relative signal intensities, namely that the alkyl structures are much more numerous than the ether or alcoholic groups, one results that the two types of groups belong to different molecules.

The most intense signals in the region of 0.5–1.5 ppm, the quasi triplet at about 0.85 ppm and the quasi singlet at 1.25 ppm, may be rather certainly attributed to $-(CH_2)_n-CH_3$ fragments. Using signal intensity ratios, one resulted $n$ = 3.93 ~ 4. These $-(CH_2)_n-CH_3$ fragments are end groups and they can be linked between them in various ways, two of the most probable ones being presented in table 1.

As a singlet, the signal from 3.65 ppm can only arise from polyethylene glycol segments, $HO-(CH_2CH_2O)_m-H$, the number m representing the degree of polymerization. A value $m \cong 7$ resulted from the ratio between $CH_2$ (3.4–3.6 ppm) and OH signal intensities.

Table 1

| POSSIBLE COMBINATION OF THE FRAGMENTS $-(CH_2)_4-CH_3$ | | |
|---|---|---|
| **Structural formula** | **General formula** | **Note** |
| $[H_3C-(CH_2)_4]_k\ CH_{4-k}$ | $C_{5k+1}H_{10k+4}$ | $U_k$ |
| $[H_3C-(CH_2)_4]_l\ C_2H_{6-l}$ | $C_{5l+2}\ H_{10l+6}$ | $U_l$ |

The fact that structures of ethylene glycol etherified or esterified with alkyl groups, namely $(CH_2CH_2O)-CH_2(CH_2)_3CH_3$ or $(CH_2CH_2O)\text{-}COCH_2-(CH_2)_3CH_3$, are not present results from the absence of signals specific to the groups $-O-CH_2(CH_2)_3CH_3$ (triplet at 3.2–3.4 ppm) and $-CH_2-OCO-CH_2\ (CH_2)_3CH_3$ (triplets at 3.9–4.2 ppm and 2.2–2.3 ppm).

All these assessments resulted for the liquid component, encoded *LM*, lead to the conclusion that this component is composed of alkyl molecules with the average structures shown in table 1 and polyethylene glycol with average polymerization degree of about 7. Taking into consideration that:

- the liquid products *LM* are composed of alkyl molecules known also as paraffin oils with general formula $C_nH_{2n+2}$, with $n$ between 8 and 18 [1];
- the formula in table 1, one can be concluded that the lubricants mainly contain paraffin oils of $U_k$ type, with $k$ between 1.2 and 3.4.

The second component is polyethylene glycol of low molecular weight (1). According to the NMR spectra, the ratio between the two components corresponds to an alkyl-to-glycol group molar ratio of about 4.

$$HO-(CH_2CH_2O)_7-H \qquad (1)$$

Such a conclusion is also supported by FT-IR spectra (fig. 6) where the main absorption band at around 2 900 $cm^{-1}$ is associated to C–H bond stretching vibrations, respectively, the band at 2 954 $cm^{-1}$ for asymmetric vibrations in $CH_2$ groups and the band of 2 854 $cm^{-1}$ for $CH_2$ symmetric vibrations. C–H bending vibrations appear at 1 462 $cm^{-1}$ for $CH_2$ groups and 1 377 $cm^{-1}$ for $CH_3$ groups.

## Identification of the solid component

The proton NMR spectrum of this component *SM* is shown in figure 5. There are two singlet signals of the same intensity and placed 4.68 and 8.10 ppm, respectively. These signals correspond to methylene and aromatic protons of the polyethylene terephthalate structural unit. Some traces of paraffin oil and polyethylene glycol are associated to the signals at 0.8 and 3.7 ppm, respectively.

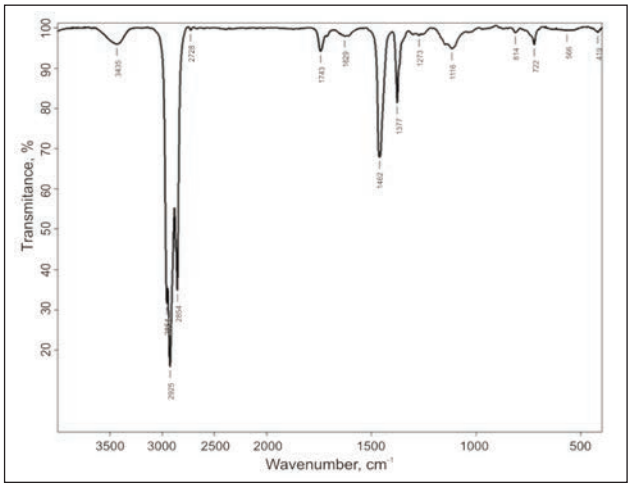


Fig. 6. FT-IR spectrum of liquid component, *LM*

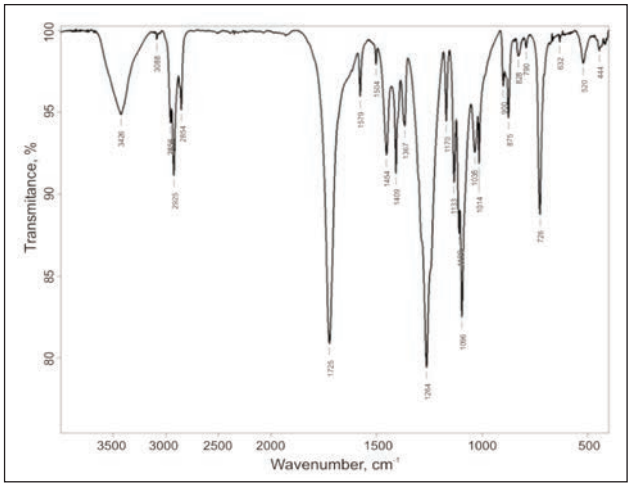


Fig. 7. IFR spectrum of the solid part (*VB - MS*)

The hypothesis of polyethylene terephthalate is confirmed by the FTIR spectra (fig. 7) by vibration bands of C–H bond at 2 956 $cm^{-1}$ for asymmetric vibration from the benzene ring, 2 925 $cm^{-1}$ for asymmetric vibration from the $CH_2$ group, 2 854 $cm^{-1}$ for symmetric vibration from the $CH_2$ group, C–O intense vibration band at 1 725 $cm^{-1}$, C–O vibration intense band at 1 264 $cm^{-1}$ for CO–O group, C–O vibration intense band at 1 096 $cm^{-1}$ for COH ends, O–H band deformation in $CH_2$ group at 1 454 $cm^{-1}$, and O–H band deformation for COH ends at 726 $cm^{-1}$.

The presence of a significant absorption band at 3 426 $cm^{-1}$ which is normally attributed to alcoholic and water molecules shows that the products *SM* consists of relatively short chains of polyethylene terephthalate (soluble in chloroform) ended by the alcoholic groups, as follows:

$$HO\text{-}CH_2CH_2\text{-}[OOC\text{-}pC_6H_4\text{-}COOO\text{-}CH_2CH_2]_{2\text{-}3}\text{-}OH \quad (2)$$

However the presence of polyethylene terephthalate in the extraction products is due to the fact that chloroform extracts short molecular chains of this polymer from the threads. Being lower than 0.1% of the weight of the fibres subjected to extraction, these short chains can be caused by hydrolysis, a process favoured by the rather high surface temperature of the friction areas between the filaments and processing machines.

## CONCLUSIONS

The spectral analyses showed that the lubricant used during the polyester yarns processing consists of paraffin oils with general formula $C_pH_{2p+4}$, where $1.2 < p < 3.4$ ppm and polyethylene glycol of low molecular weight ($HO\text{–}(CH_2CH_2O)_7\text{–}H$). The ratio of the two components can be estimated from the molar ratio between the alkyl and ethylene groups that was approximated to be 4.

A solid component found in very small percentage in the chloroform extraction products of fibres was found to be composed of short polyester chains and such molecules are supposed to be the result of a hydrolysis process which happens due to the friction between polyester threads and processing machines.

## BIBLIOGRAPHY


[1] Nenițescu, C. D. *Tratat de chimie organică*. Editura Didactică și Pedagogică, București, 1980

[2] Seymour, R. B., Carraher, C. E. *Polymer chemistry introduction*. 3rd Ed. Marcel Dekker, New York, 1992

[3] Herman, F. M. *Encyclopaedia of polymer science and technology*, vol. 6. Ed. J. Wiley, New York, 1985, p. 818,

[4] Cioara L., Cioara I., Aspects of the behavior to cyclic tensioning for the woven filters with simple structure, In: Industria Textila 2013, Vol. 64, Issue: 3, pp. 136-140

[5] Lorentz, Jäntschi. *Physics chemistry. Chemical and instrumental analyses*. Ed. Academic Direct, ISBN 973-86211-7-8, 2004



**Authors:**

*Lect. dr. ing.* DANIELA FĂRÎMĂ
Universitatea Technică Gheorghe Asachi
Facultatea de Textile, Pielărie și Management Industrial
Bd. Dimitrie Mangeron nr. 53
700050 Iaşi
e-mail: dfarima@tex.tuiasi.ro

*Dr. ing.* IULIAN MANCAȘI
Majutex Ltd. Iasi
e-mail: iulian.mancasi@majutex.ro

*Cerc. şt. dr. ing.* ALEXANDRA ENE
Institutul Național de Cercetare-Dezvoltare pentru Textile și Pielărie
Str. Lucreţiu Pătrăşcanu nr. 16, 030508 Bucureşti
e-mail: certex@ns.certex.ro

# Properties of the knitted upper clothes used by primary school children

NILGÜN ÖZDİL
SERKAN BOZ
ZÜMRÜT BAHADIR UNAL
GAMZE SÜPÜREN MENGÜÇ

**REZUMAT – ABSTRACT**

**Proprietățile confecțiilor tricotate purtate în partea superioară a corpului de către elevii de școală primară**

*Pe măsura dezvoltării tehnologiei, o atenție din ce în ce mai mare a fost acordată confortului personal conferit de articolele de îmbrăcăminte și caracteristicilor ergonomice ale creațiilor vestimentare. Ca urmare, caracteristicile tehnice ale tricoturilor au devenit mai accesibile utilizatorilor și nu mai reprezintă o categorie de lux. O importanță foarte mare se acordă utilizării unor tricoturi destinate confecționării îmbrăcămintei elevilor din școala primară care să confere un confort fiziologic sporit. Creațiile vestimentare nu trebuie să limiteze libertatea de mișcare a copiilor, ci să posede caracteristici care să faciliteze activitățile zilnice ale acestora, contribuind la menținerea sănătății lor. În lucrare sunt investigate caracteristicile de performanță și de confort ale tricoturilor destinate confecționării uniformelor școlare. În acest scop, au fost utilizate șase tipuri de tricoturi glat, din diverse materiale. Au fost analizate următoarele caracteristici: grosimea tricotului, rezistența la abraziune și la piling, rezistența la rupere, elasticitatea, permeabilitatea la aer, permeabilitatea la vapori de apă și managementul umidității. Rezultatele testelor au fost comparate prin metode statistice. Au fost identificate cele mai adecvate materiale, în funcție de sezon.*

*Cuvinte-cheie: uniformă școlară, material tricotat, proprietăți fizice, proprietăți de confort*

**Properties of the knitted upper clothes used by primary school children**

*Along with the development in the technology, products that supply personal comfort and ergonomically appropriate designs have become more significant. For this purpose, the technical characteristics of fabrics make lives easier and they are no longer luxury. In particular physiological comfort properties of the materials used in the design of primary school students' school clothes have great importance. Designs should not limit the movements of the children, should be appropriate for health and be enriched with features to facilitate the daily lives of the children. In this study, performance and various comfort properties of knitted fabrics that are used in the production of school outwears were investigated. For this purpose, six different single jersey fabrics made from different materials were used. Thickness, abrasion and pilling resistance, bursting strength, stretchability, air permeability, water vapor permeability and moisture management properties of the fabrics were measured. Test results were compared by using statistical methods. By taking the seasonal changes into account, the most appropriate material for usage was aimed to be suggested.*

*Key-words: school clothing, knitted fabric, physical properties, comfort properties*

People prefer comfortable and easy-to-use dresses in order to remove the fatigue and stress brought by daily life. As it is known, knitted clothes provide comfortable movement probability compared to woven clothing, since they are better adapted to the body [1]. Furthermore, light weight of knitted fabrics prevents sense of extra weight of dress at the body and consequently increases the sense of comfort [2].

Clothing comfort is an extremely complex subject. A recent overview and position paper on the conceptualization of clothing comfort defined it as “State of satisfaction indicating physiological, psychological, and physical balance between the person, his/her clothing, and his/her environment” [3]. Clothing comfort is not only an important subject for young people and adults, but also for the children. According to the experts, children don't like to wear tight clothes, necked sweaters and clothes with zippers. Besides the model of children clothes, the suitability of the fabric, freedom of movement, good handle and ease-of-use are very important [4]. It is an important parameter for the primary school-age children to wear their school clothes willingly, since they spend most of their time in them. The tensile strength and abrasion resistance properties of garments have traditionally been considered as the most obvious indicators of the service life of apparel. Secondly, they have to be enough stretchable and not limit the movements of the children. Thirdly, they have to be qualified to meet the expectations like thermophysiological and tactile comfort. School clothes consist of upper clothes which contact with the human skin and they have great importance by means of garment ergonomics and comfort. Since the children are more active, they move faster and sweat more than adults, who are comparatively less active. Their clothes have to facilitate water vapour and liquid moisture to be transferred from skin surface to the other side of the garments to avoid the possibility of illnesses [5].

The clothes should allow perspiration to be transferred to the atmosphere in order to maintain the thermal balance of the body. Moisture transmission through textile materials has been recognized as an

important factor in many applications [6]. Moisture transport properties of textiles are maintained by perspiring both in vapour and liquid form. The process of moisture transport through clothing under transient humidity conditions is an important factor which influences the dynamic comfort of the wearer in practical use [7]. Water vapor can pass through the fabric by different processes, diffusion of the water vapour through the fibre layers, absorption–desorption of vapour by fibres and transmission of water vapour by forced convection. Liquid moisture flow through textile materials is a combination of wetting and wicking. Wetting is the initial process involving the fluid spreading wherein the fibre-air interface is displaced with the fibre-liquid interface. In the case of textile material, as soon as water wets the fibre it enters into the inter-fibre capillary channel and is dragged along by the action of capillary pressure and the process of "wicking" takes place [6].

Capillary action or capillarity can be defined as the macroscopic motion or flow of a liquid under the influence of its own surface and interfacial forces in narrow tubes, cracks and voids. The surface tension is based on the intermolecular forces of cohesion and adhesion. When the forces of adhesion between the liquid and the tube wall are greater than the forces of cohesion between the molecules of the liquid, then capillary motion occurs. Flow ceases when the pressure difference becomes zero. The primary driving forces responsible for the movement of moisture along the fabric are the forces of capillarity [8].

Wetting behaviour of the fibre is mainly dependent on its chemical nature and roughness of the fibre surface, whereas capillary action through the inter-fibre and inter-yarn channel is also dependent on the number of capillaries formed, diameter of the capillary and tortuosity of the channels [6].

The two forms of perspiration raise separate problems: one is the ability of water vapour to pass through the fabric, particularly the outer layer and the other is the absorption ability of the fabric in contact with the skin or otherwise dealing with the liquid sweat. A fabric of low moisture vapour permeability is unable to pass sufficient perspiration and this leads to sweat accumulation in the clothing and hence discomfort. The fabrics most likely to have a low permeability are the ones that have been coated to make them waterproof. The coatings used to keep out liquid water will also block the transport of water vapour [9]. During exercise, liquid water accumulates on the skin and starts to wet the clothing layers above the skin. Depending on the temperature and humidity gradient across the clothing, the water vapour either leaves the clothing or condenses and freezes somewhere in its outer layers [10]. In sweating conditions, wicking is the most effective process to maintain a feel of comfort. In the case of clothing with high wicking properties, moisture coming from the skin is spread throughout the fabric offering a dry feeling and the spreading of the liquid enables moisture to evaporate easily [7].

Different fibres thus absorb different amounts of water. Cotton fabrics have good water absorptivity. They are heavy when wet and sag due to the extra weight. Cotton fibres collect moisture in spite of flowing it out. As a result, it creates a clammy feeling in high sweating conditions. And also it takes too long to dry, sticks to the skin, restricts movement and after the activity ends, the wearer often feels cold. Cotton fabric's absorbent capacity can be reduced by making the fabric thinner by using finer yarns and by making more open constructions [11]. In the case of polyester fabrics, even though capillarity is good, due to the poor wettability they are not comfortable to wear. The fabrics produced from polyester micro denier fibres have a high water uptake and due to the high number of capillaries a large amount of moisture can pass very quickly through them to the atmosphere, thus providing a dry and comfortable feeling to the wearer [7]. Viscose is another important cellulosic fibre mostly used in textiles. Viscose fibres are hydrophilic, absorbent, and skin-friendly. Viscose fibres have higher moisture regain properties and good moisture management compared to other cellulosic fibres. When it is wetted, it absorbs much water but higher amount of the amorphous region in fibre structure causes a decrease in fabric strength [12]. Apart from moisture management properties, air permeability is also an important factor in the comfort of a fabric as it plays a role in transporting moisture vapour from the skin to the outside atmosphere [13].

There are several studies in the literature related with usage performance of school uniforms. Üstün and Çeğindir (2006) investigated the comfort satisfaction of the primary school students and their mothers about the school uniforms. For this purpose, they applied a questionnaire to 204 students (7–14 age range) and to their mothers. It was determined that 67% of the participants were satisfied with their uniforms, however 60% of them were unsatisfied with the usage performance [14].

Ağaç and Harmankaya (2009) researched the effects on the school uniform preferences and they applied a questionnaire to 220 students (7–11 age range). It was pointed out that "mother" is the most effective person on shopping preferences of students and the students need help during fastening the button, while they are dressing. Therefore, the zipper is more often preferred [15].

There are not many researches related to mechanical and comfort properties of the upper school uniform in the literature. The aim of the study is to investigate the mechanical and comfort properties of fabrics produced from alternative materials and used for school uniforms.

## MATERIALS AND METHODS

There are several types of fabrics that are used in the production of school clothes. Most of them are knitted in various constructions by using cotton yarns in different yarn counts. In some types, such as single jersey, elastane yarn could also be used to increase

Table 1

| FABRICS USED IN THE EXPERIMENT | | | | | | |
|---|---|---|---|---|---|---|
| **Fabric code** | **Fabric type** | **Fabric weight**, g/m$^2$ | **Fabric thickness**, mm | **Yarn count** | **Coefficient of twist**, $\alpha_e$ | **Tightness factor**, $K$ |
| *1* | 100% Co | 202.9 | 0.73 | Ne 30 | $\alpha_e$ = 3.8 | 1.56 |
| *2* | 97% Co – 3% elastane | 254.5 | 0.89 | Ne 30 | | 1.66 |
| *3* | 100% PET | 192.9 | 0.49 | Ne 27 | | 1.74 |
| *4* | 50% Co – 50% PET | 158.5 | 0.63 | Ne 30 | | 2.65 |
| *5* | 100% viscose | 202.3 | 0.58 | Ne 27 | | 1.59 |
| *6* | 97% micro PET – 3% elastane | 235.8 | 0.61 | Denier 150 | - | 1.43 |

stretchability of the fabrics. In this study, six different fabrics were knitted by using the same fabric structure (single jersey) in circular knitting machine. Fabrics were produced from cotton, PET, micro PET, viscose and cotton blended yarns. The twist coefficients of the yarns were kept constant (*αe* = 3,8) for the spun yarns. The mechanical, surface and comfort characteristics of six different single jersey fabrics were investigated. Properties of the fabrics were summarized in table 1.

After conditioning of the fabrics for 24 hours under the standard atmosphere conditions (20 ± 2°C temperature and 65 ± 4% relative humidity), fabrics were tested for their physical properties. Mass per unit area was measured according to EN 12127 standard, thickness was measured according to ISO 5084 standard, abrasion resistance of the fabrics was determined by using Martindale Abrasion Tester (ISO 12947-3) under 9 kPa pressure till fabrics were rubbed 20 000 cycles and mass losses were calculated. Pilling resistance of the fabrics was determined according to ISO 12945-2 standard and the assessments were done using PillGrade Automated Pilling Grading System. Bursting strength values were measured according to ISO 13938-2 in 7.3 cm$^2$ test area in TruBurst Bursting tester. Stretchability of the fabrics in course direction was tested according to TS 10985 standard.

Besides mechanical and handle properties, comfort characteristics of the fabrics are also important for the primary school uniforms. Therefore, various comfort parameters were also measured in the experiment. Air permeability tests are processed (by FX3300-Tester) according to ISO 9237 standard (Test area: 20 cm$^2$, 100 Pa air pressure). The primary school students have generally higher activity, therefore they sweat more. Hence, vapour and liquid moisture transfer properties of their clothes have great importance in terms of their health and comfort.

Relative water vapour permeability of the fabrics was tested according to ISO 11092 standard by using skin model. In order to determine the liquid water transfer properties, Moisture Management Tester was used and the tests were conducted according to AATCC Test Method (TM) 195-2009. The MMT is designed to sense, measure and record the liquid moisture transport behaviours in multiple directions. When moisture is transported in a fabric, the contact electrical resistance of the fabric changes. The change of resistance value depends on two factors: the components of liquid and the water content in the fabric. The liquid components are fixed, so that the measured electrical resistance is related to the water content in the fabric. In order to simulate sweating, a special solution (including NaCl) was dropped onto the fabric's top surface. During the test, the same mass of solution (0.15 g) was applied onto each specimen's top surface automatically by the instrument. The test liquid is dropped from the top part of the instrument to the top surface of the fabric, which is used as inner surface that will be in touch with the human skin [16], [17].

Overall Moisture Management Capacity (OMMC), which is calculated by the MMT, was used to define the liquid transport properties of the fabrics. OMMC is an index to indicate the overall capability of the fabric to manage the transport of liquid moisture. The overall moisture management capacity is defined as:

$$OMMC = 0.25\,BAR + 0.5\,OWTC + 0.25\,SS_b \quad (1)$$

where:

*BAR* is the moisture absorption rate at the bottom side;

*OWTC* – the one-way transport capacity (the difference of the cumulative moisture content between the two surfaces of the fabric);

$SS_b$ – the spreading/drying rate of the bottom side ($SS_b$), which is represented by the maximum *SS* [16] – [19].

The larger the *OMMC*, the higher is the overall moisture management ability of the fabric.

In order to determine the statistical significance of the variables on the related properties, variance analysis method and post hoc tests were used. To deduce whether the parameters are significant or not, p values were examined according to the significance level of $\alpha$ = 0.05.

## RESULTS AND DISCUSSIONS

### Abrasion test results

The mass loss values (%) of the fabrics for the cycles 5 000 to 20 000 are given in figure 1 and statistical

Table 2

| MULTIPLE COMPARISON TEST (SNK) RESULTS FOR MASS LOSS FOR 20 000 CYCLES | | | | | | |
|---|---|---|---|---|---|---|
| **Fabric type** | ***N*** | **Subset** | | | | |
| | | ***1*** | ***2*** | ***3*** | ***4*** | ***5*** |
| 97% micro PET – 3% elastane | 3 | –0.6631 | - | - | - | - |
| 100% Co | 3 | - | 4.9122 | - | | - |
| 97% Co – 3% elastane | 3 | - | 5.2556 | - | - | - |
| 100% PET | 3 | - | - | 6.6500 | - | - |
| 50% Co – 50% PET | 3 | - | - | - | 7.9379 | - |
| 100% viscose | 3 | - | - | - | | 12.2188 |
| Sig. | - | 1.000 | 0.247 | 1.000 | 1.000 | 1.000 |

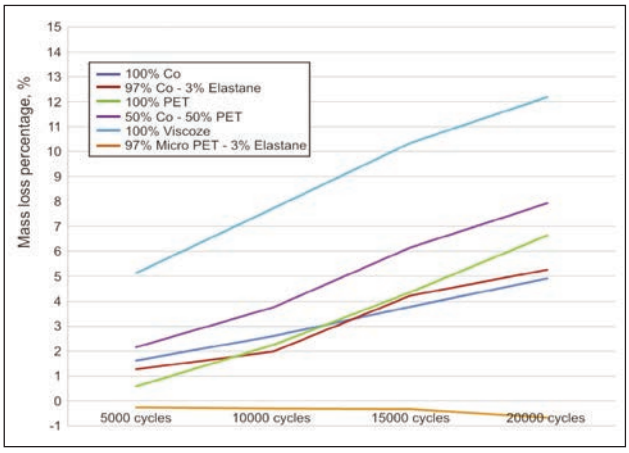


Fig. 1. Mass loss values of the fabrics for different cycles

analysis for the mass loss values at 20 000 cycles is given in table 2. As the mass loss values of the fabrics were analyzed, it can be seen that fabric including 100% viscose has the highest mass loss value for all cycles. Higher mass loss values were obtained for 100% cotton fabrics rather than 100% PET fabrics until 13 000 cycles. After 13 000 cycles the mass loss values of the 100% PET fabrics were higher. Although PET fibres have higher fibre strength, as the number of the cycles increased the fibres holding the pills breaks and mass loss increase.

The difference between the mass loss values of the 100% Co and 97% Co – 3% elastane fabric is statistically insignificant and their mass losses are lower than the other fabrics. The fabric including 97% micro PET – 3% elastane pulls out the fibres of abradant fabric as a result of rubbing and combines them into its own structure. Therefore, an increase was observed in its mass at the end of the 20 000 cycles of rubbing. For an overall evaluation, it can be stated that fabrics including polyester and cotton fibres have lower mass loss, whereas the fabrics including viscose fibres have a higher mass loss.

## Pilling test results

Pilling degrees of the fabrics are given in figure 2. As the pilling degrees of the fabrics were examined, it can be said that fabric including 97% micro PET – 3% elastane fabric has the highest pilling resistance, since the PET fibres are in a filament form. However, fabrics including 50% Co – 50% PET fibres have the lowest pilling resistance. There were not any statistical significant differences between the fabrics made of 100% viscose, PET and 97% Co – 3% elastane fibres (table 3).

Table 3

| MULTIPLE COMPARISON TEST (SNK) RESULTS FOR PILLING DEGREES | | | | | |
|---|---|---|---|---|---|
| **Fabric type** | ***N*** | **Subset** | | | |
| | | ***1*** | ***2*** | ***3*** | ***4*** |
| 50% Co – 50% PET | 3 | 1.4 | - | - | - |
| 100% viscose | 3 | - | 2.3 | - | - |
| 97% Co – 3% elastane | 3 | - | 2.3 | - | - |
| 100% PET | 3 | - | 2.4 | - | - |
| 100% Co | 3 | - | - | 3.9 | - |
| 97% micro PET – 3% elastane | 3 | - | - | - | 5.0 |
| Sig. | - | 1.000 | 0.764 | 1.000 | 1.000 |

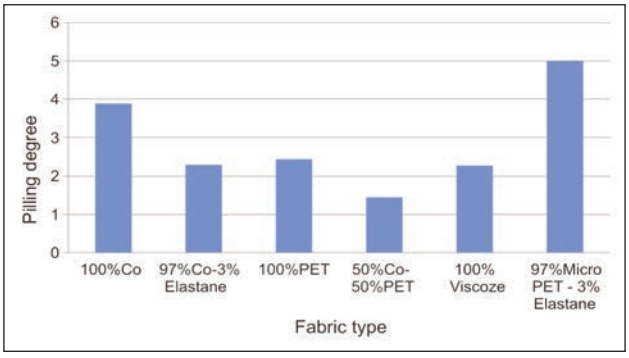


Fig. 2. Pilling degrees of the fabrics

## Bursting strength test results

Bursting strength values of the fabrics are given in figure 3 and table 4. Bursting strength of the 100% PET and 97% micro PET – 3% elastane fabrics have the highest value, whereas fabric containing 100%

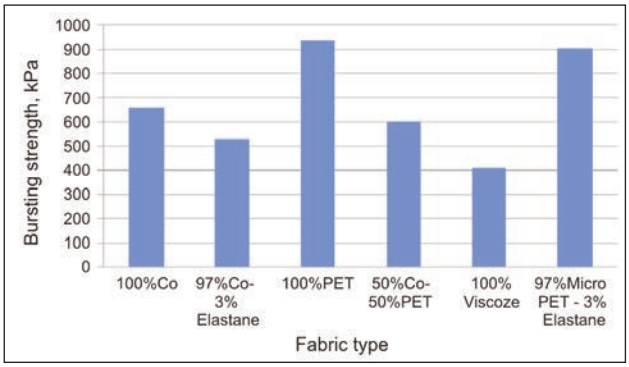


Fig. 3. Bursting strength values of the fabrics

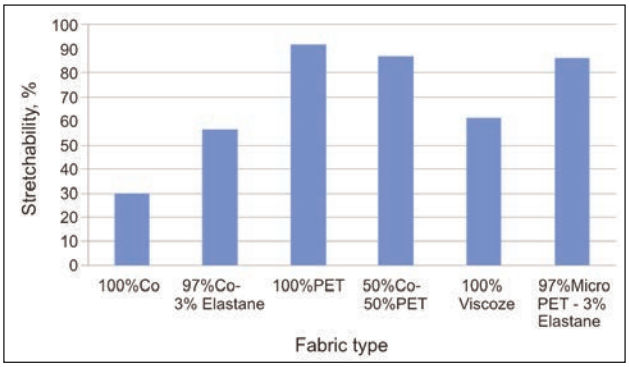


Fig. 4. Stretchability test results of the fabrics

Table 4

MULTIPLE COMPARISON TEST (SNK) RESULTS FOR BURSTING STRENGTH VALUES

| Fabric type | N | Subset | | | |
|---|---|---|---|---|---|
| | | 1 | 2 | 3 | 4 |
| 100% viscose | 5 | 409.48 | - | - | - |
| 97% Co – 3% elastane | 5 | - | 529.56 | - | - |
| 50% Co – 50% PET | 5 | - | 602.76 | 602.76 | - |
| 100% Co | 5 | - | - | 647.50 | - |
| 97% micro PET – 3% elastane | 5 | - | - | - | 907.80 |
| 100% PET | 5 | - | - | - | 938.70 |
| Sig. | - | 1.000 | 0.052 | 0.223 | 0.396 |

Table 5

MULTIPLE COMPARISON TEST (SNK) RESULTS FOR STRETCHABILITY VALUES

| Fabric type | N | Subset | | |
|---|---|---|---|---|
| | | 1 | 2 | 3 |
| 100% Co | 3 | 30.0000 | - | - |
| 97% Co – 3% elastane | 3 | - | 56.4000 | - |
| 100% viscose | 3 | - | 61.2000 | - |
| 97% micro PET – 3% elastane | 3 | - | - | 86.4000 |
| 50% Co – 50% PET | 3 | - | - | 86.8000 |
| 100% PET | 3 | - | - | 92.0000 |
| Sig. | - | 1.000 | 0.275 | 0.405 |

Table 6

MULTIPLE COMPARISON TEST (SNK) RESULTS FOR AIR PERMEABILITY VALUES

| Fabric type | N | Subset | | | |
|---|---|---|---|---|---|
| | | 1 | 2 | 3 | 4 |
| 97% micro PET – 3% elastane | 10 | 117.80 | - | - | - |
| 97% Co – 3% elastane | 10 | 160.00 | - | - | - |
| 100% Co | 10 | - | 271.70 | - | - |
| 100% viscose | 10 | - | - | 1107.90 | - |
| 50% Co – 50% PET | 10 | - | - | 1142.60 | - |
| 100% PET | 10 | - | - | - | 1332.00 |
| Sig. | - | 0.364 | 1.000 | 0.455 | 1.000 |

viscose has the lowest value. The tenacity of the PET fibres (0.47 N/tex) is higher than cotton (0.32 N/tex) and viscose (0.18 N/tex) fibres. Therefore, these fabrics are more resistant to bursting force. It can also be stated that the usage of elastane yarns in the structure causes a decrease in the bursting strength when compared with the usage of pure cotton yarns.

## Stretchability test results

Stretchability of the fabrics can be seen in figure 4. According to figure 4, fabrics containing PET fibres have higher stretchability, while fabrics produced from cotton fibres have lower stretchability values. The fabrics produced from viscose fibres have higher stretchability than cotton fabrics in accordance with the fibres extension values (breaking elongation of PET staple fibres is around 37%, viscose staple fibre is 16%, and cotton fibre is 7%) [20]. Elastane yarns increase stretchability of the fabrics expectedly (table 5).

## Air permeability test results

Air permeability test results of the fabrics are given in figure 5 and statistical analysis is given in table 6. Air permeability is related to the porosity of the fabrics. Closer fabric structures cause lower air permeability, due to the higher cover factor. In the study, the fabrics containing elastane yarns showed lower air permeability. The usage of elastane in fabric causes close fabric structure. The staple fibres having lower uniformity than staple PET and viscose fibres caused higher yarn hairiness. Because of that cotton fabrics have lower air permeability.

## Test results for water vapour permeability and moisture management property

Relative water vapour permeability test results and the statistical evaluation of the experimental fabrics

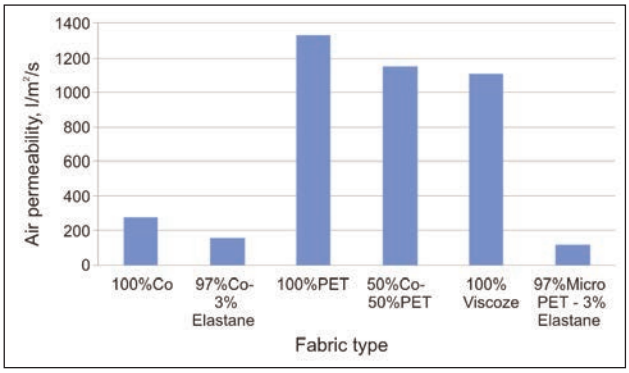


Fig. 5. Air permeability values of the fabrics

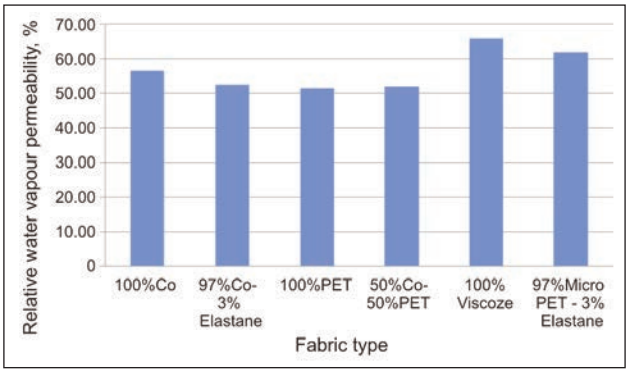


Fig. 6. Relative water vapour permeability values of the fabrics

Table 7

MULTIPLE COMPARISON TEST (SNK) RESULTS FOR WATER VAPOUR PERMEABILITY VALUES

| Fabric type | N | Subset | | | |
|---|---|---|---|---|---|
| | | 1 | 2 | 3 | 4 |
| 100% PET | 3 | 51.3333 | - | - | - |
| 50% Co – 50% PET | 3 | 52.0333 | - | - | - |
| 97% Co – 3% elastane | 3 | 52.6333 | - | - | - |
| 100% Co | 3 | - | 56.5333 | - | - |
| 97% micro PET – 3% elastane | 3 | - | - | 62.2667 | - |
| 100% viscose | 3 | - | - | - | 65.8667 |
| Sig. | - | 0.520 | 1.000 | 1.000 | 1.000 |

Table 8

FOVERALL MOISTURE MANAGEMENT CAPACITY (OMMC) VALUES OF THE FABRICS

| Fabric type | OMMC values | Evaluation |
|---|---|---|
| 100% Co | 0.39 | Poor |
| 97% Co – 3% elastane | 0.54 | Good |
| 100% PET | 0.25 | Poor |
| 50% Co – 50% PET | 0.34 | Poor |
| 100% viscose | 0.64 | Very good |
| 97% micro PET – 3% elastane | 0.47 | Good |

are given in figure 6 and table 7 respectively. According to figure 6, it can be stated that viscose and 97% micro PET – 3% elastane fabrics have higher relative water vapour permeability as compared to the fabrics including cotton and PET.

Overall moisture management capacity (OMMC) values of the fabrics are given in table 8 and the values are compared with the grading scale given by the manufacturing company (0 – 0.2: very poor; 0.2 – 0.4: poor; 0.4 – 0.6: good; 0.6 – 0.8: very good; > 0.8: excellent) [16].

According to the test results, it can be stated that relative water vapour permeability and OMMC values of the fabrics were found compatible with the information given in the literature. As these parameters were evaluated together, it can be considered that 100% viscose fabric has the highest OMMC value and the highest water vapour permeability. However, 100% PET fabric has the lowest values in both tests. Since the total surface area of the micro fibres is higher than the classic polyester fibres, the usage of micro polyester fibre in the structure has a positive impact by means of relative water vapour permeability and OMMC values.

## CONCLUSIONS

The improvements in the comfort of school uniforms affect the comfort of primary school children and their school life. Especially in cities having hot climates, the school uniforms are classified in two groups, which can be used in winter and summer terms. Summer term school uniforms are garments used as t-shirt with round collar or polo shirt combined with shorts.

In this experiment, six different single jersey fabrics, which are commonly used in school t-shirts and polo shirts were investigated for their physical, mechanical and moisture management properties. The results can be summarized as follows:

- In case of using 100% Co fabric, although this type of fabric has good abrasion and pilling resistance, the lowest stretchability and poor moisture management property was determined from this fabric.
- In contrary to the good moisture management property of 97% Co – 3% elastane fabric, it has low air permeability and relative water vapour permeability.
- 50% Co – 50% PET fabric has high stretchability and air permeability. However, it has the lowest pilling resistance and poor water vapour and liquid moisture transfer properties.
- The highest bursting strength and air permeability results were obtained from the 100% PET fabric. It has also high stretchability, however the water

vapour and liquid moisture transfer properties of this fabric were found relatively lower.

- 100% viscose fabric has the highest relative water vapour permeability and "very good" moisture management property, besides having the lowest bursting strength and abrasion resistance.
- 97% micro PET – 3% elastane fabric has the best pilling resistance among the researched fabrics. It also has high bursting strength, high stretchability and good moisture management property; however it has the lowest air permeability.

According to all test results, it can be concluded that viscose and micro PET fabrics can be suggested for school upper clothes due to their better comfort properties. However, micro PET fabric has also an advantage in terms of mechanical properties.

## BIBLIOGRAPHY


[1] Marmaralı, A., Kretzschmar, S., Özdil, N., Oğlakcıoğlu, N. *Giysilerde Isıl Konforu Etkileyen Parametreler*. In: Tekstil ve Konfeksiyon, 2006, vol. 16, issue 4, pp. 241-246

[2] Erdoğan, M. Ç. *Örme Kumaşların Konfeksiyon Problemleri ve Çözüm Önerileri*. Tekstil ve Makine Dergisi, 1990, V. Tekstil Sempozyumu Özel Sayısı, November, p. 166

[3] Sweeney, M. M., Branson, D. H. *Sensorial comfort. Part I: A pschophysical method for assessing moisture sensation in clothing*. In: Textile Research Journal, 1990, vol. 60, issue 7, pp. 371-377

[4] Öndoğan, Z., Ünal, Z. B. *Çocuk Giyiminin Önemi*. In: Tekstil ve Konfeksiyon, 2001, vol. 11, issue 4, pp. 225-228

[5] Bahadır, Ünal Z., Yıldız, E. Z., Özdil, N. *İlköğretimde Kullanılan Pantolonluk Kumaş Özelliklerinin İncelenmesi ve İyileştirilmesi Üzerine Bir Araştırma*. In: Tekstil ve Konfeksiyon, 2011, issue 3, pp. 244-248

[6] Das, B., Das, A., Kothari, V. K. Fanguiero, R., Araújo, M. *Studies on moisture transmission properties of PV-blended fabrics*. In: The Journal of the Textile Institute, 2009, vol. 100, issue 7, pp. 588–597

[7] Das, B., Das, A., Kothari, V. K., Fanguiero, R., Araújo, M. *Moisture transmission through textiles. Part I: Processes involved in moisture transmission and the factors at play*. In: AUTEX Research Journal, 2007, vol. 7, issue 2, pp. 100-110

[8] Sharabaty, T., Biguenet, F., Dupuis, D., Viallier, P. *Investigation on moisture transport through polyester/cotton fabrics*. In: Indian Journal of Fibre & Textile Research, December 2008, vol. 33, pp. 419-425

[9] Saville, B. P. *Physical testing of textiles*. Woodhead Publishing, 1999, Cambridge England, pp. 215-216

[10] Haghi, A. K. *Moisture permeation of clothing a factor governing thermal equilibrium and comfort*. In: Journal of Thermal Analysis and Calorimetry, 2004, vol. 76, pp. 1 035–1 055

[11] Cotton Incorporated, Cary North Carolina. *100% Cotton Moisture Management*. In: Journal of Textile and Apparel, Technology and Management, 2002, issue 2, p. 3

[12] Roggenstein, W. *Viscose fibres with new functional qualities*. In: Lenzinger Berichte, 2011, vol. 89, pp. 72-77

[13] Oğulata, R. T., Mavruz, S. *Investigation of porosity and air permeability values of plain knitted fabrics*. In: Fibres & Textiles in Eastern Europe, 2010, vol. 18, issue 5 (82), pp. 71-75

[14] Üstün, G., Çeğindir, N. Y. *İlköğretim Çağı Çocukları ve Annelerinin Okul Önlük ve Formalarının Konforundan Memnuniyet Durumlarının İncelenmesi*. Hacettepe Üniversitesi, Sosyolojik Araştırmalar e-Dergisi, 2006; http://www.sdergi.hacettepe.edu.tr/cercevearsiv.htm

[15] Ağaç, S., Harmankaya, H. *İlköğretim Birinci Kademe Öğrencilerinin Giysi Tercihleri ve Giysi Satın Alma Davranışlarına Etki Eden Faktörler*. In: Selçuk Üniversitesi Sosyal Bilimler Enstitüsü Dergisi, 2009, vol. 22, pp. 1-13

[16] Özdil, N., Süpüren, G., Özçelik, G., Pruchova, J. *A study on the moisture transport properties of the cotton knitted fabrics in single jersey structure*. In: Tekstil ve Konfeksiyon, 2009, issue 3, pp. 218-223

[17] Hu, J., Li, Y., Yeung, K. W., Wong, A. S. W., Xu, W. *Moisture management tester: A method to characterize fabric liquid moisture management properties*. In: Textile Research Journal, 2005, vol. 75, pp. 57–62

[18] Moisture Management Tester Operation Manual, 2009, SDL Atlas Inc.

[19] Süpüren, G., Oğlakçıoğlu, N., Özdil, N., Marmaralı, A. *Moisture management and thermal absorptivity properties of double-face knitted fabrics*. In: Textile Research Journal, 2011, vol. 81, issue 13, pp. 1 320-1 330

[20] Morton, W. E., Hearle, J. W. S. *Physical properties of textile fibres*. Woodhead Publishing in Textiles: Number 68, 2008, CRC Press, Boca Raton Boston New York Washington, DC, Woodhead Publishing Limited, Cambridge, England



**Authors:**

NİLGÜN ÖZDİL
ZÜMRÜT BAHADIR UNAL
Ege University Textile Engineering Department
Bornova-İzmir, Turkey
e-mail: nilgun.ozdil@ege.edu.tr;
e-mail: zumrut.bahadir.unal@ege.edu.tr

SERKAN BOZ
GAMZE SÜPÜREN MENGÜÇ
Ege University Emel Akın Vocational Training School
Bornova-İzmir, Turkey
e-mail: serkan.boz@ege.edu.tr;
e-mail: gamzesupuren@gmail.com

**Corresponding author:**
NİLGÜN ÖZDİL

# Mobile laboratory for developing the latent prints

WOJCIECH BŁASZCZYK
LONGINA MADEJ-KIEŁBIK
ELŻBIETA MAĆKIEWICZ
ELŻBIETA WITCZAK

**REZUMAT – ABSTRACT**

**Laboratorul mobil pentru developarea amprentelor latente**

*Lucrarea prezintă realizările Consorțiului științific-industrial, coordonat de Institutul pentru Tehnologii de Securitate "Moratex", privind realizarea unui laborator mobil inovator pentru developarea amprentelor latente. Laboratoarele mobile extind semnificativ capacitățile de testare ale serviciilor de poliție. Spre deosebire de laboratoarele tradiționale (camerele fixe), acestea permit executarea testelor direct la locul infracțiunii și oferă un spațiu operațional mai mare. În lucrare sunt prezentate câteva dintre soluțiile existente în prezent la nivel mondial, activitățile consorțiului privitoare la elaborarea propriei proiectări, precum și rezultatele testelor metrologice și posibilitățile de utilizare a laboratorului realizat.*

*Cuvinte-cheie: laborator, mobilitate, cort, dactiloscopie, ester al acidului cianoacrilic*

**Mobile Laboratory for Developing the Latent Prints**

*The paper presents the achievements of the Scientific-Industrial Consortium led by the Institute of Security Technologies „Moratex" on the elaboration of the innovative mobile laboratory for developing latent prints. The mobile laboratories expand remarkably the testing capabilities of police services. Unlike traditional labs (the stationary chambers), they allow executing the tests directly at the place of crime and they have much more operational space. The paper presents examples of worldwide solutions for that situation, activities of the Consortium when developing their own design, as well as the results of metrological and usage tests of the developed laboratory.*

*Key-words: laboratory, mobility, tent, dactyloscopy, cyanoacrylate acid ester*

Developing the Latent Prints is a process aiming to find traces of the friction ridges, existing at the scene of an incident, and sometimes also to improve their visibility. Such a process may be conducted with various methods. One of them, the most often used nowadays in the fixed chambers is the cyanoacrylate method. It belongs to the chemical methods of developing the traces of fingerprints. First time it has been used by the Japanese Police in late 70-ties of previous century, but it is now commonly in use all around the world [1] – [2]. The method is particularly useful for developing old, invisible traces, especially on the non-absorbent medium i.e.: glass, metals, plastics, leather, paint and enamel surfaces or aluminum foil [3] – [4]. Such basis feature compact and smooth structure, which results in avoiding the trace-creative substances (such as sweat and fat) to penetrate an object, but keeps them on the surface [5].

In order to develop the latent prints, the action of methyl or ethyl ester of 2-cyanoacrylic acid is exploited. If the adequate conditions are provided (temperature, humidity) a process of polymerization of cyanoacrylate ester occurs, according to the following formula:

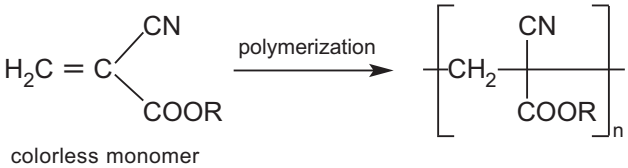


colorless monomer

As a result of the polymerization process on the invisible traces of latent prints a white substance appears, being the polymer of 2-cyanoacrylate acid. This makes disclosure of latent prints possible, which could not be disclosed by conventional (powder) method.

The cyanoacrylate method can be used by placing tested items in a homeostatic chamber (cyanoacrylate chamber), specially designed for this purpose. In devices of such type, the temperature and humidity are strictly measured, which allows for significant acceleration of the disclosure of evidence process and its full control. These chambers have different sizes depending on the dimensions of objects, for which traces are to be disclosed.

A significant problem arises when it is necessary to disclose traces on the large-size objects (eg cars, trucks), especially when there is a need to gather evidence of a crime at its scene. A compact, portable system in the form of a tent with equipment necessary for the visualization of traces might be useful. Foster & Freeman company proposed such a solution. The product called SUPERfume-TENT is dedicated for disclosing latent prints with cyanoacrylate method [www.fosterfreeman.com, Foster & Freeman, SUPERfume-TENT [07.2013]. It consists of a tent with metal support and the systems which provide proper parameters for the process of developing the latent prints.

But it is possible to propose another solution. The tent presented in this paper with the systems that

control the conditions in its interior (NUS) is characterized by the use of a line of amenities designed for efficient process of disclosing the latent fingerprints at the crime scene.
Mobile laboratories for disclosing the latent prints eliminate deficiencies of stationary laboratories in two ways. They allow carrying out the testing directly on the crime scene and also have much bigger workspace. However, the research effectiveness of such a laboratory is related with solving the design problems of both tent and apparatus for emission and purifying the operational gas as well as generating and controlling the climate of operational zone.
Institute of Security Technologies "Moratex" has undertaken developing of such a solution within the frame of the development project „Developing the technology of the tent for disclosing the traces with the vapours ester of cyanoacrylic acid" being realized by the Scientific-Industrial Consortium.
The aim of this research was to design new idea of the mobile laboratory made using the textile materials, for the detection of the traces with the vapours ester of cyanoacrylic acid.

## EXPERIMENTAL PART

### Materials used

The laboratory tent itself is made of the following basic elements:

- pneumatic rack;
- outer shell;
- inner shell.

The tent features front gates as big as possible for tents joining, inspection windows to observe the process of traces development and elements for stabilization of tents foundation. The basic parts i.e. the shells and rack were made of materials featuring properties adequate to their tasks within the tend structure. The were selected from the wider range during development and assessment of model batch of the NUS.
The pneumatic rack was made of H 55128 fabric of Heytex GmbH, both sides coated with polyvinyl chloride, areal density of 600 g/m$^2$. The material features the following properties: durability of usage, high gas-tightness and high parameters of mechanical strength, especially resistance to abrasion, tear, break and puncture, resistance to atmosphere conditions and to short-term exposition to vapours ester of cyanoacrylic acid. The structure of rack is equipped with nodes for fixing the outer and inner shells as well as with handles which allow for fixing it to the ground.
The outer shell is made of P190-160 polyester fabric of the areal density 190 g/m$^2$. It is a fabric coated with polyurethane, very flexible, waterproof, watertight, featuring high parameters of mechanical strength, especially to tear and break as well as resistant to short-term exposition to the vapours ester of cyanoacrylic acid.
The inner coating is made of polyethylene (threelayers) technology foil of areal density as low as 100 g/m$^2$ (Research and Development Centre for Petroleum Industry J.S.C.). This foil features relevant parameter values for mechanical resistance, light transmittance and is resistant to short-term exposition to the ester of cyanoacrylic vapours. The material has a low coefficient of light transmission, £ 0.5% [6], which is essential for the efficiency of the process of revealing latent prints.
The materials were subjected to detailed tests of physical, mechanical and chemical parameters, during the process of developing the structure of the NUS. The tests were executed at the accredited laboratories: Laboratory of Metrology of Moratex Institute and Laboratory for Packaging Materials and Consumer Packaging Testing at the Polish Packaging Research and Development Centre in Warsaw, according to the applicable requirements for flat textiles coated with rubber or plastics, and with technology foils.
Listings of required parameters and their values, both required and obtained for these materials are presented in the project reporting documentation. Due to the large volume of research material, those results are not presented in this paper.
A particular parameter tested was the resistance of the above mentioned materials and the nodes to the operating gas i.e. ester of cyanoacrylic acid. This resistance was assessed by measuring the change in tensile strength. It was presumed that the strength of the material exposed to these conditions should not be less than 70% of the original strength of the material/node conditioned at room temperature. The results achieved were in all cases consistent with the assumptions. Summary results of this parameter for the fabrics and construction nodes are shown in table 1 and table 2.

### Design of NUS laboratory

The idea of mobile laboratory is based on two key elements: the tent itself (fig. 1 *a, b*) and the system of reliable emission of operational gas (fig. 2) [7].
In order to gain optimum adaptation of operational zone to the size of objects under research, the structure of tent itself was elaborated in two sizes as can be seen in table 3. The same goal induced their joint design – modularity. It is possible to join two versions of small sizes or a small one with the medium-size tent. This is illustrated by the figure 3.
The NUS laboratory, when folded, is ready for transporting with regular vehicles of police forces.

## RESULTS AND DISCUSSIONS

The models developed of the tent itself, selected structural parts and testing works are presented in figures 4 – 6.
Another basic element of NUS laboratory is the system for reliable emission of operational gas (fig. 2). Its task is to create and monitor the optimum climate within the operational zone of NUS, to emit vapours ester of cyanoacrylic acid and air purification upon completing a test. The system consists of a control

Table 1

| RESULTS OF RESISTANCE TEST OF MATERIALS OF THE TENT ITSELF TO THE VAPOURS ESTER OF CYANOACRYLIC ACID RELATED TO CONDITIONING UNDER A NORMAL CLIMATE | | | | |
|---|---|---|---|---|
| **Parameter** | **Value after conditioning** | | **Change of the parameters value, %** | **Method of testing** |
| | ***In normal conditions*** | ***In the vapours ester of cyanoacrylic acid*** | | |
| **H 55128 fabric coated on both sides** | | | | |
| Breaking force, N/5 cm:<br>- lengthwise;<br>- crosswise | <br>2 582 ± 82<br>1 653 ± 67 | <br>2 562 ± 62<br>1 823 ± 75 | <br>– 0.8<br>+ 10.3 | *PBM-40/ITB-2012 |
| **P190-160 coated fabric** | | | | |
| Breaking force, N/5 cm:<br>- lengthwise;<br>- crosswise | <br>1 722 ± 35<br>1 230 ± 34 | <br>1 683 ± 35<br>1 248 ± 61 | <br>– 2.3<br>+ 1.5 | *PBM-40/ITB-2012 |
| **Foil (from OBR Płock)** | | | | |
| Breaking force, N/5 cm:<br>- lengthwise;<br>- crosswise | <br>22.4 ± 0.6<br>22.2 ± 1.1 | <br>24,9 ± 0.9<br>16,6 ± 0.7 | <br>+ 2.2<br>– 25.2 | *PBM-40/ITB-2012 |

* The Institute of Security Technologies "Moratex" developed its own procedure for determining the breaking force (PBM-40). This procedure is based on international standards: PN-EN-ISO 13934-1:2002 and PN-EN-ISO 1421:2001. Tests of samples were executed with the application of test methodology based on standards: PN-EN-ISO 13934-1:2002 and PN-EN-ISO 1421:2001.

Table 2

| RESULTS OF RESISTANCE TEST OF MATERIALS OF THE TENT'S STRUCTURAL NODES TO THE VAPOURS ESTER OF CYANOACRYLIC ACID RELATED TO CONDITIONING UNDER A NORMAL CLIMATE | | | | |
|---|---|---|---|---|
| **Parameter** | **Value after conditioning** | | **Change of the parameters value, %** | **Method of testing** |
| | ***In normal conditions*** | ***In the vapours ester of cyanoacrylic acid*** | | |
| **H 55128 fabric/2cm wide welded join/H 55128 fabric** | | | | |
| Breaking force, N/5 cm:<br>- lengthwise;<br>- crosswise | <br>2 581 ± 95<br>1 758 ± 115 | <br>2 422 ± 93<br>1 861 ± 141 | <br>– 6.2<br>+ 5.9 | **PBM-29/ITB-2008 |
| **H 55128 fabric/sewed join/P 190-160 polyester fabric coated with PU** | | | | |
| Breaking force, N/5 cm:<br>- lengthwise;<br>- crosswise | <br>1 293 ± 39<br>1 209 ± 19 | <br>1 316 ± 53<br>1 245 ± 22 | <br>+ 1.8<br>+ 3.0 | **PBM-29/ITB-2008 |
| **H 55128 fabric/hooks-loops join/ foil from OBR Plock** | | | | |
| Breaking force, N/5 cm:<br>- lengthwise;<br>- crosswise | <br>12.6 ± 1.5<br>12.0 ± 1.3 | <br>12.1 ± 1.3<br>11.4 ± 0.5 | <br>– 4.0<br>– 5.0 | **PBM-29/ITB-2008 |
| **H 55128 fabric/4cm wide welded join/H 55128 fabric** | | | | |
| Breaking force, N/5 cm:<br>- lengthwise;<br>- crosswise | <br>2 053 ± 105<br>2 613 ± 147 | <br>2 000 ± 60<br>2 645 ± 45 | <br>– 2.6<br>+ 1.2 | **PBM-29/ITB-2008 |

** PBM-29 – is a testing procedure developed by Institute of Security Technologies "Moratex". This procedure is based on standards: PN-EN-ISO 13935-1:2002.

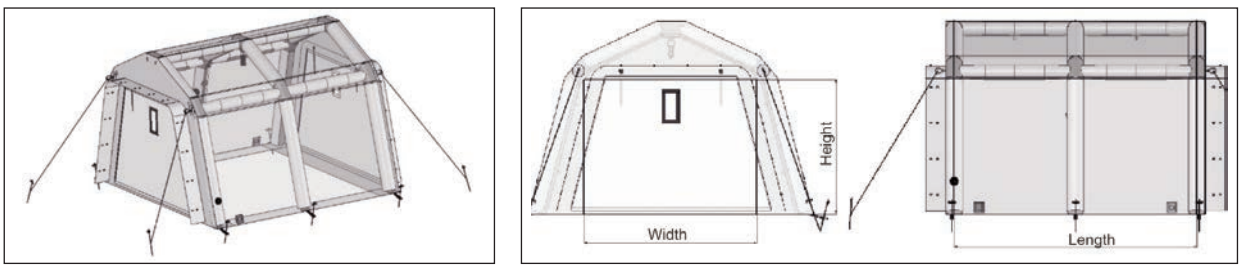


*a* *b*

Fig. 1: *a* – the tent design; *b* – main tent design [8]

Table 3

| TENT SIZES | | |
|---|---|---|
| **Dimensions**, m | **Version** | |
| | Small-size | Medium-size |
| Length | 3.6 ± 0.1 | 7.0 ± 0.1 |
| Width | 2.6 ± 0.1 | 4.0 ± 0.1 |
| Height | 2.0 ± 0.1 | 4.0 ± 0.1 |

Fig. 2. Operation gas emission system [7]

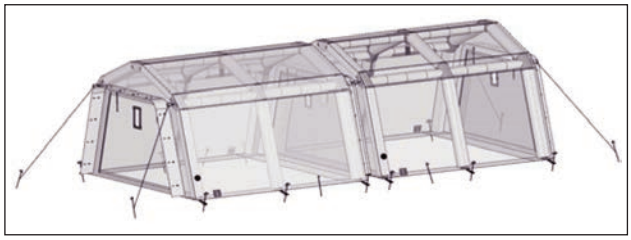

Fig. 3. Modular joint set of two small-size tents [8]

unit and controlled functional devices. Under field conditions it may be powered by a power generator. It includes the following devices and parts [8]:

- a module for controlling the ambient parameters inside the tent (NUS-MS):
  – humidity and temperature sensors (NUS-ZC);
- devices that provide the required climatic conditions:
  – air humidifier (NUS-MN),
  – electric heater (NUS-MG);
- a device for producing vapours ester of cyanoacrylic acid (NUS-MCP);
- device for air purification upon completing a test (NUS-MO).

Fig. 4. The medium-size tent

Fig. 5. The small-size tent

Fig. 6. The pneumatic rack

The elaborated system executes in an automatic manner the program of optimum carrying out the process of developing the latent prints.
Equipment and system components is illustrated by the figures 7 – 12. Schematic diagram showing the location of equipment and components of the system on the floor of NUS is presented in the figure 13.
Correctness of the system operation and of the efficiency of developing the latent prints were assessed on the basis of usage tests executed by the Central Forensic Laboratory of the Police in Warsaw. They

Fig. 7. Module for controlling the ambient parameters inside the tent – NUS-MS


Fig. 8. Humidity and temperature sensors – NUS-ZC

Fig. 9. Device for producing vapours ester of cyanoacrylic acid – NUS-MCP

Fig. 10. Electric heater – NUS-MG

Fig. 11. Air humidifier – NUS-MN

Fig. 12. Device for air purification upon completing a test – NUS-MO

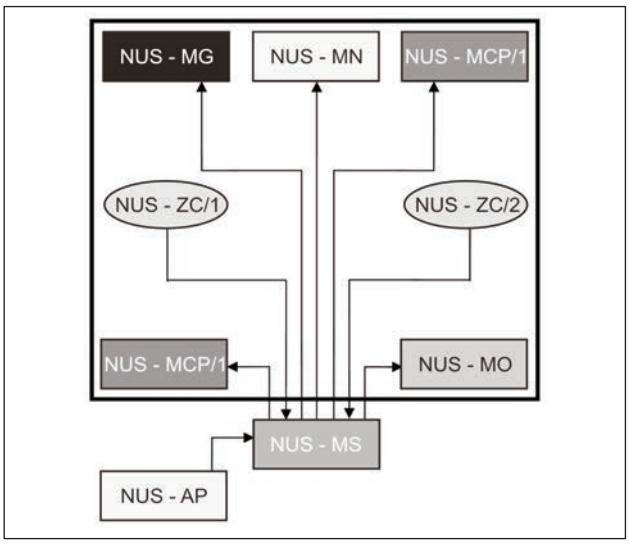


Fig. 13. Location of the devices and components of the NUS laboratory [8]

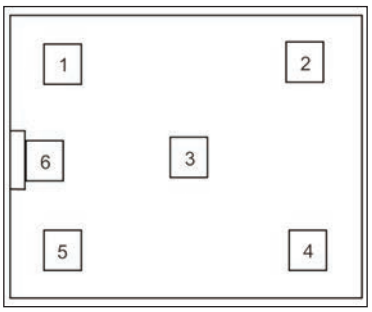


Fig. 14. The checkpoints [9]

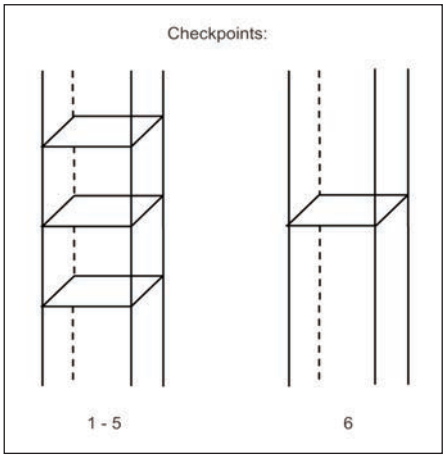


Fig. 15. Levels of placing the samples [9]

were involved through the process of visualizing latent prints by a specially elaborated program of research [9], which concerned the test samples, their location (fig. 14, 15) and the exposure time.

In order to determine the optimum time of the process of developing the latent prints, various types of research materials in the form of glass and plastic bottles, metal cans and plastic boxes with marked traces of fingerprints was placed in a tent. After reaching the assumed environmental conditions (temperature and humidity), developing traces with vapours ester of cyanoacrylic acid after 15, 30, 45, 60 and 75 minutes began. On the basis of tests it was found that for all samples tested the optimum time of disclosing the latent fingerprints is 30 minutes. Examination of the uniformity of the propagation ester of cyanoacrylic acid vapours in the inner space of the tent was also made. Therefore plates made of black plastic which was deprived of impurities, and then a natural fat/sweat substance was applied onto them. The plates were then placed in the tent, at the previously designated measurement points located at different heights. After obtaining the required environmental conditions inside the tent, the process of disclosing the traces was started. It was found that the time of disclosing the traces on the test plate varied depending on the position of the sample. The process was shortest for plates that were at a short distance from the fan distribution the operational gas in the tent room. The effectiveness of the process of disclosing the latent prints was rated very well.

## CONCLUSIONS

The usage tests carried out by Central Forensic Laboratory of the Police in Warsaw were the assessment of the structure of NUS laboratory. Trials and demonstration of NUS model, consisted in carrying out the process of developing the latent prints in under near-to-realistic conditions. The object of the demonstration were tent models of small and medium-sized version, equipped with all necessary operational systems which were those used to control the atmosphere inside the tent and operating gas emissions as well as air purifying upon completing a test. During the demonstration a tent was pitch, the

operational system installed and run and a process of developing the latent prints executed. The systems works were controlled by the module located outside the tent.

According to the presumptions, the test sample was placed in the sphere formed by the inner shell of the tent. Rating of the development of latent prints was carried out by a team of professionals from Central Forensic Laboratory of the Police with a positive result.

Construction of the NUS has been applied for protection to the Polish Patent Office (No P. 403281).


## ACKNOWLEDGEMENTS

Project funded by the National Centre for Research and Development in frame of the project No. O ROB 0020 01/ID 20/1, entitled: "Developing the technology of the tent for disclosing the traces with the vapours ester of cyanoacrylic acid". Construction of the NUS was awarded the Silver Medal at the 122 edition of the International Exhibition of Innovation Concours Lépine 2013, 30.04. – 12.05. 2013, Paris, France.


## BIBLIOGRAPHY


[1] Czubak, A. *The use of cyanoacrile glues for revealing fingerprints on various surfaces.* In: Problems of Forensic Science, 2002, vol. 52, p. 87

[2] Newton, D. E. *Forensic chemistry.* Fact on File, Inc. 2007

[3] Zubański, S. *Raport z badań dotyczących wizualizacji śladów linii papilarnych metodami chemicznymi.* Prokuratura Okręgowa w Zielonej Górze. http://www.zielona-gora.po.gov.pl/esi-admin/upload/lektury_elektroniczne/daktyloskopia-metody-chemiczne-sl-zubanski-2.pdf [07.2013]

[4] Holder, E. H. Jr., Rob Vinson, L. O., Laub, J. H. *The fingerprint Sourcebook, Chapter 7*. Latent Print Development. U.S. Department of Justice. Office of Justice Programs. National Institute of Justic

[5] Pękała, M., Rybczyńska-Królik, M. *Przewodnik po metodach wizualizacji śladów daktyloskopijnych.* wyd. Centralnego Laboratorium Kryminalistycznego, Warsaw, 2006

[6] Godlewska, E., Zdanowski, B., Kolado, W. *Research report no. DOJ-531-412/12*. Unpublished materials, Laboratorium Badań Materiałów i Opakowań Jednostkowych Centralnego Ośrodka Badawczo-Rozwojowego Opakowań w Warszawie, Warsaw, 2012

[7] Osmoła, P., Staniszewski, P., Staniszewski, S. *Study no. D.3.3/1: Projekt systemu do prawidłowej emisji gazu operacyjnego dla partii prototypowej wraz z dokumentacją techniczną*. Unpublished materials, Stanimex, Lublin, 2013

[8] Strzelczyk, J., Bojanowski, Z., Sykuła, P., Lewandowski, L. *Study no. D.3.5: Dokumentacja konstrukcyjna modeli NUS*. Unpublished materials, Przedsiębiorstwo Sprzętu Ochronnego „Maskpol" S.A., Konieczki, 2012

[9] Rogoża, E., Drzewiecka, K., Chyczewska, A. *Program badań skuteczności ujawniania śladów linii papilarnych parami estru kwasu cyjanoakrylowego w prototypach NUS*. Unpublished materials, Centralne Laboratorium Kryminalistyczne Policji, Warsaw, 2013



**Authors:**

WOJCIECH BŁASZCZYK

ELŻBIETA MAĆKIEWICZ

LONGINA MADEJ-KIEŁBIK

ELŻBIETA WITCZAK

Institute of Security Technologies Moratex

3 M Sklodowskiej-Curie Street

90-965 Lodz, Poland

e-mail: wblaszczyk@moratex.eu


# INFORMATION FOR AUTHORS

***Industria Textila magazine*** is an international peer-reviewed journal published by the National Research & Development Institute for Textiles and Leather – Bucharest, in print editions.

**Aims and Scope**: *Industria Textila* magazine welcomes papers concerning research and innovation, reflecting the professional interests of the Textile Institute in science, engineering, economics, management and design related to the textile industry and use of fibres in consumer and engineering applications. Papers may encompass anything in the range of textile activities, from fibre production through textile processes and machines, to the design, marketing and use of products. Papers may also report fundamental theoretical or experimental investigations, practical or commercial industrial studies and may relate to technical, economic, aesthetic, social or historical aspects of textiles and the textile industry.

## Submission of Manuscripts

The paper submitted for publication shall concern problems associated with production and application of fibers and textiles.

*Please include full postal address as well as telephone/ fax/e-mail details for the corresponding author, and ensure that all correspondence addresses are included. Also include the scientific title of the authors.*

*Industria Textila* magazine considers all manuscripts on the strict condition that they have been submitted only to the *Industria Textila* journal, on this occasion, and that they have not been published already, nor are they under consideration for publication or in press elsewhere. Authors who fail to adhere to this condition will be charged with all costs which *Industria Textila* magazine incurs and their papers will not be published.

## Manuscripts

Manuscripts of the following types are accepted:
*Research Papers* – An original research document which reports results of major value to the Textile Community
*Notes* – see below
*Book Reviews* – A brief critical and unbiased evaluation of the current book, normally invited by the Editor
*Correspondence* – Communications based on previously published manuscripts

Manuscripts shall be submitted in English in double-spaced typing, A4 paper, size font 12, Times New Roman, margins 2 cm on all sides, under electronic version in Word for Windows format.

The volume of the submitted papers shall not exceed 10 pages (including the bibliography, abstract and key words), typescript pages including tables, figures and photographs.

All articles received are reviewed by a reviewer, renowned scientist and considered expert in the subject the article concerns, which is appointed by the editorial board. After the article has been accepted, with the completions and the modifications required by the reviewer or by the editorial staff, it will be published.

The submission of the above-mentioned papers is by all means the proof that the manuscript has not been published previously and is not currently under consideration for publication elsewhere in the country or abroad.

There may also be published papers that have been presented at national or international scientific events, which have not been published in volume, including the specification related to the respective event.

The articles assessed as inappropriate by the reviewer or by the editorial staff, concerning the subject matter or level, shall not be published.

The manuscript shall be headed by a concise title, which should represent in an exact, definite and complete way the paper content. Authors should also supply a shortened version of the title, suitable for the running head, not exceeding 50 character spaces.

The manuscript shall also be headed by complete information about the author(s): titles, name and forename(s), the full name of their affiliation (university, institute, company), department, city and state, as well as the complete mailing address (street, number, postal code, city, country, e-mail, fax, telephone).

Tables and figures (diagrams, schemes, and photographs) shall be clear and color, where possible.

The photographs shall be sent in original format (their soft), or in JPEG or TIF format, having a resolution of at least **300 dpi**.

All tables and figures shall have a title and shall be numbered with Arabic numerals, consecutively and separately throughout the paper, and referred to by the number in the text.

Generally, symbols and abbreviations shall be used according to ISO 31: specifications for quantities, units and symbols. SI units must be used, or at least given comprehensive explanations or their equivalent.

Cited references shall be listed at the end of the paper in order of quotation and contain: **for a paper in a periodical** – the initials and surname of the author(s), title of journal and of the article, year and number of issue, number of volume and page numbers; **for a book** – the initial and surname of the author(s), full name of the book, publisher, issue, place and year of publishing, and the pages cited; **for patents** – the initial and surname of the author(s), the title, the country, patent number and year.

[1]. Grégory, P., Marketing, 2e edition, Édition Dalloz, Paris, 1996

Authors are requested to send an abstract of the paper, preferably no longer than 100 words and a list of 5-6 key words (preferably simple, not compound words, in alphabetical order). Avoid abbreviations, diagrams and direct reference to the text.

All manuscripts with the material proposed for publication, shall be sent to:

**marius.iordanescu@certex.ro**

**Complimentary issue** – The corresponding author will receive a complimentary print copy of the issue in which his/her article appears. It will be up to the corresponding author if he/she decides to share or route his/her copy to his/her co-author(s).